Lessons learned from (A)ATSR and prelaunch calibration of SLSTR

Dr David L Smith
RAL Space
STFC, Harwell Oxford, United Kingdom

ATSR Series

RAL Space

1991-2000 ATSR-1

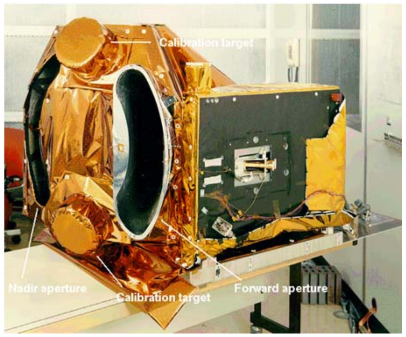

1995-2008 ATSR-2

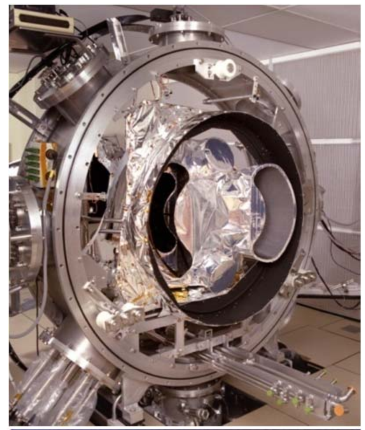

2002-2012- AATSR

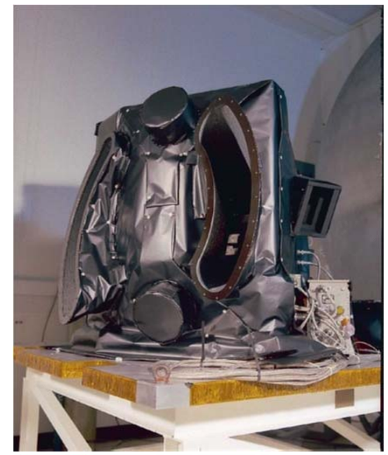

What is ATSR?

- The **A**long **T**rack **S**canning **R**adiometer - ATSR for short
  - an imaging space-borne infrared radiometer

- Designed in the early 1980's by UK and Australian scientists – who were then ahead of their time in recognising climate change as an important issue.
  - **Specifically** designed to measure sea surface temperature (SST) for:
    - **a) climate change detection – the first sensor aimed at this task!**
    - b) to support a range of oceanography studies
  - Later capabilities added for land, cloud, and aerosol remote sensing

- Three instruments have been flown since 1991 on ESA EO missions:
  - ATSR(-1) on ERS-1 – initial experimental instrument
  - ATSR-2 on ERS-2
  - AATSR on ENVISAT

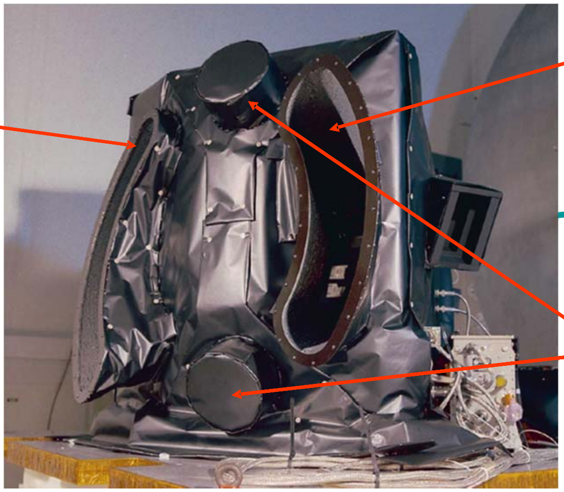

Design Features – Dual View

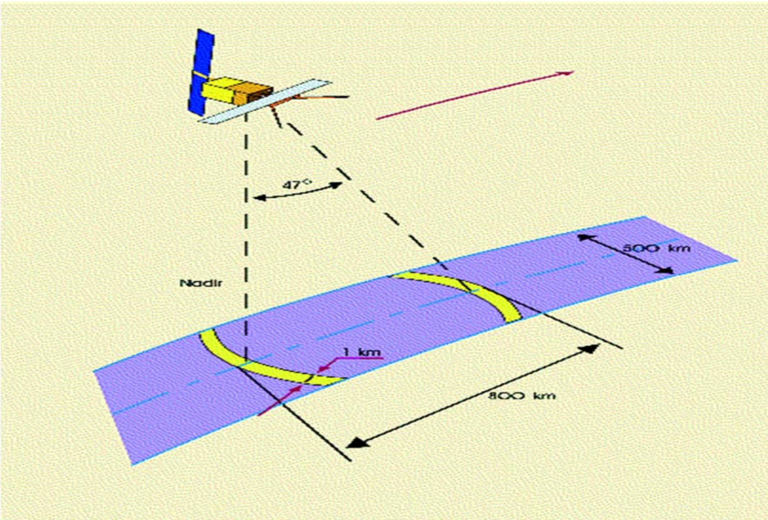

- Conical Scan Geometry provides dual view
  - Allows atmospheric corrections
  - 555km swath width

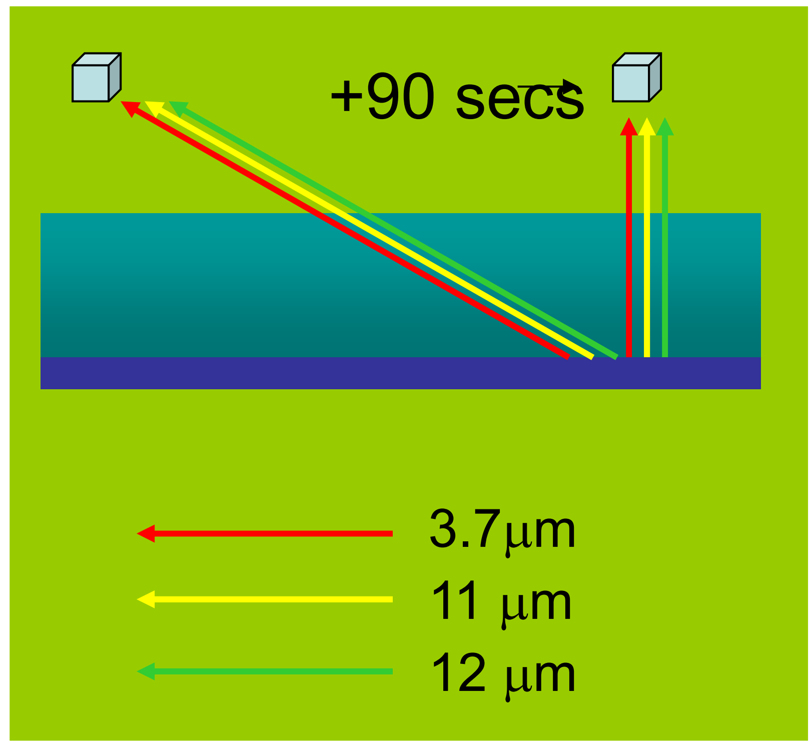

Design Features - Channels

- Thermal IR channels at 12µm, 11µm and 3.7µm
  - Actively cooled to 80K using a Stirling cycle
- Visible/Near Infrared Channels at 1.6µm, 0.87µm, 0.66µm and 0.56µm

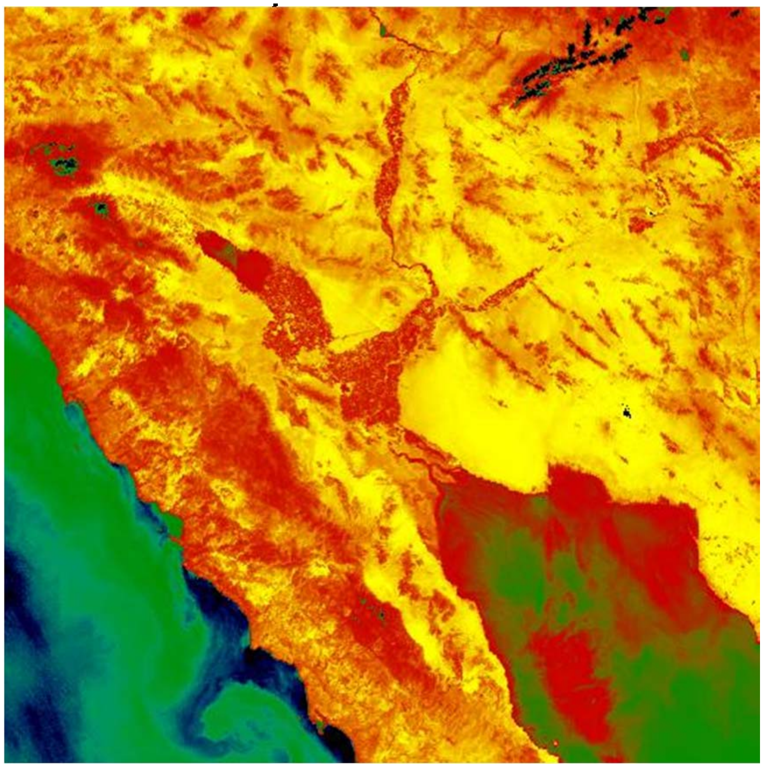

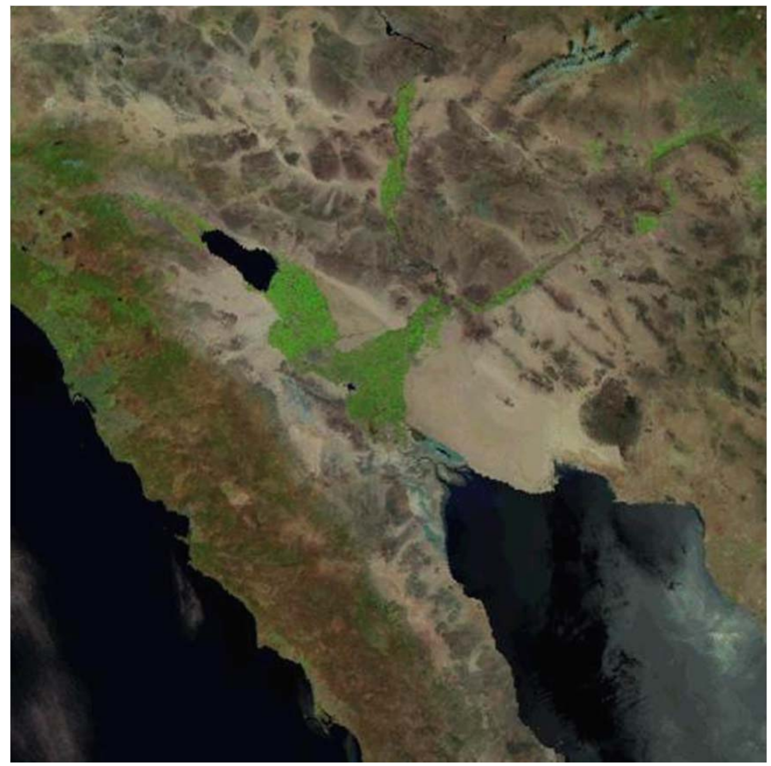

Sea Surface Temperatures

- Dual view allows aerosol robust SST retrieval

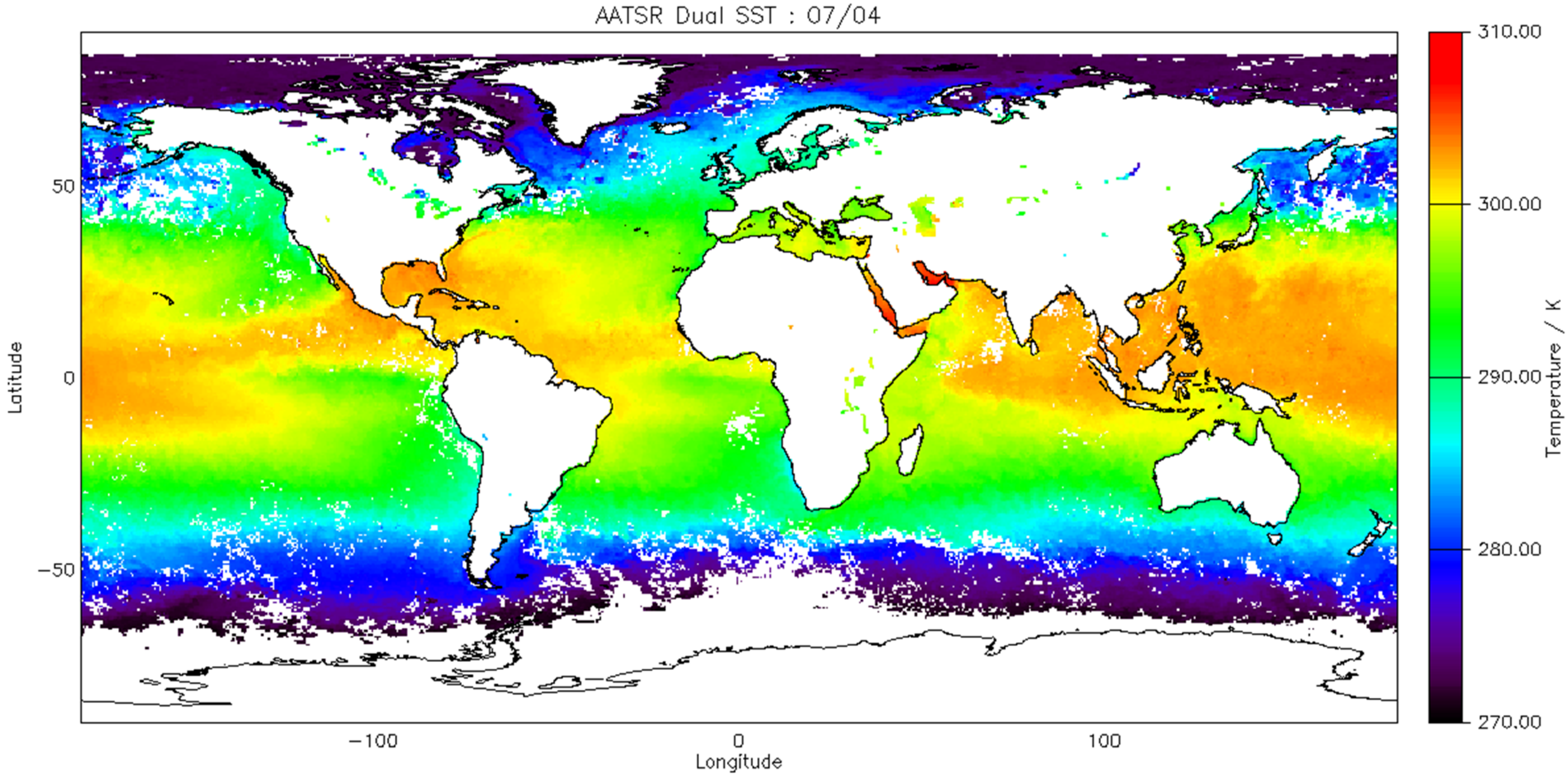

Calibration Topics

Spectral Response Calibration

- In-band response
- Out of band response
- Temperature dependency of response

Geometric Calibration

- Pointing Direction (LoS)
- Spatial Sampling
- Co-Registration
- Image Quality (MTF)

Polarisation

IR Radiometry

- Blackbody calibration
- Radiometric accuracy over dynamic range
- Linearity
- Radiometric noise performance
- Orbital Stability

Solar Channel Radiometry

- Calibration of VISCAL system
- Radiometric response over dynamic range
- Linearity
- Radiometric noise performance

Thermal Infrared Channels

TIR Channels Optical Chain

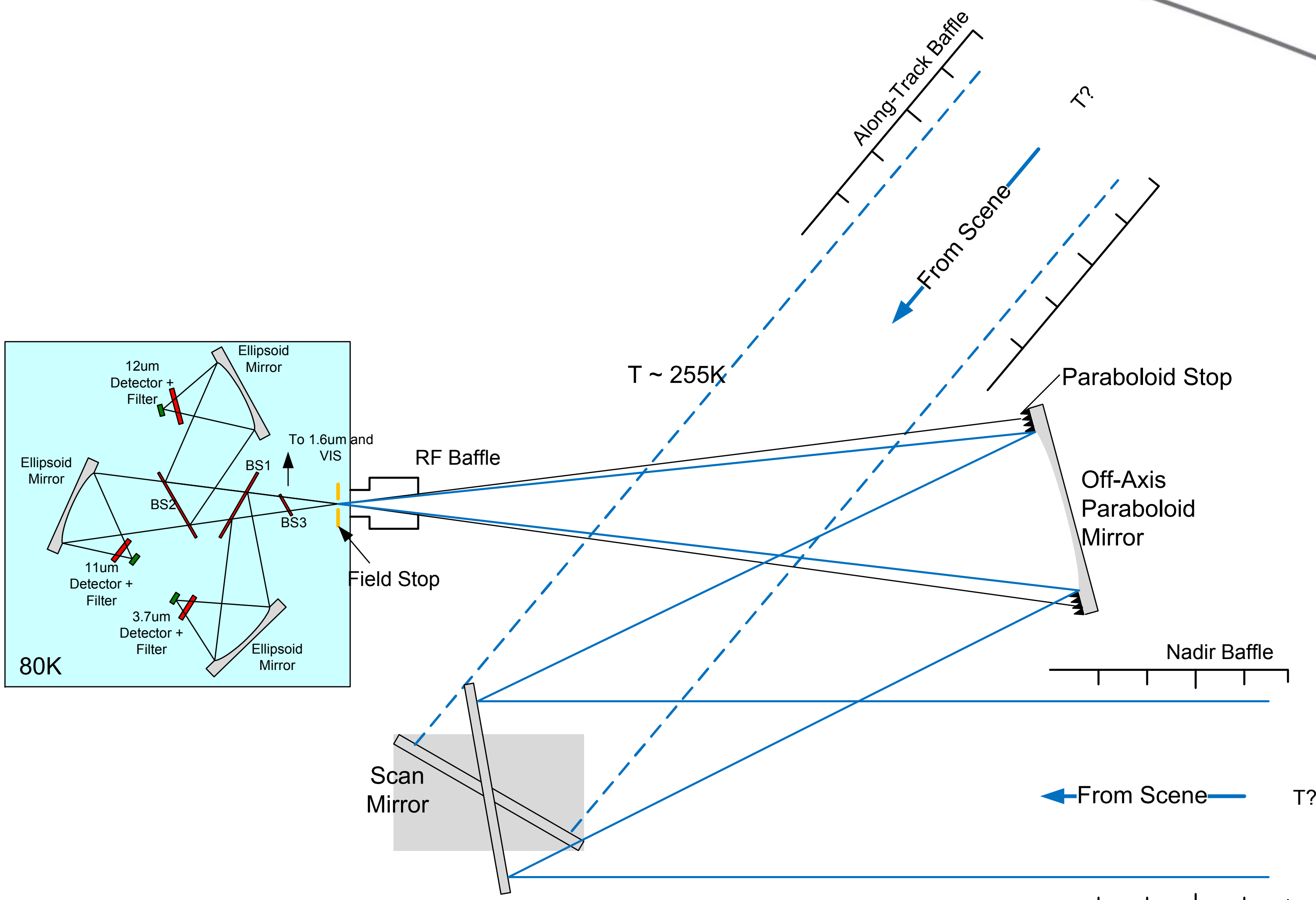

IR Calibration System

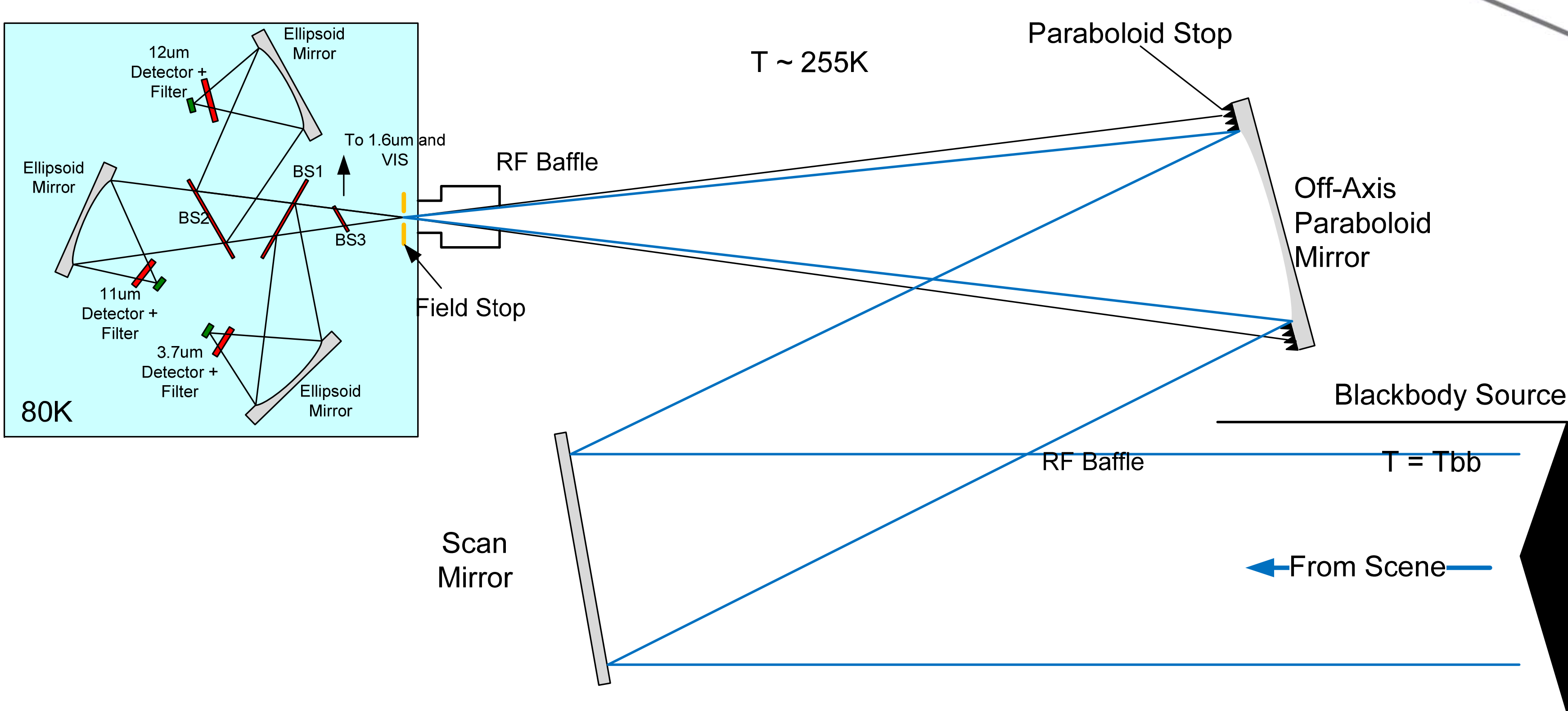

(A)ATSR Calibration System

Blackbodies viewed every scan.

- 2-point scheme covering the range of expected SST
  - Cold bb ~300K
  - Hot bb ~256K (floating at optics temperature)
- High Emissivity >0.999
- Precision Thermometry
  - 5 baseplate sensors
  - Calibration traceable to ITS-90
- Illuminates the full optical chain.
- Calibration system does not involve the use of ‘special’ modes, mechanisms or additional optics.

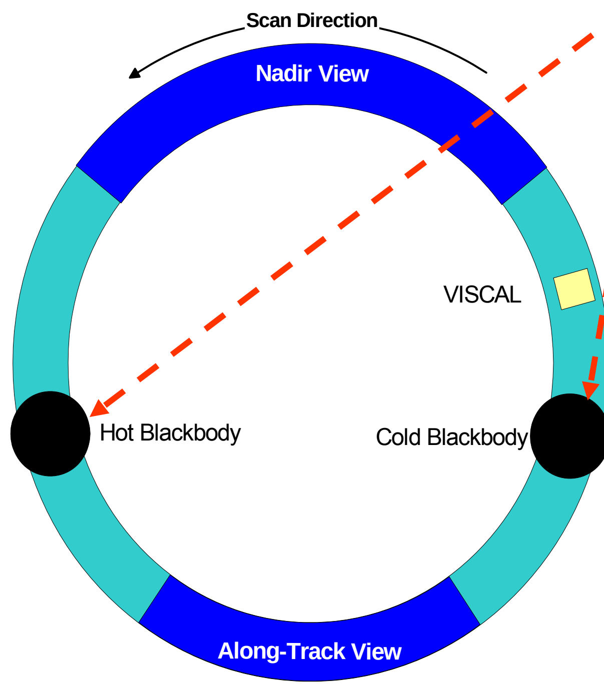

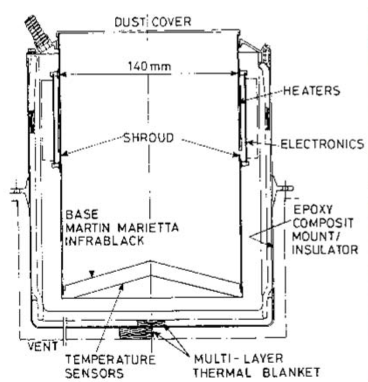

ATSR Radiometric Model

- Radiant flux at the detector is given by

$$\varphi_\lambda = A_\lambda \left(\begin{array}{l} (\pi - \Omega_\lambda) L_{FPA,\lambda} + \\ \Omega_\lambda \left(\begin{array}{l} (1 - \tau_{FPA,\lambda}) L_{FPA\lambda} + \\ \tau_{FPA,\lambda} \left(\begin{array}{l} (1 - \xi_\lambda) L_{surr,\lambda} + \\ \xi_\lambda \left(\begin{array}{l} (1 - r_{para,\lambda}) L_{para,\lambda} + \\ r_{para,\lambda} \left(\begin{array}{l} (1 - r_{scan,\lambda}) L_{scan,\lambda} + \\ r_{scan,\lambda} L_{scene,\lambda} \end{array} \right) \end{array} \right) \end{array} \right) \end{array} \right) \end{array} \right)$$

- Signal from 80K FPA surrounding is negligible and assuming that optical enclosure is isothermal and stable (by design)

$$\begin{aligned} \varphi_\lambda &= A_{i,\lambda} \Omega_{i,\lambda} \tau_{FPA,\lambda} \left(\xi_\lambda r_\lambda^2 L_{scene,\lambda} + \left(1 - \xi_\lambda r_\lambda^2\right) L_{inst,\lambda} \right) \\ &= \varphi_{scene,i,\lambda} + \varphi_{inst,i,\lambda} \end{aligned}$$

- Assuming linear detector and amplifier measured signal can be expressed as

$C_{scene} = gL_{scene} + C_0$

IR Radiometric Calibration Model

- Scene radiance at T(K) is a linear function of the measured signal

  $L_{scene} = GainC_{scene} + Offset$

- Using Signals from Hot and Cold Blackbodies we can obtain *Gain* and *Offset*

  $Gain = (L_{hot}-L_{cold})/(C_{hot}-C_{cold})$ and

  $Offset = (L_{hot}C_{cold} - L_{cold}C_{hot})/(L_{hot}-L_{cold})$

- L_{hot} and L_{cold} are the blackbody radiances derived using the Planck function from the measured blackbody temperatures and emissivities.

  $L = \varepsilon P(T_{BB}) + (1-\varepsilon)P(T_{inst})$ and

  $P(T) = \int R(\lambda)2hc^2/(\lambda^5 exp(hc/\lambda kT)-1)d\lambda$

- In practice we use look-up tables to convert from temperature to radiance and vice versa.

Pre-Flight Calibration (AATSR)

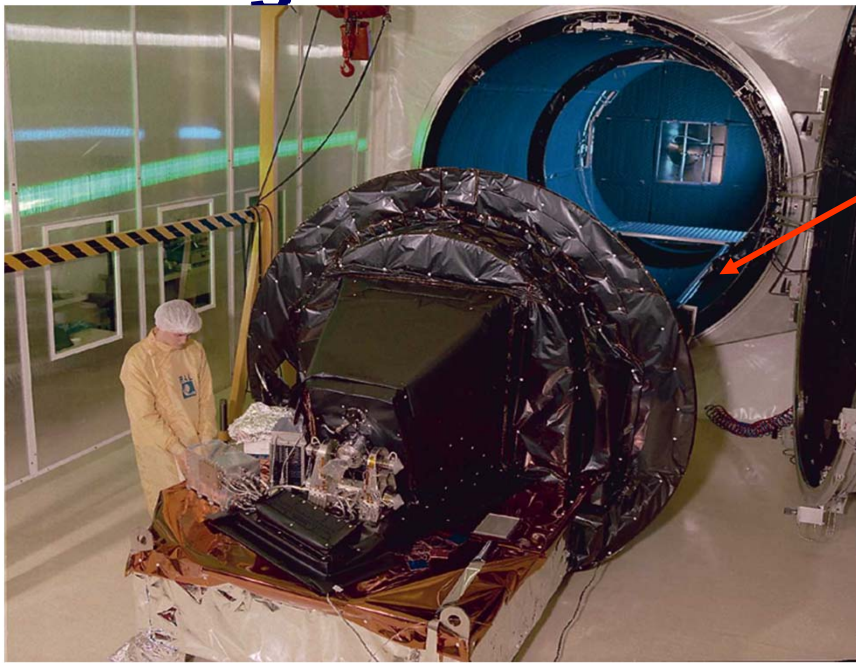

Calibration tests performed under representative thermal environment to control stray light

Radiometric Test Equipment previously used for ATSR-1/2 & AATSR-2

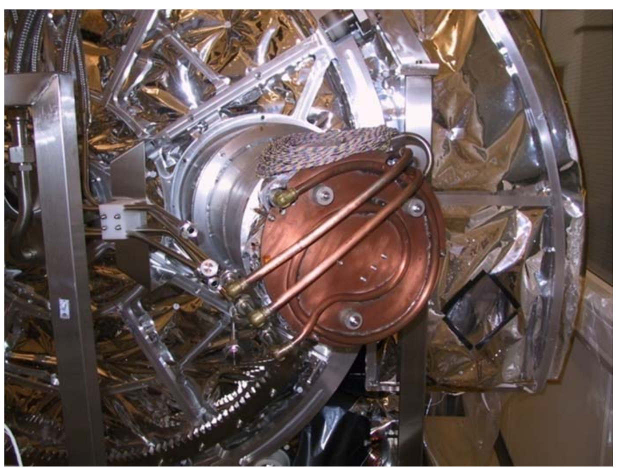

Precision RIRTs Calibrated to ITS90 < 0.01K

Radiometric Accuracy < 0.05K

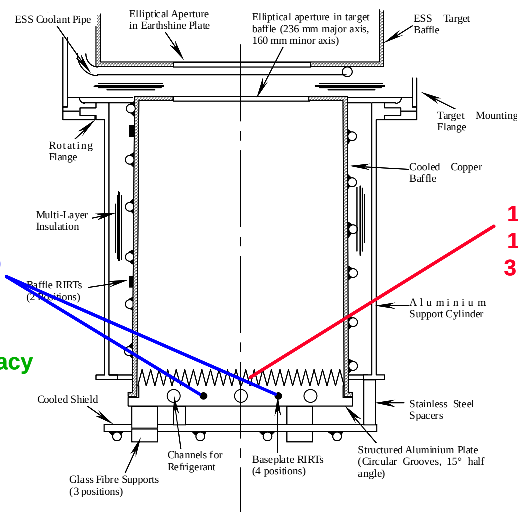

Emissivity
12µm = 0.99871
11µm = 0.99870
3.7µm = 0.99911

Standards

ATSR

ATSR-2

AATSR

Comparison of ATSR BBs with external BBs

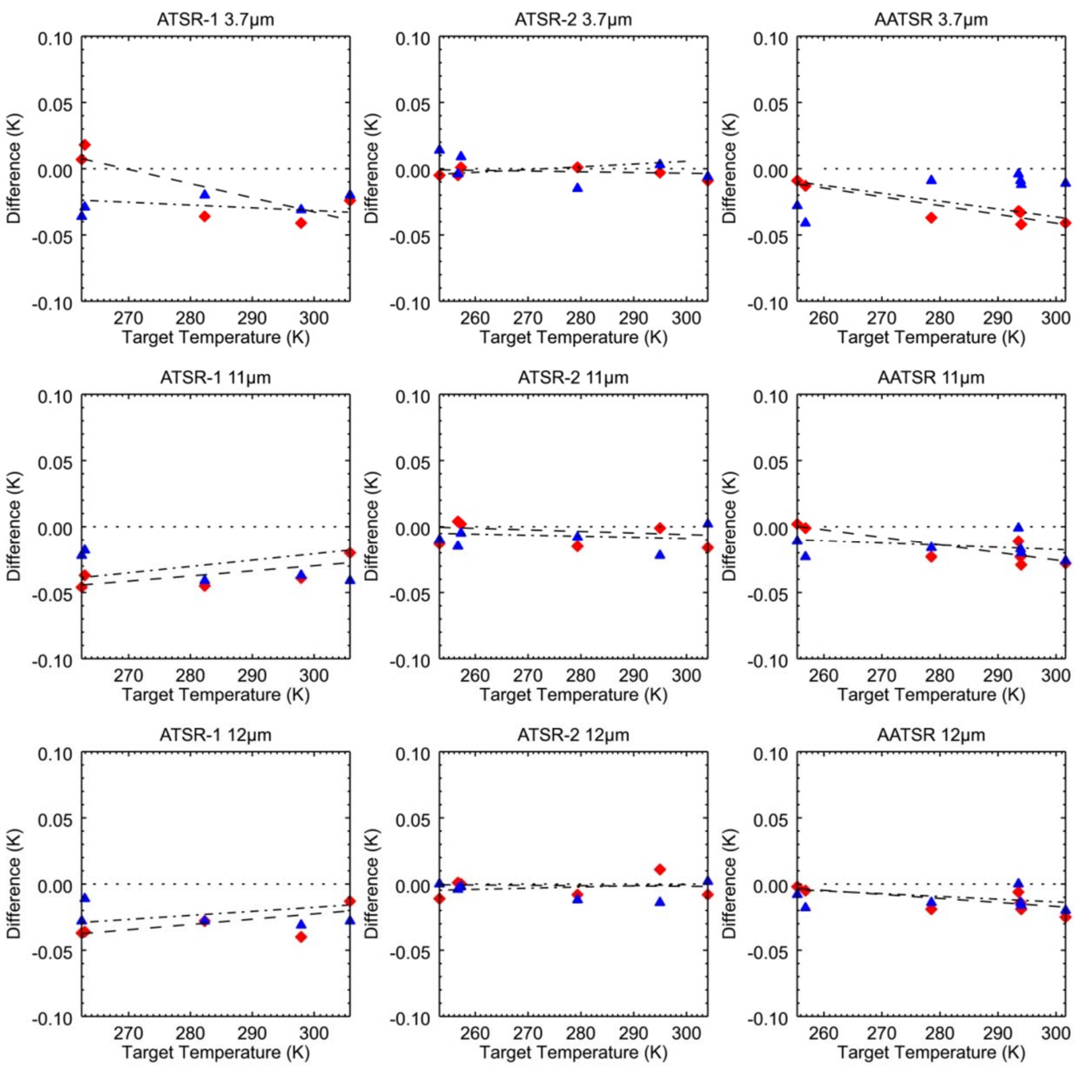

- For each of the calibration runs, measurements were taken with the external blackbody temperatures matched to the on-board target temperatures.
- Effect of non-linearity is negligible at these points
- Provides a ‘direct’ comparison of the flight blackbodies against external sources.

Calibration vs. Target Temperature

RAL Space

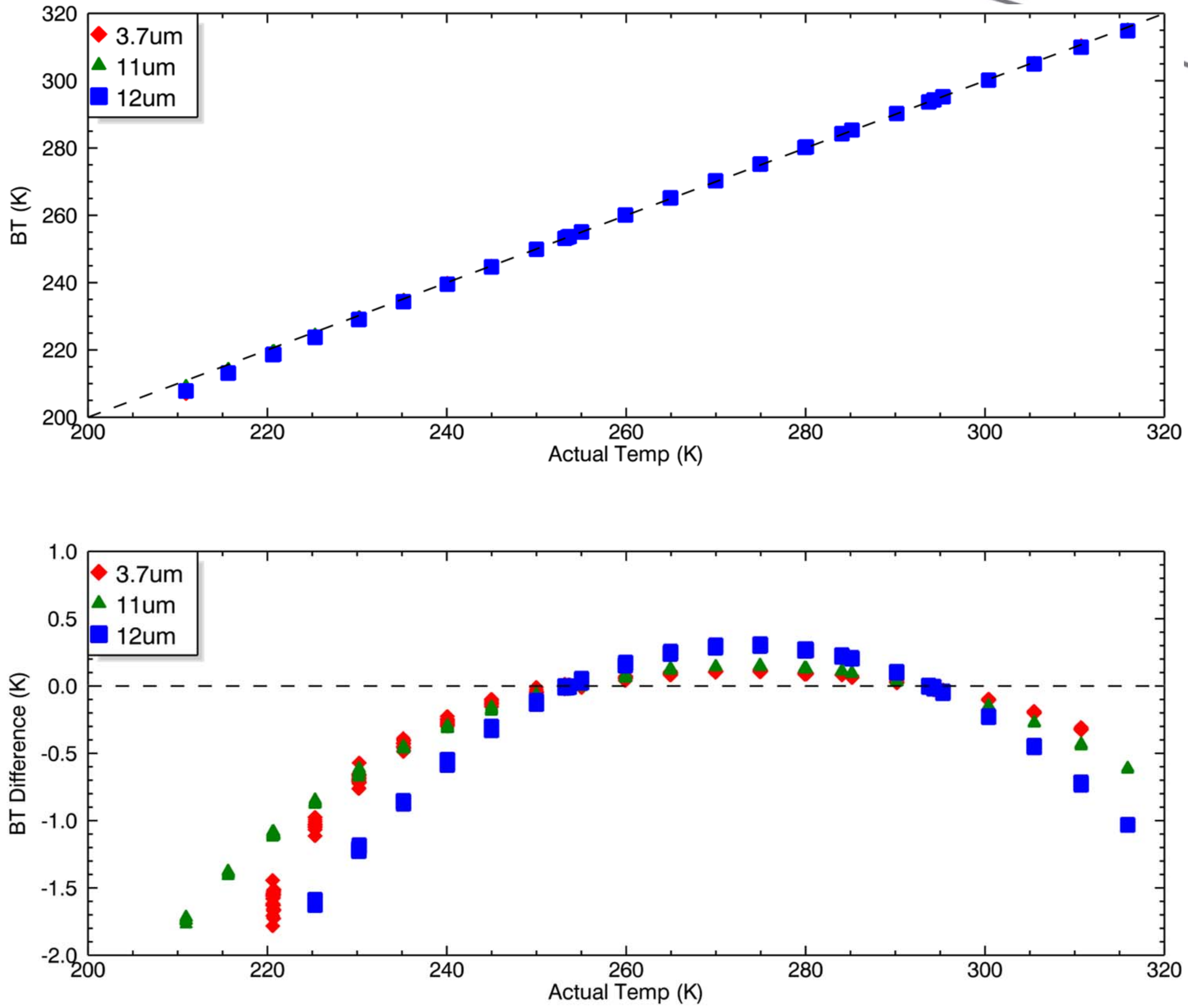

IR Channels Nonlinearity

RAL Space

- Nonlinearity is defined as the ratio of the measured response against the linear response.
  - NL = Vout/Vin

- Strictly speaking NL for AATSR is a function of the flux at the detector.

- For practical reasons on ATSR NL is defined as a function of scene radiance
  - Good enough for SST measurements

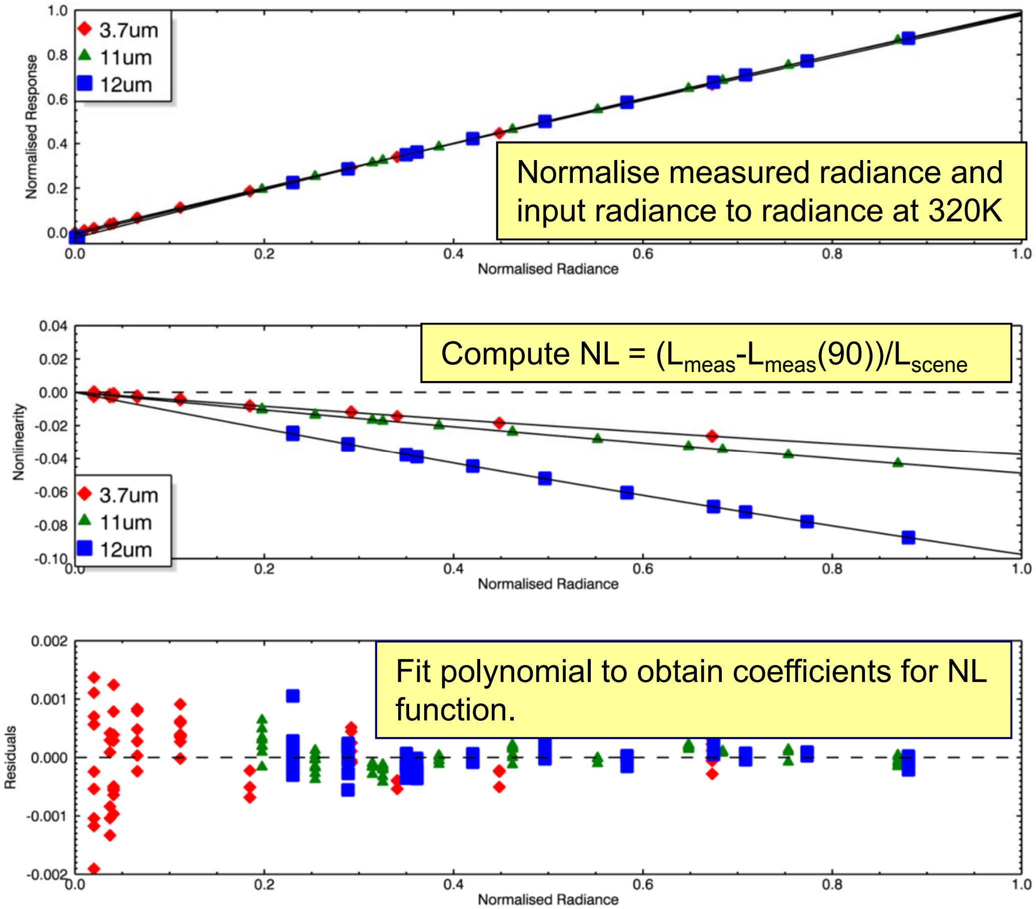

Modify temperature to radiance LUTs such that

L'(T) = f(T)L(T)

Calibration Summary

		ATSR	ATSR-2	AATSR
3.7μm	NEΔT	0.046	0.051	0.037
	T_λ-T_{RIRT}	-0.021	-0.010	-0.014

10.8μm	NEΔT	0.023	0.021	0.025
	T_λ-T_{RIRT}	-0.034	-0.014	-0.030

12.0μm	NEΔT	0.031	0.024	0.023
	T_λ-T_{RIRT}	-0.028	-0.014	-0.020

Blackbody Crossover Test

- Test is performed by switching heated blackbodies
  - Performed at yearly intervals

- The basic idea is to compare the radiometric signals in the thermal channels when the two blackbodies are at identical temperatures.
  - Any significant difference would imply a drift in the blackbody thermometer calibration or change in target emissivity caused by a deterioration of the black surface finish.

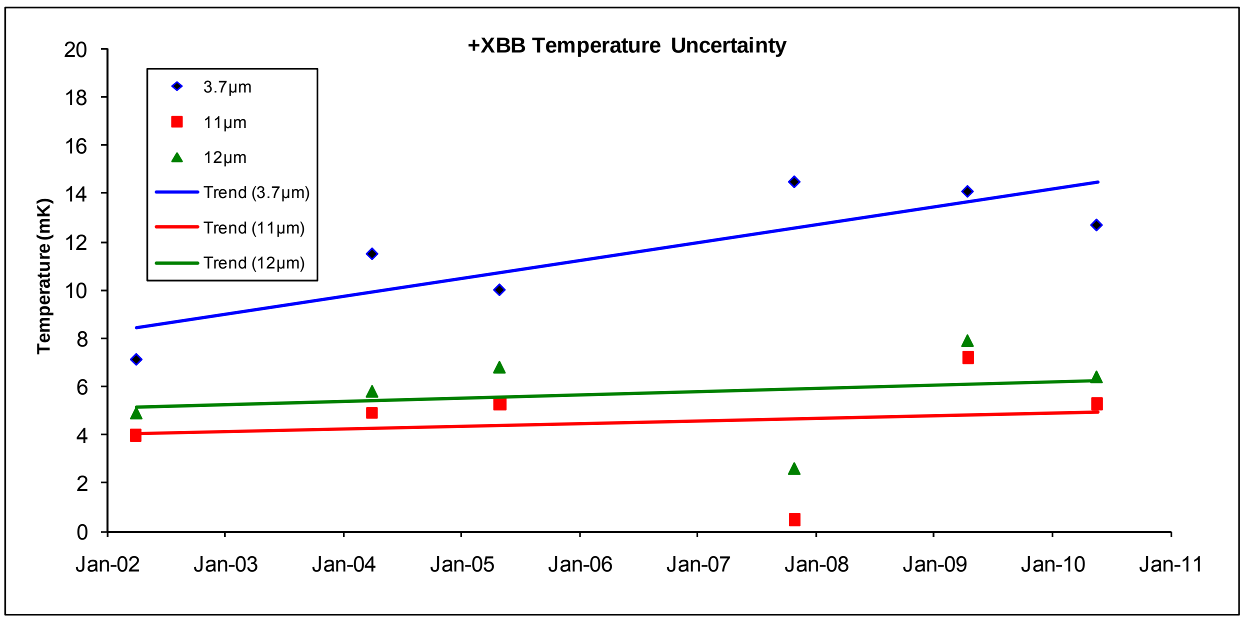

AATSR-ATSR-2 BT Intercomparisons

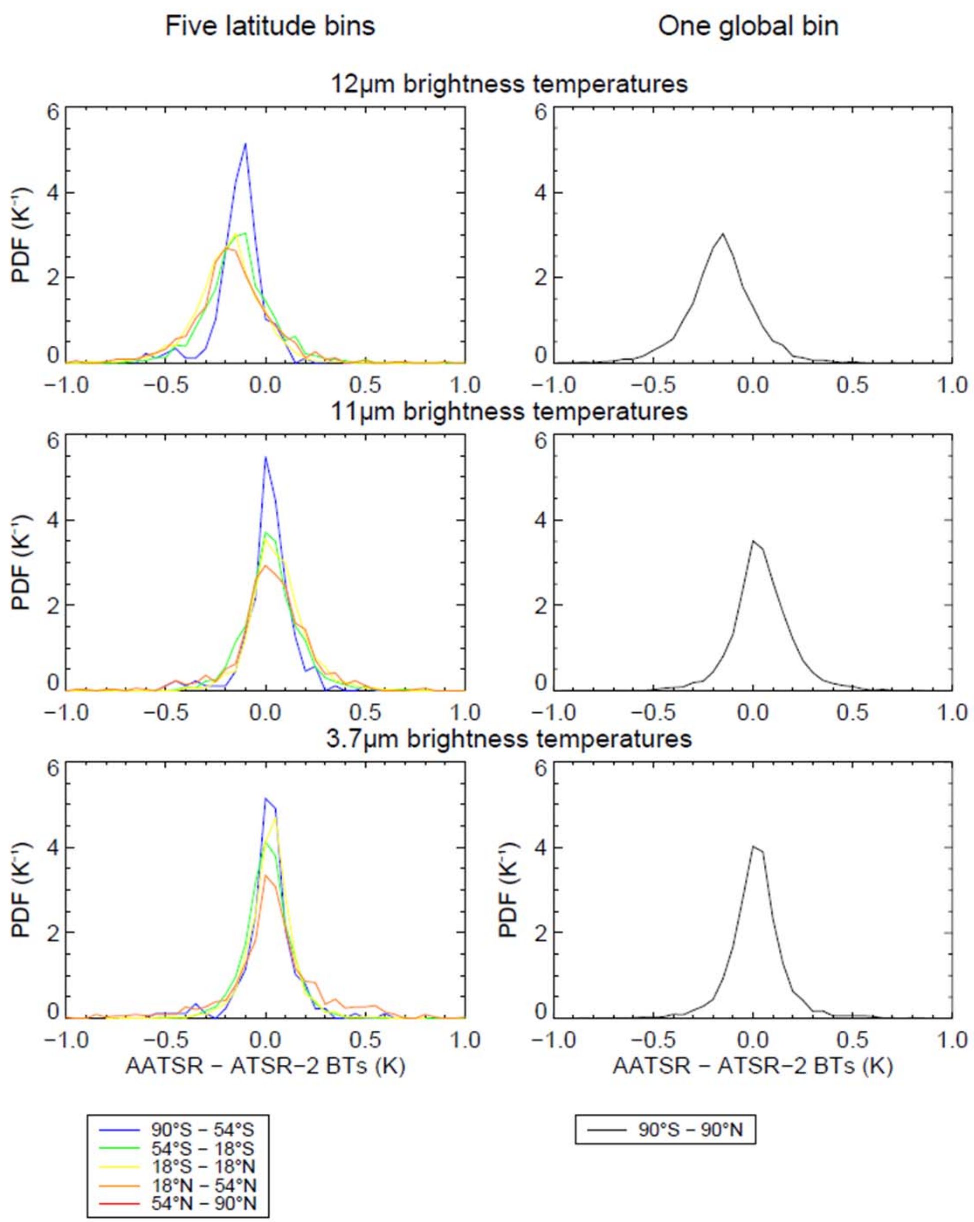

The overlap period between consecutive missions is critical for comparing calibrations of sensors to ensure consistency

ATSR-1 -> ATSR-2
ATSR-2 -> AATSR

Night Time

12um Anomaly Review Board

- Following a recommendation from the AATSR Exploitation Board (AEB) and Quality Working Group (QWG), an Anomaly Review Board was established to consider the differences in signal response which have been consistently observed between the ATSR-2 and AATSR signal channels, particularly, though perhaps not exclusively, in the 12 µm wavelength signal channels of the two instruments.

- The ARB team is composed of many people with experience of the design, manufacture, calibration and usage of the AATSR under an independent chair.

- Secretarial services to the ARB were provided by Telespazio Vega under contract to DECC.

12µm Conclusion

AATSR minus IASI | **ATSR-2 minus AATSR**

Before

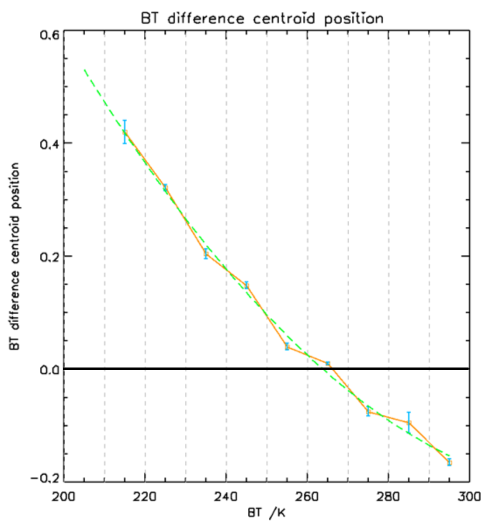

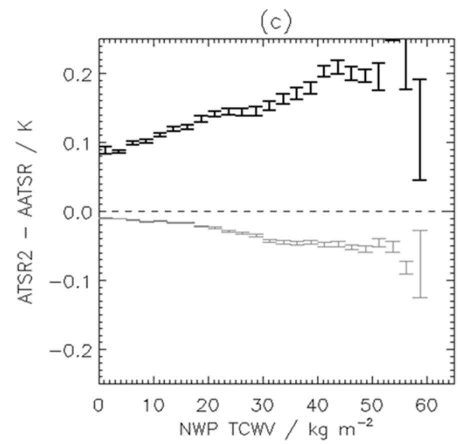

Subtraction of non-linearity adjustment factor and long wavelength shift by ~50nm

After

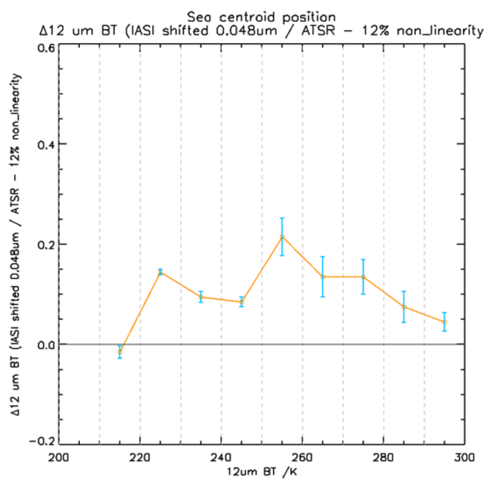

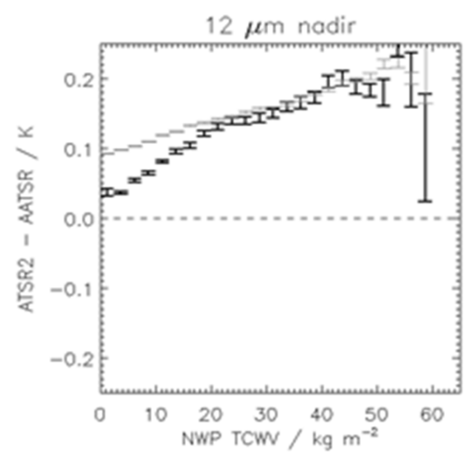

Large range of T (ocean and cloud)

Reduced range of T (ocean only)

VIS-SWIR Channels

VIS-SWIR Channels

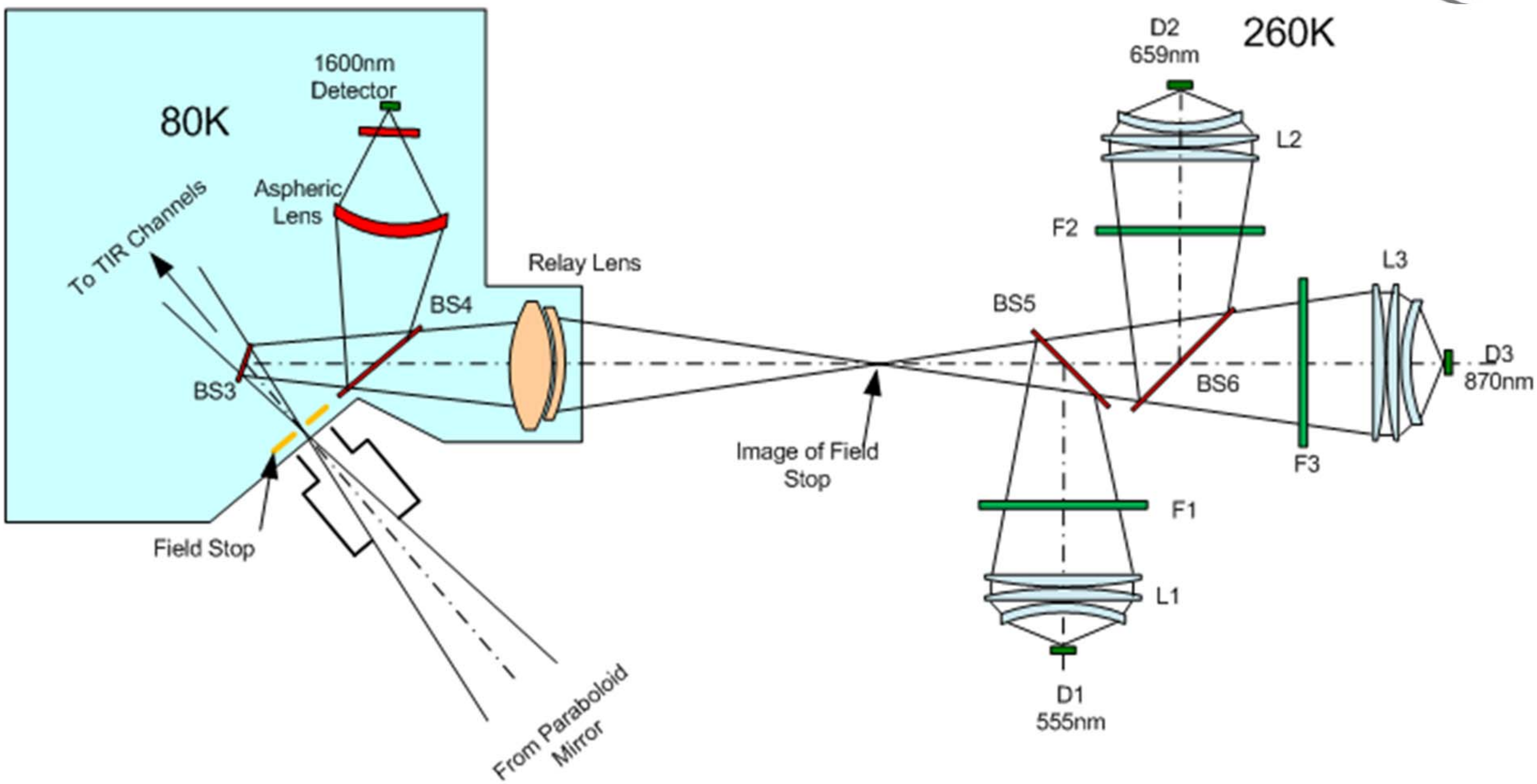

VIS-swir CALibration system

- ATSR-2 introduced a prototype VISCAL system which provides a calibration reference proportional to the solar irradiance, so

$R_{scene} = R_{VISCAL} (C_{scene} - C_{dark}) / (C_{VISCAL} - C_{dark})$

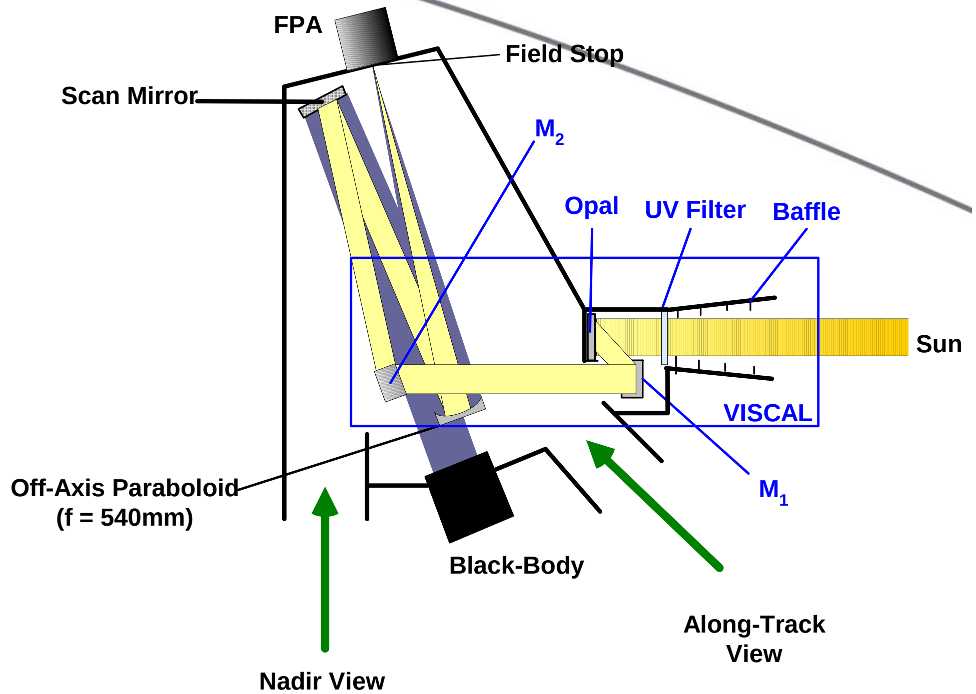

- AATSR has an developed version of the VISCAL system
  - Improved stray light baffling
  - Wider FOV for diffuser

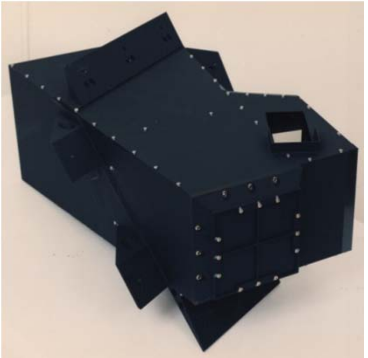

Calibration Budget

Component	Expression	Source	Uncertainty
Reflectance Factor For VISCAL	Δr_{viscal}	Pre-Launch Calibration Diffuser BRDF Relay Mirror Reflectances UV window transmission VISCAL geometry	3%
Degradation of VISCAL Reflectance Factor	Δr_{drift}	Post-Launch Vicarious Calibration	1%
Orbital Gain Stability	Δr_{orbit}	By design & Pre-Launch Testing	0.1%
Signal Channel Noise (VISCAL Source Signal)	$\Delta r_{noise,viscal}$	Measured from On-Board Sources	<0.01%
Signal Channel Noise (VISCAL Dark Signal)	$\Delta r_{noise,dark}$	Measured from On-Board Sources	<0.01%
Signal Channel Noise (Scene Signal)	$\Delta r_{noise,scene}$	Measured from On-Board Sources	<0.01%
Signal Channel Noise (Dark Signal)	$\Delta r_{noise,dark}$	Measured from On-Board Sources	<0.01%
Non-Linearity	Δr_{nonlin}	Pre-Launch Calibration	1%
Total Uncertainty	$\boldsymbol{\Delta r_{scene}}$		

Solar Irradiance Error	ΔI_0	Solspec Reference Spectrum Spectral Response (Pre-Launch)	2%
Total Uncertainty	$\boldsymbol{\Delta L_{scene}}$		

Pre-flight Calibration

- Radiometric Response
- Linearity
- Polarisation Sensitivity
- Variation around scan
- VISCAL Reflectance Factor

	Expected	Measured
1600nm	0.192±0.005	0.192±0.006
870nm	0.156±0.004	0.154±0.005
659nm	0.163±0.003	0.163±0.005
555nm	0.165±0.003	0.165±0.005

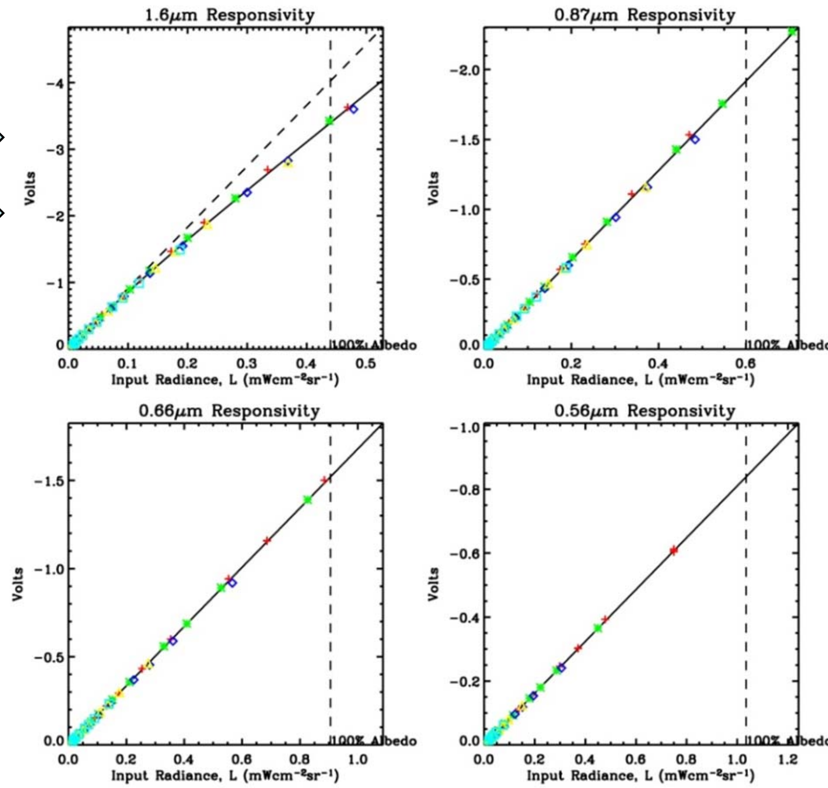

VIS-SWIR Channels Performance

The optical throughput of the 1600nm, 860nm, 660nm and 560nm channels is monitored using the VISCAL system.

Performance of the visible channels was strongly affected by the build-up of contamination on the IR-FPA.

Prior to November 2002, the throughput of short wavelength channels fell off sharply after running the IR-FPA at 80K for a few weeks.

After November 2002, the fall off in signal was much less as the condensation rate had reduced to rates approaching that seen at the start of the ATSR-2 mission.

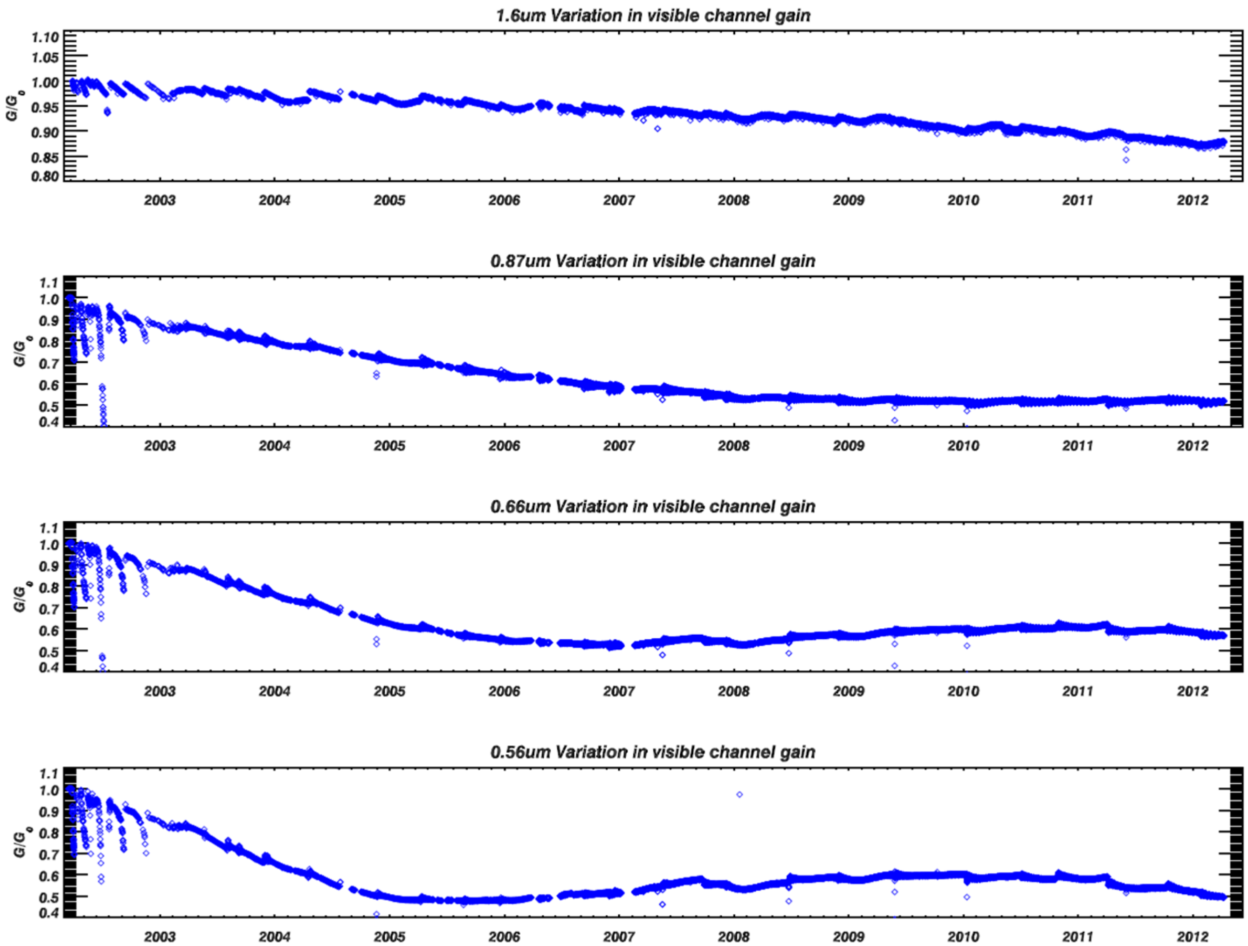

VIS-SWIR Channels Performance

Detail for the period from 01-Oct-2011 to 31-Dec-2011 showing the 1600nm, 860nm, 660nm and 560nm visible channel calibration levels, G, relative to the level at the start of the mission, G_0.

The oscillations in the signal are due to the build-up of a thin condensation layer causing a thin film interference effect.

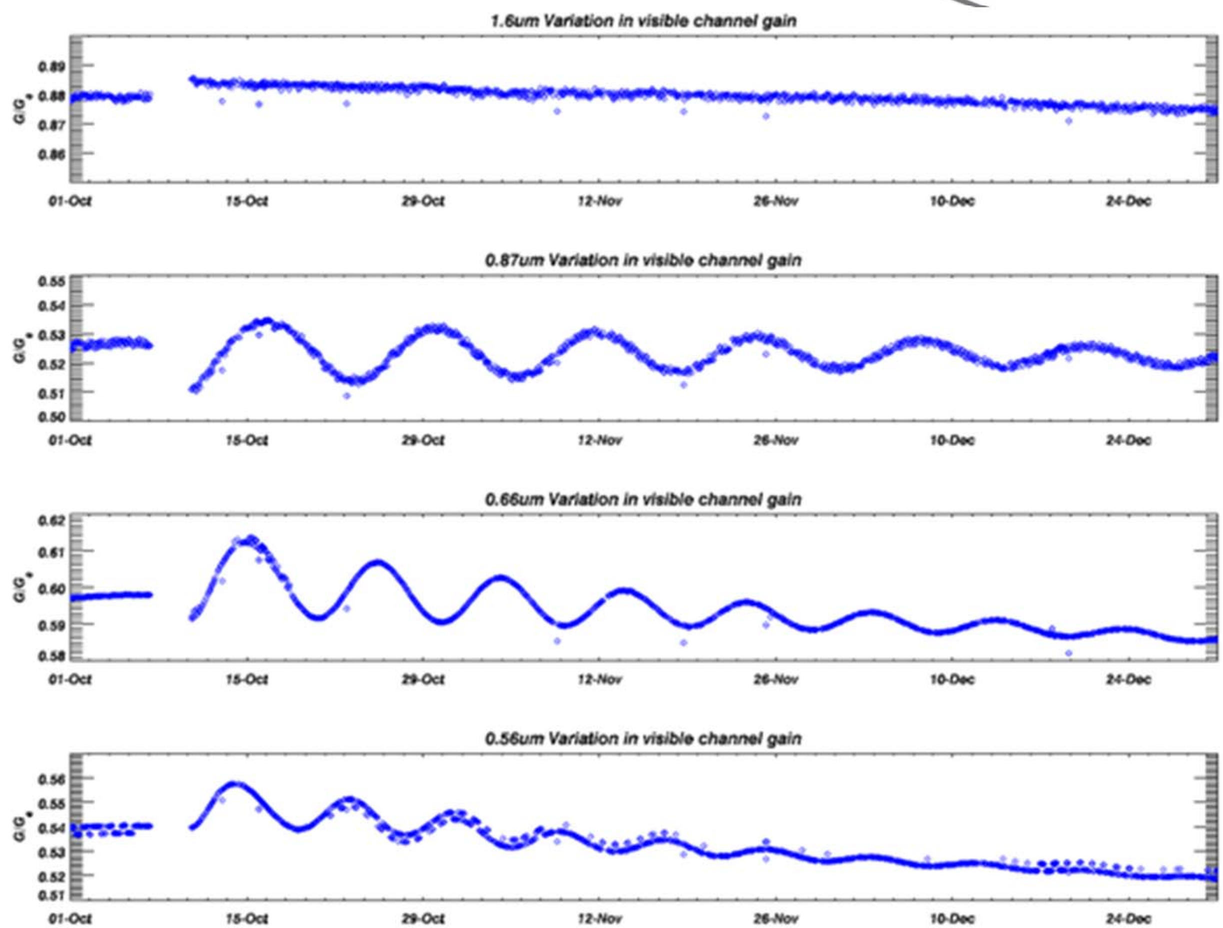

Calibration over stable targets

- ATSR-2 and AATSR carry in-flight systems for calibrating the VIS-SWIR channels.

- Quasi stable desert and ice targets allow monitoring of long-term stability and comparisons between sensors (e.g. AATSR, MERIS, MODIS)

Site selection criteria:

Uniform reflectance over large area

Long term-radiometric stability of the calibration sites

Ensures long-term stability of the top-of-the atmosphere (TOA) albedo (and of seasonal variations, if any) or reflectance over large spatially uniform areas.

High surface reflectance to maximise the signal-to-noise and minimise atmospheric effects on the radiation measured by the satellite

Site Data Extractions

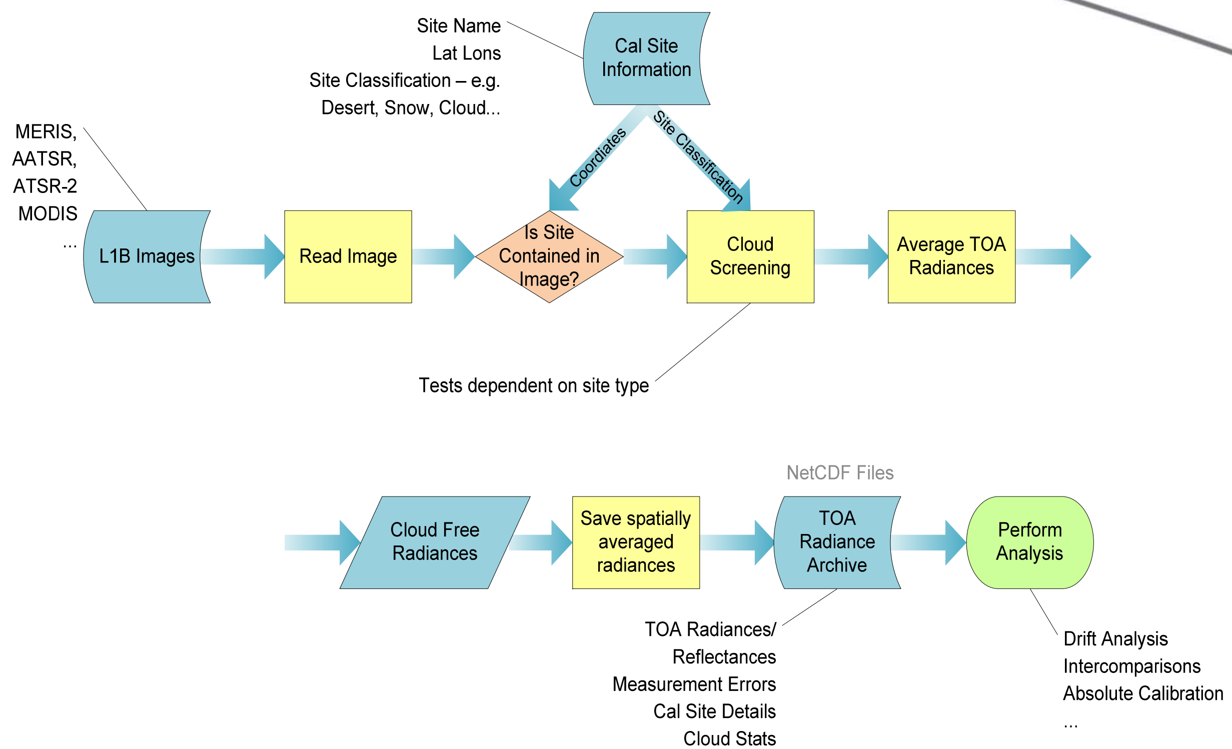

No of extractions

AATSR – 7782
ATSR-2 – 1562
ATSR-1 – 1267
MERIS - 16050 (Desert sites provided by ACRI using METRIC)
1359 (Dome-C and Greenland from L1b products)
MODIS-A – 11149 (Dome-C and Libya 4 only!)

1.6um nonlinearity correction

- Early intercomparisons between AATSR and ATSR-2 showed that the 1.6um non-linearity had not been implemented correctly in the L1 processing chain.
- Although non-linearity correction table had been implemented - the radiometric scaling was inconsistent with the internal variables in the IPF
- Problem was rectified in December 2004 using a table with a non-linearity correction table.

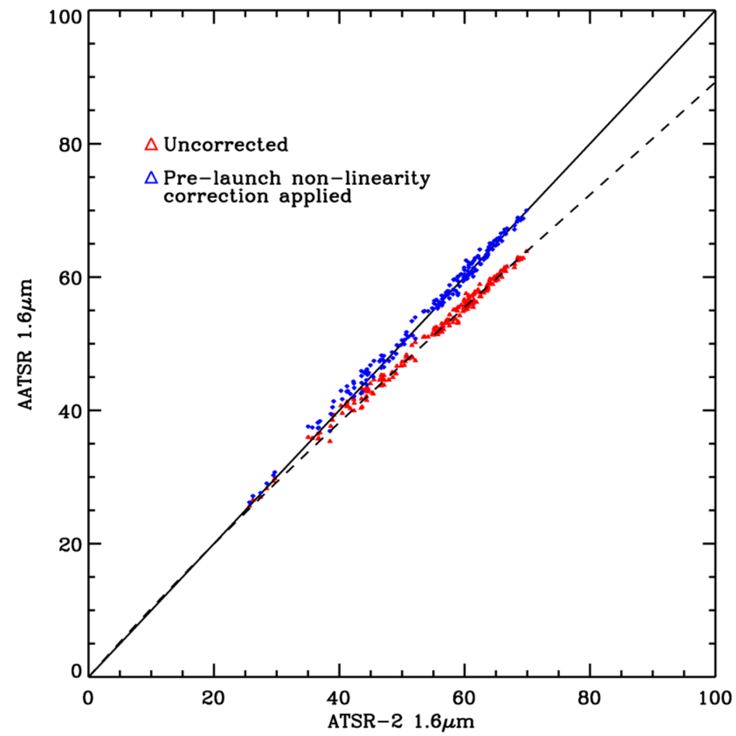

AATSR vs. ATSR-2 desert targets

ATSR-2 VISCAL Drift

To obtain drift we compare measured BRF against reference BRF for all sites

Trend is obtained by averaging drift for all sites of 90day window filtering for values <2sigma from mean.

ATSR-2 degradation follows model of Barnes et al

Results provide input to drift correction look-up-table

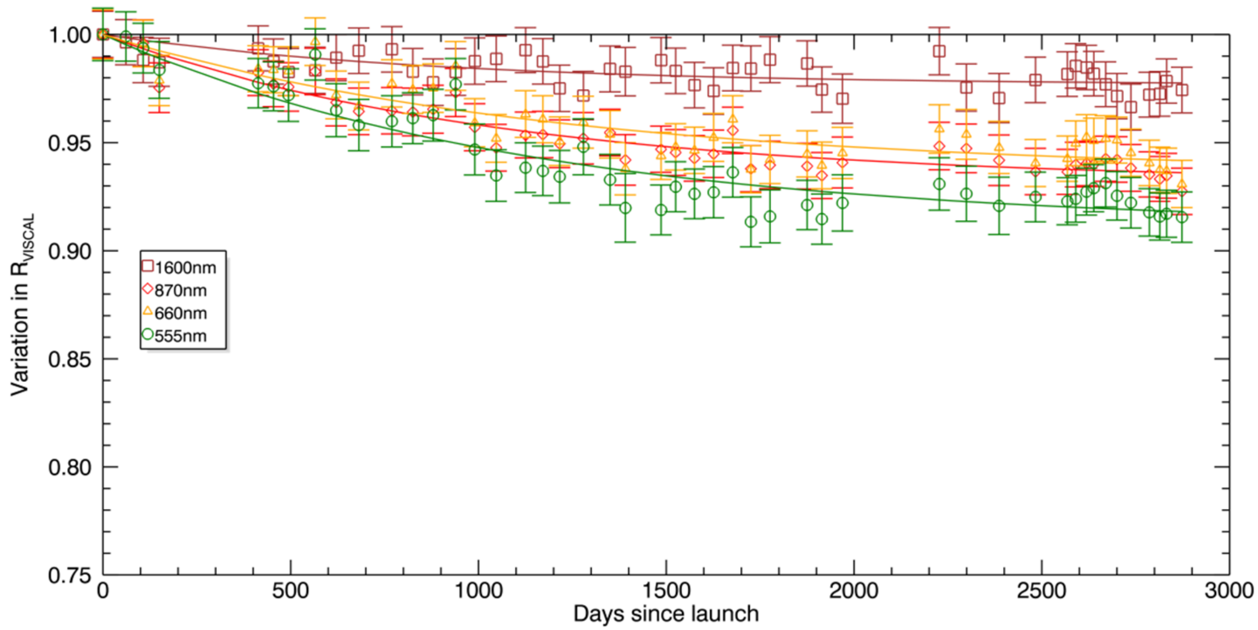

$$f(\lambda,t)=a_0(\lambda)-a_1(\lambda)\{1-\exp[-a_2(\lambda)(t-t_0)]\}$$

AATSR VISCAL Drift

AATSR drift DOES NOT follow Barnes Model as originally expected – suggests a more complex model for drift

Results provide input to drift correction look-up-table

Drift is not based on the measurements NOT a parametric model

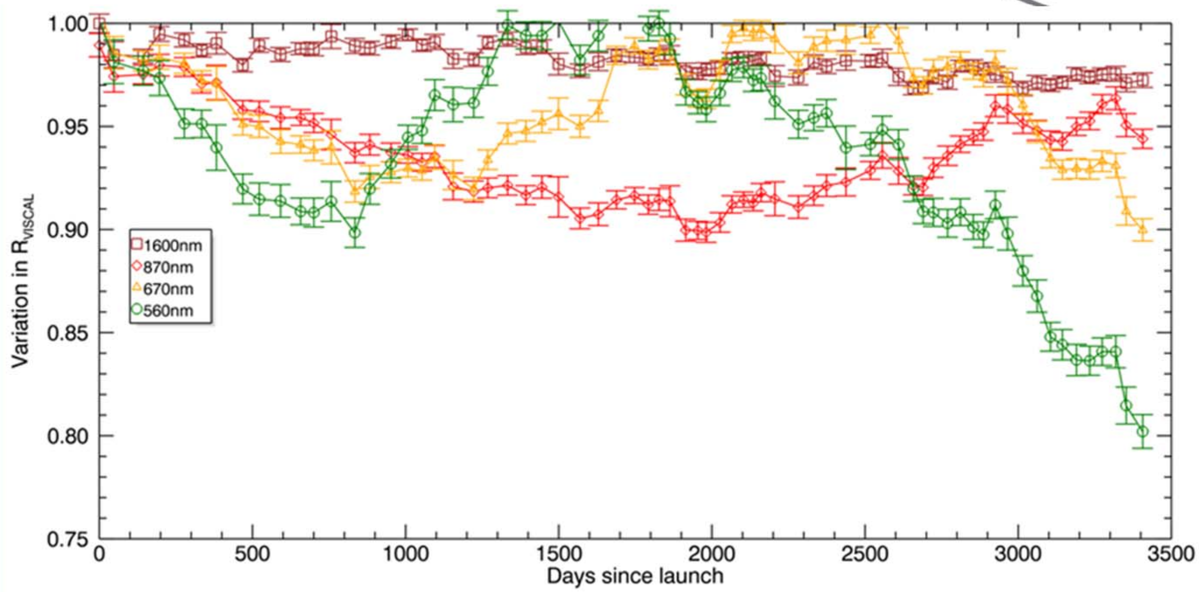

~~$f(\lambda,t) = a_0(\lambda)-a_1(\lambda)\{1-\exp[-a_2(\lambda)(t-t_0)]\}$~~

AATSR Visible Calibration History

Before 3rd Reprocessing

- Only 3 updates to AATSR visible calibration in IPF were introduced since launch
  - 14-December-2004 - 1.6um non-linearity correction introduced (PO-TN-RAL-AT-0540)
  - 29-November-2005 – Exponential Drift Correction is applied to VC1 files (PO-TN-RAL-AT-0542)
  - 18-December-2006 – Thin Film Drift Correction is introduced to VC1 files (PO-TN-RAL-AT-0552)

- Users need to apply corrections to L1b products with the drift correction look-up-table and tools provided on-line via CEOS cal-val portal http://calvalportal.ceos.org/cvp/web/guest/aatsr-envisat

AATSR Visible Calibration History

3rd Reprocessing

- Channels recalibrated using same drift correction as published
- All (A)ATSR sensors recalibrated to AATSR
- NO corrections for bias (e.g. AATSR vs. MERIS) have been introduced

Intercomparison Methodology – Direct comparisons

Approach works for sensors at similar local time and view geometry – e.g. MERIS and AATSR

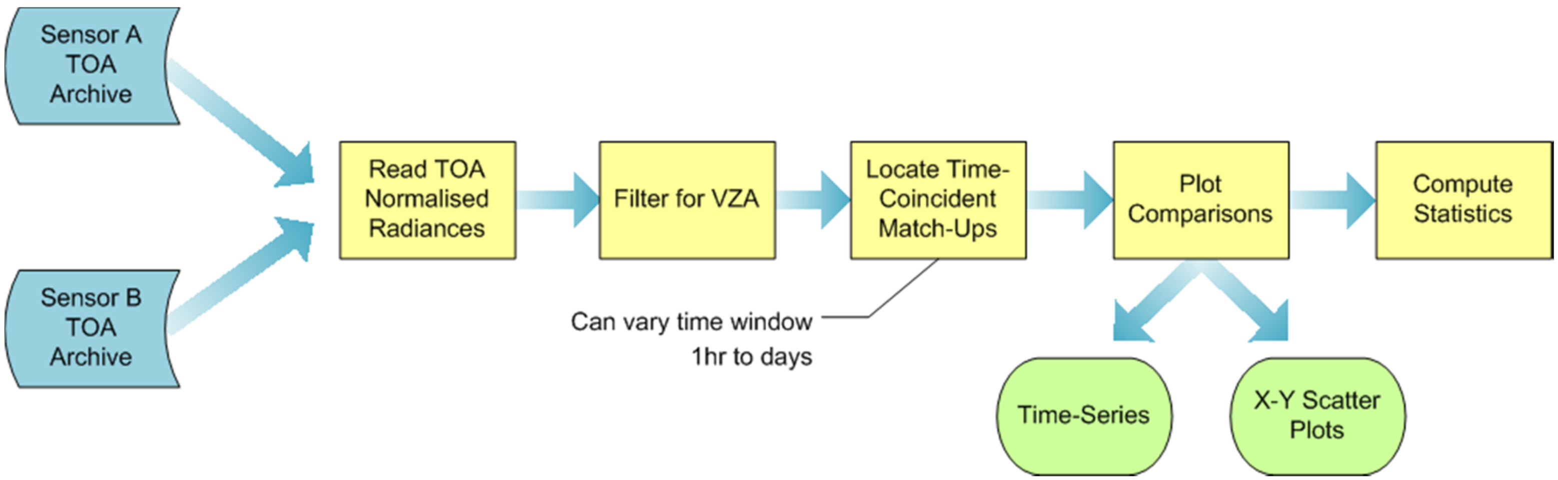

Provides Limited number of coincidences

No good for sensors at different crossing times – e.g. EOS-A/ENVISAT

Restricted to near nadir observations

Atmospheric corrections are needed where spectral bands are not coincident

Direct comparison MERIS vs. AATSR

AATSR and MERIS share same platform hence direct comparisons are possible

Corresponding channels at 865nm, 660nm and 555nm

Matchups at VZA <10°

AATSR drift corrections applied

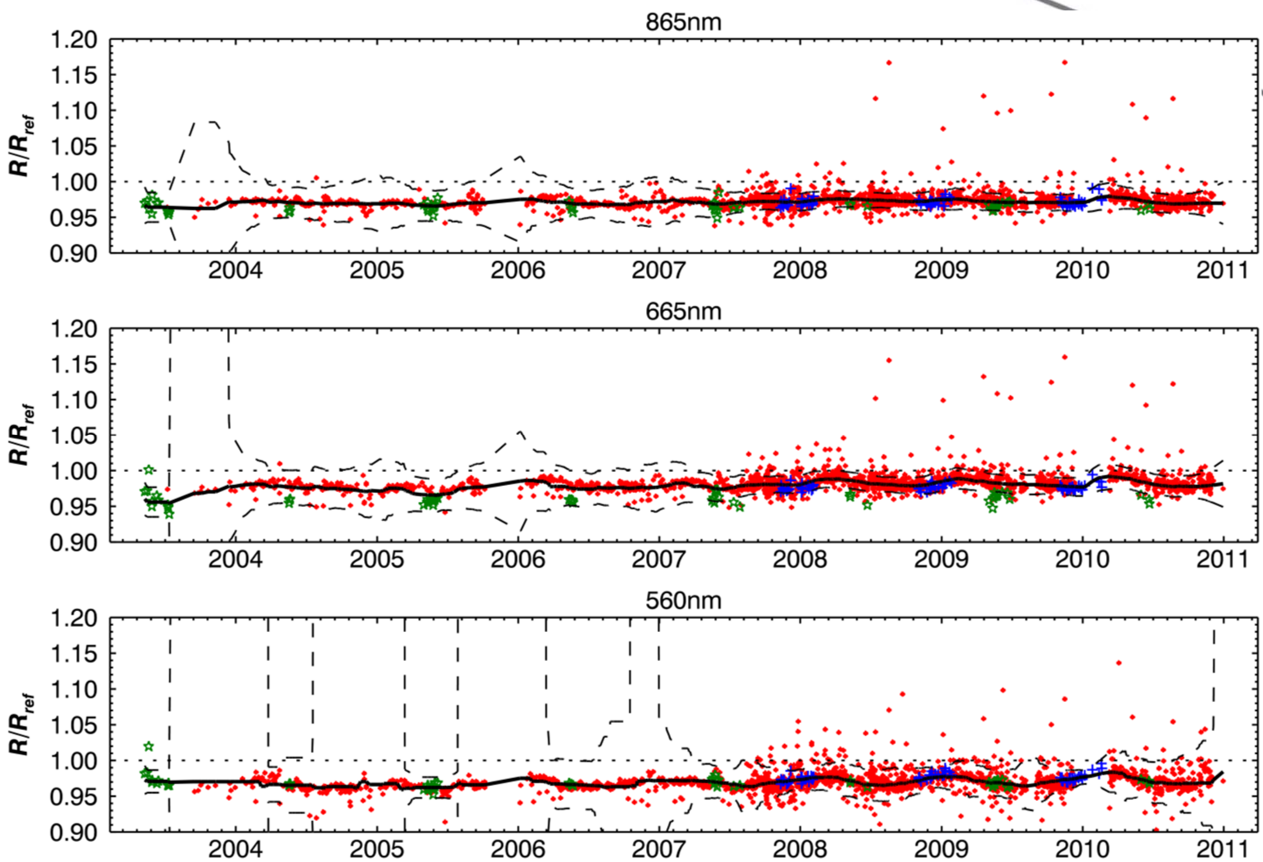

Intercomparison Methodology – Via reference BRF

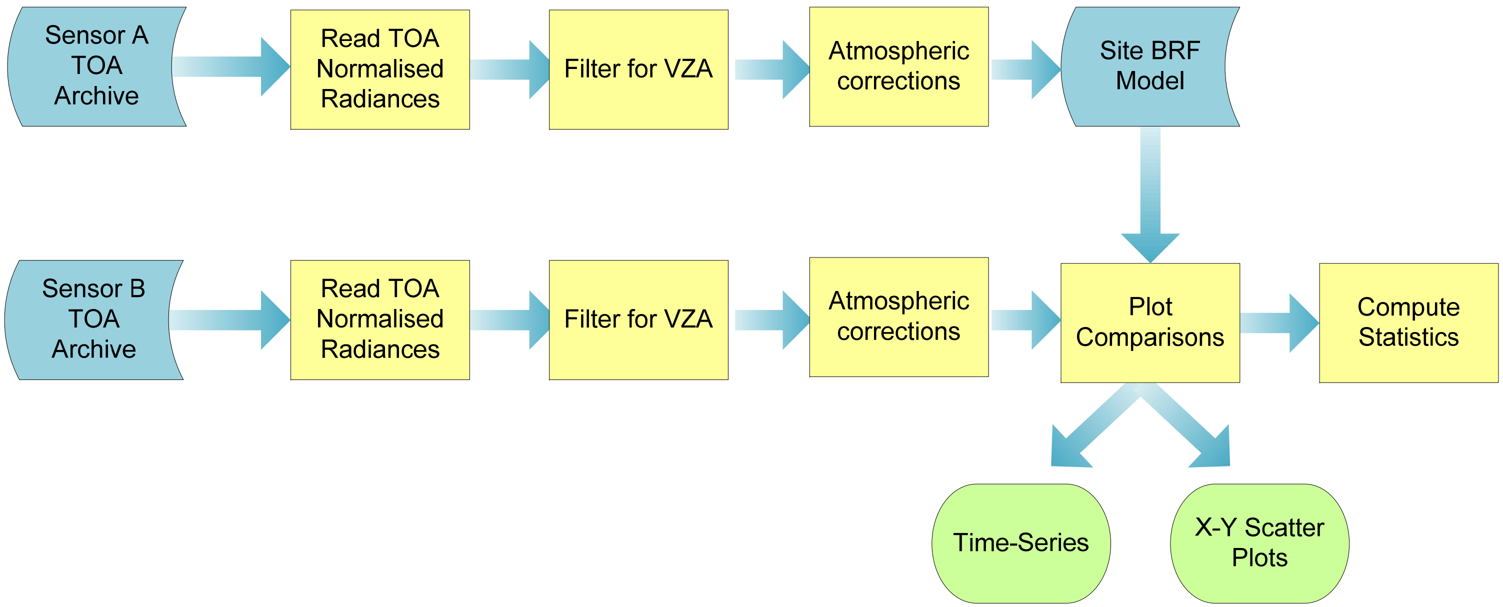

Extends range of possible cross-calibrations

- Sensors at different overpass times – e.g. EOS-A/ENVISAT
- Sensors where no direct comparisons possible – e.g. AATSR/ATSR-2

Atmospheric adjustments needed where bands are not coincident

Site BRF Model

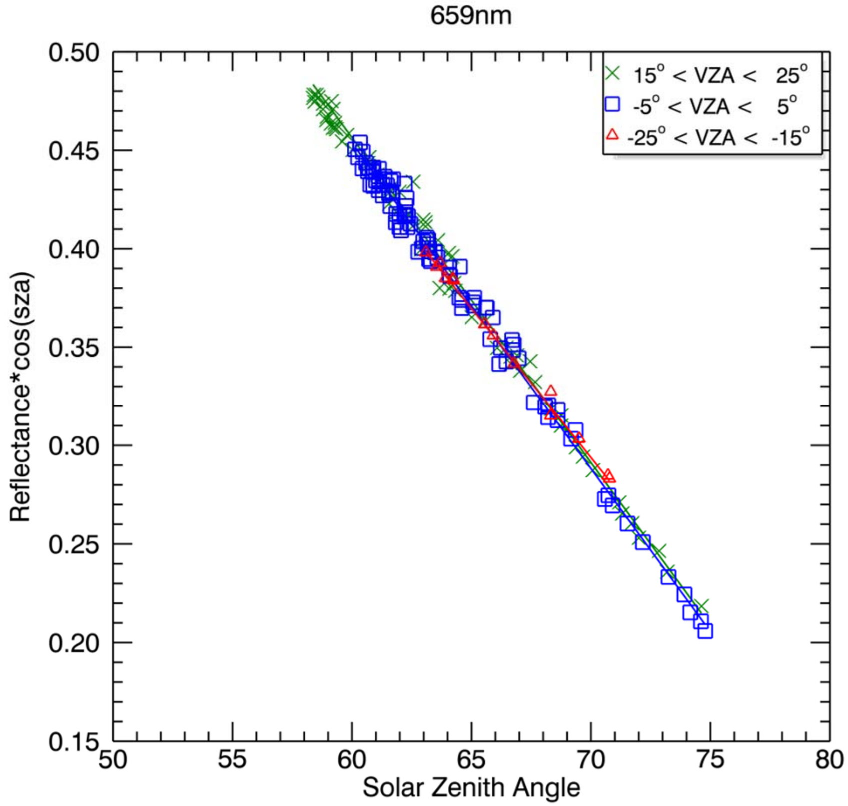

DOME-C 660nm

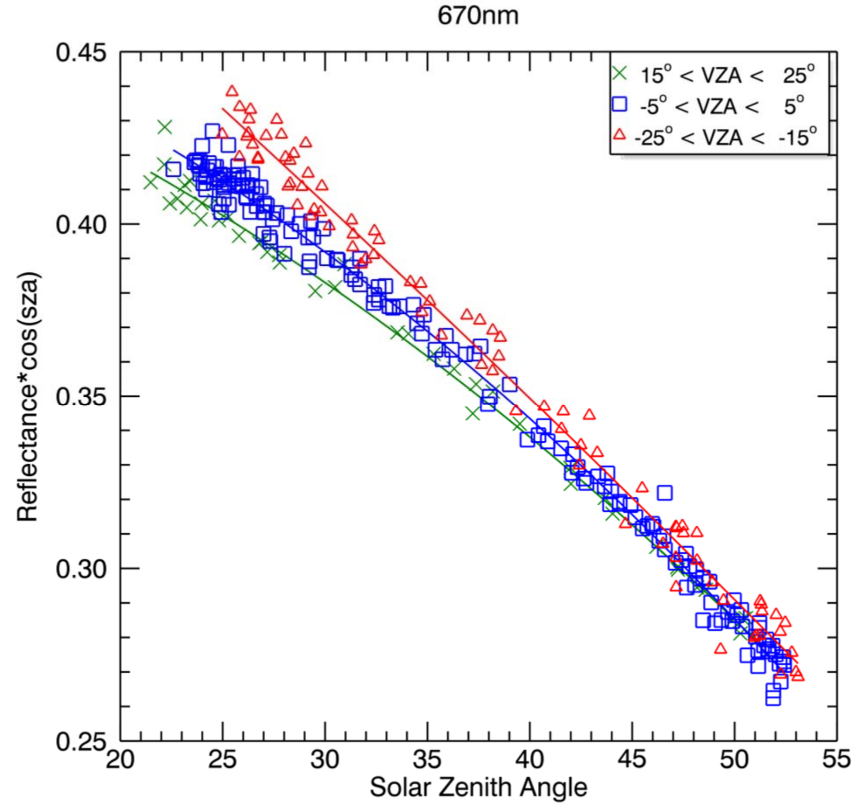

Sudan-1 660nm

Corrections for Rayleigh, O_3 and H_2O applied before fitting model

MERIS vs. AATSR BRF

Using BRF model provides more comparisons

Results are in agreement with direct comparisons

Improvements to MERIS cloud screening could reduce scatter

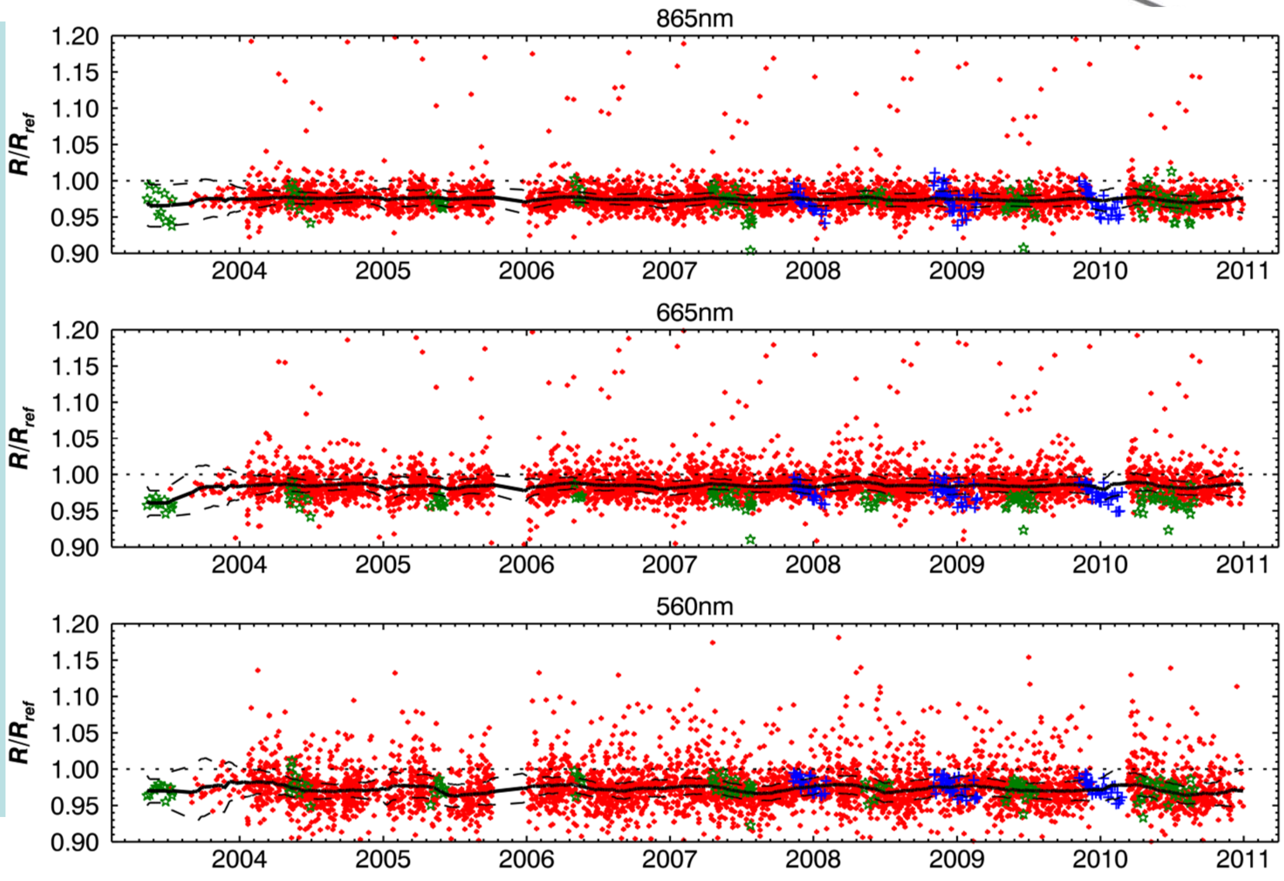

MODIS-A vs. AATSR BRF

Direct comparisons between MODIS-A and AATSR are not possible due to orbit differences

Differences between Desert and Dome-C are apparent – due to spectral variation in site reflectance

Improvements to cloud screening, spectral corrections should reduce differences

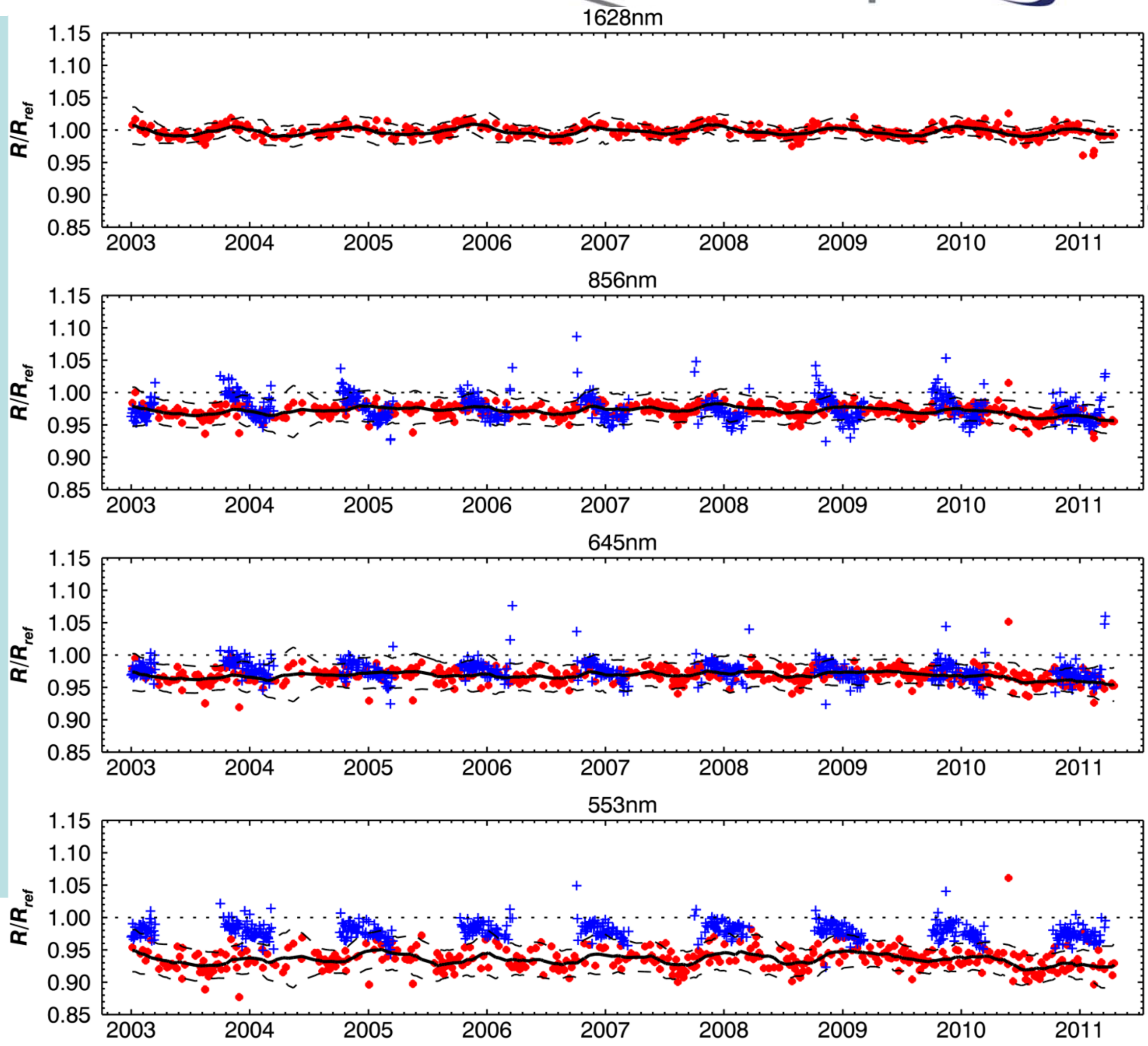

Intercomparison summary
Adjusted for estimated spectral errors

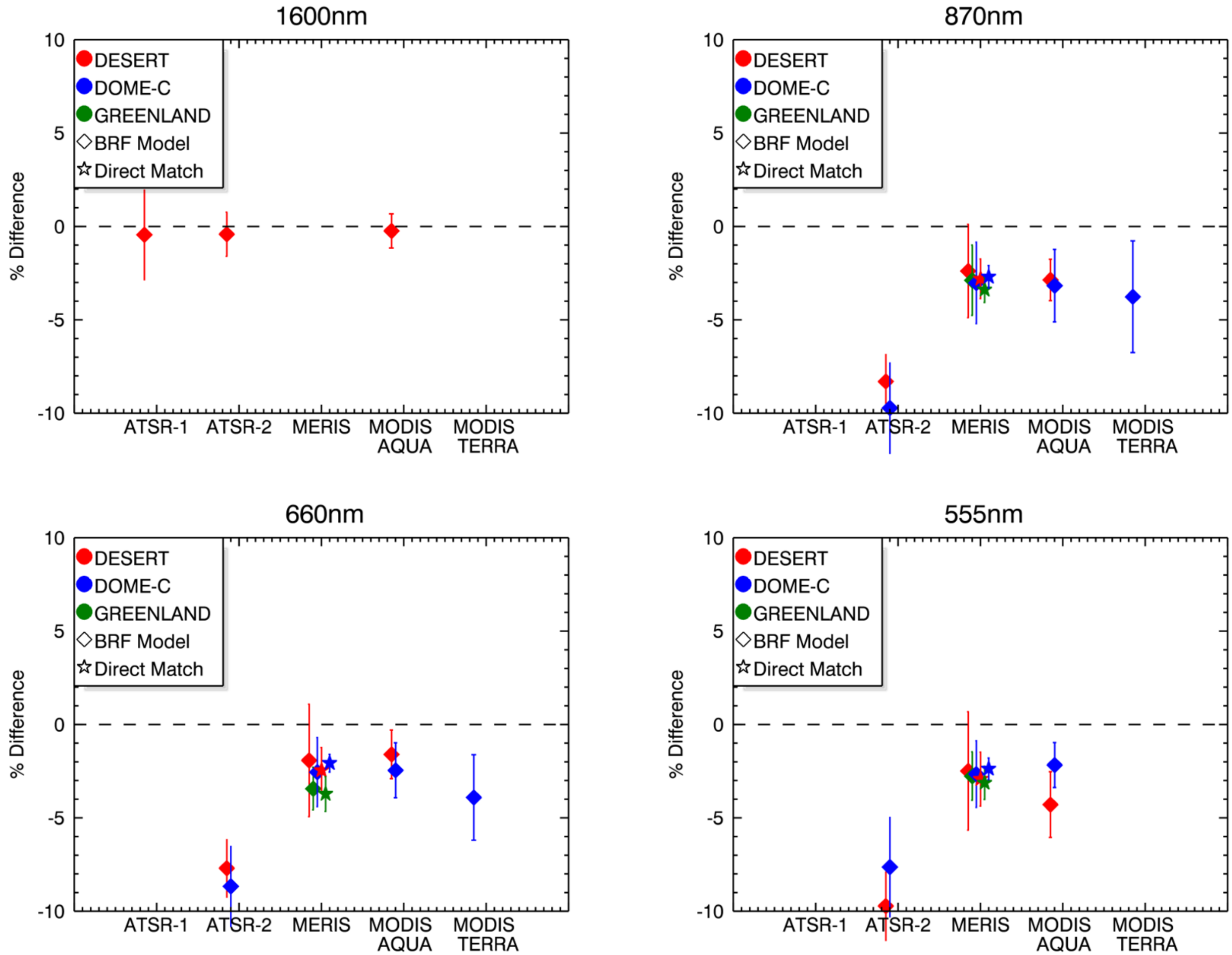

Key Issue to Address

Surface BRF model

- Most models are tied to sensor acquisitions – hence not an absolute calibration method
- Sensors on Sun synchronous orbits do not cover complete geometric space
- CNES BRF model for Libya-4 site (based on Synder model and Parasol data) has been made available – to be implemented for AATSR comparisons.

Spectral Differences

- Can give 5% bias if unaccounted for – even for small differences in bands
- Can be correlated with geometric effects – i.e. optical depth vs. sun zenith angle.

Uncertainties due to spectral differences

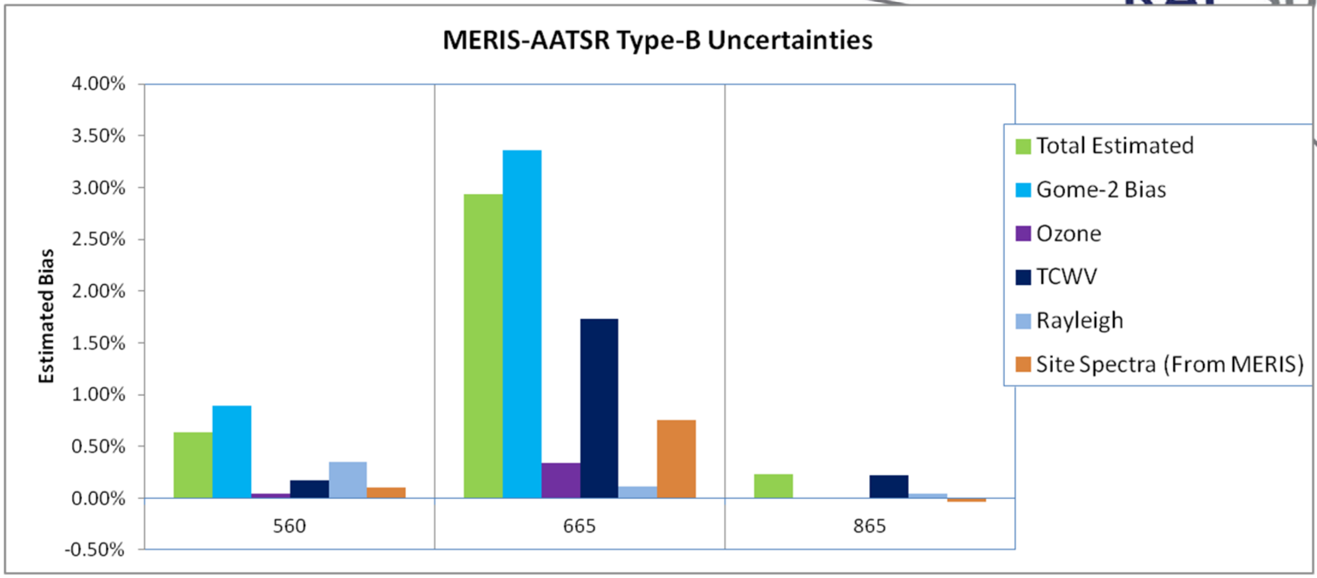

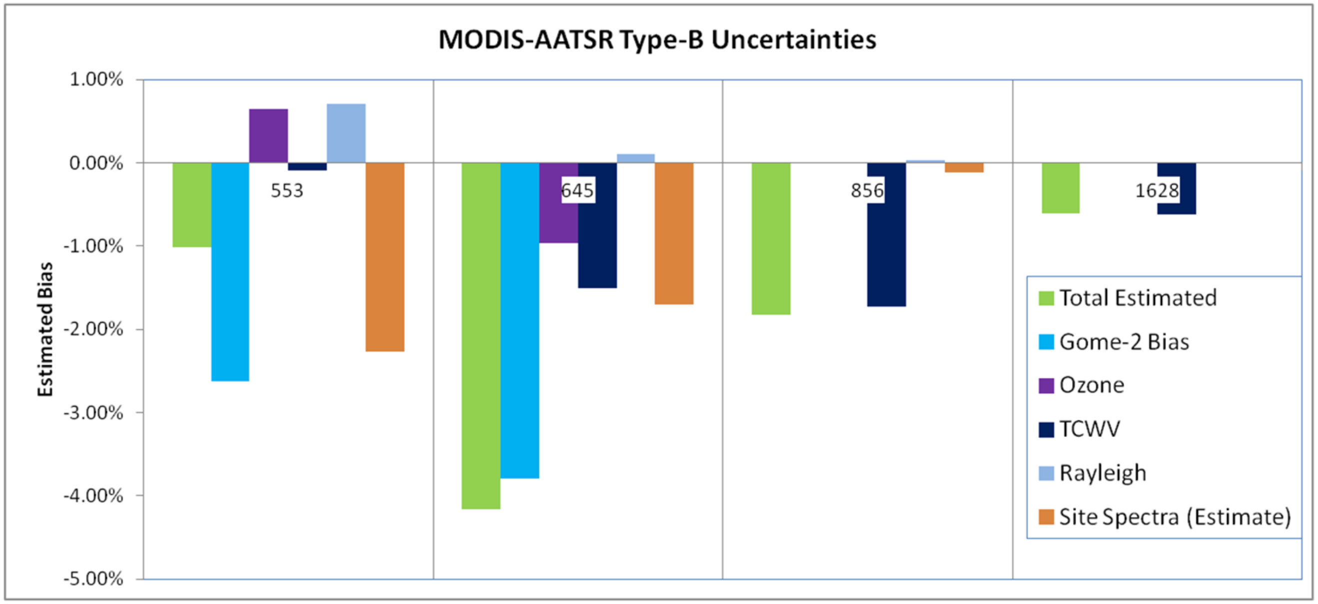

Intercomparisons via spectrometers

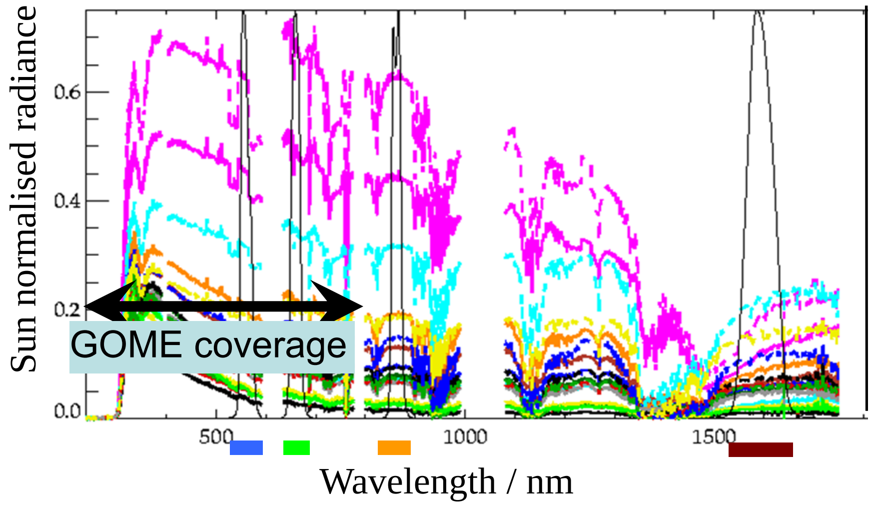

AATSR / SCIA / GOME spatial coverage

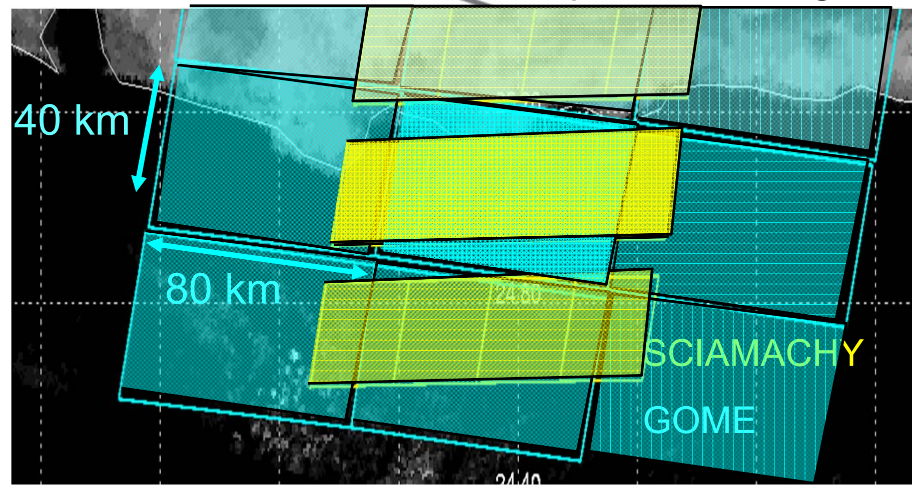

- Inter-comparison requires
  - *Spectral* averaging of SCIA/GOME
  - *Spatial* averaging of AATSR/ATSR-2
- GOME & SCIA pixels not same size or coincident, therefore
  - Perform comparison for accurately co-located GOME/ATSR-2
  - Average SCIA to give scene comparable to GOME; compare to properly averaged AATSR
  - Associate nearest GOME/SCIA pixels to allow cross platform comparison; accept “noise” due to scene variation (time difference).

AVHRR/3 vs. AATSR (via GOME-2)
(1 orbit, 30/05/2007)

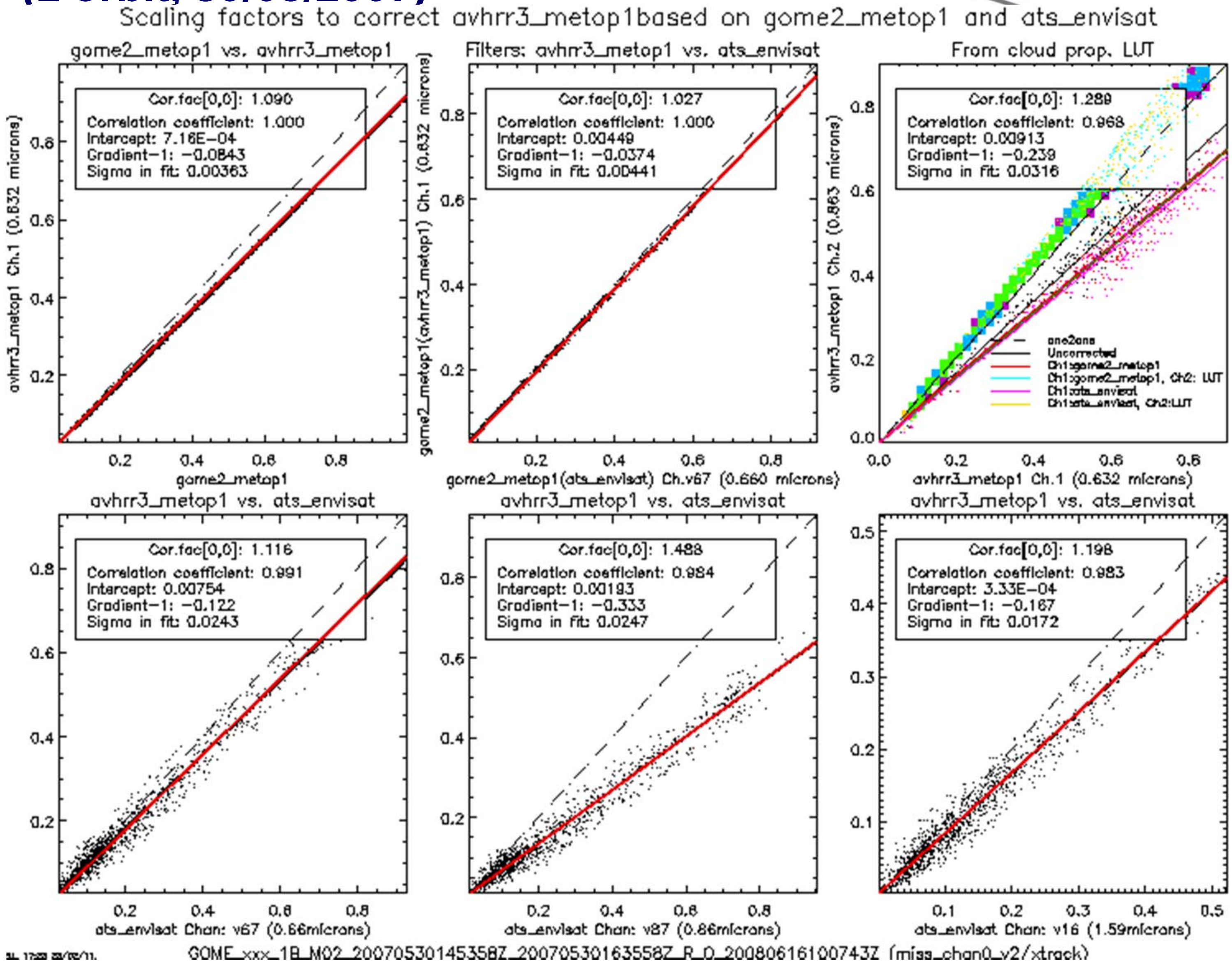

Spectrometers

GOME-2 Over Libya-4

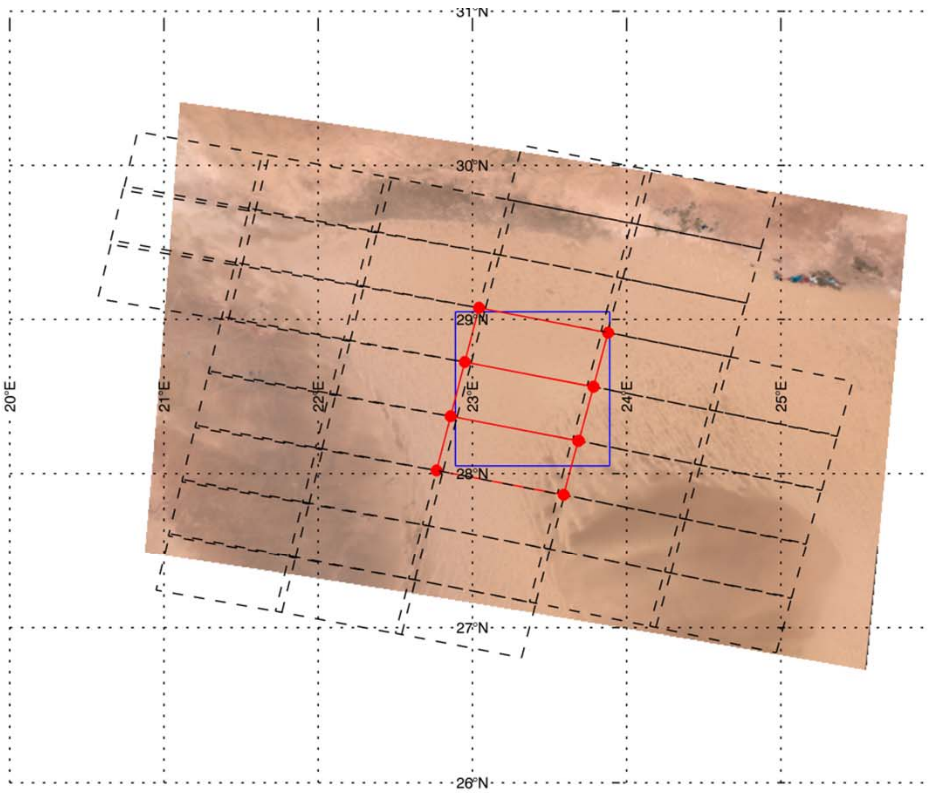

Good temporal coverage
Spatial resolution within Libya-4 site
Spectral range up to 800nm
Co-registered with METOP-AVHRR

SCIA Over Libya-4

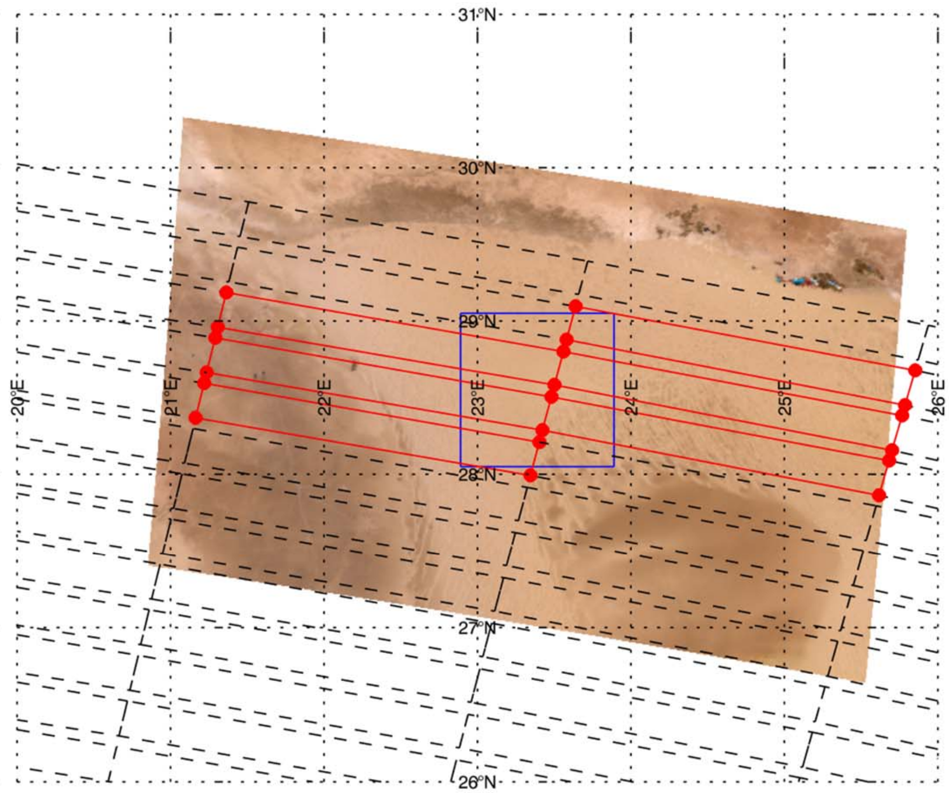

Poor temporal coverage (for Nadir)
Spatial resolution larger than site
Spectral range up to 2000nm
Co-Registered with AATSR/MERIS

GOME-2 Extractions over Libya-4

- METOP GOME-2 orbital L1 products from EUMETSAT
  - Jan-2007 to present (up to 2025 expected)
  - At Issue 4.0 on BADC
  - Latest version Issue 5.3 – to be ingested

- Extractions performed for channels 3 (400-600nm) and 4 (600-800nm) pixels within ±2ºLon, ±1.5ºLat of site centre.
  - No spectral or spatial averaging – data are at native resolution
  - Spectral sampling (0.11-0.22nm) and resolution (0.24-0.53nm) dependent on wavelength
  - Channels 1 (240-315nm) and 2 (310-403nm) not extracted for this analysis

- ERS-2 GOME-1 Data are also available for 1996-2005
  - Data quality?

Libya-4 Geometry

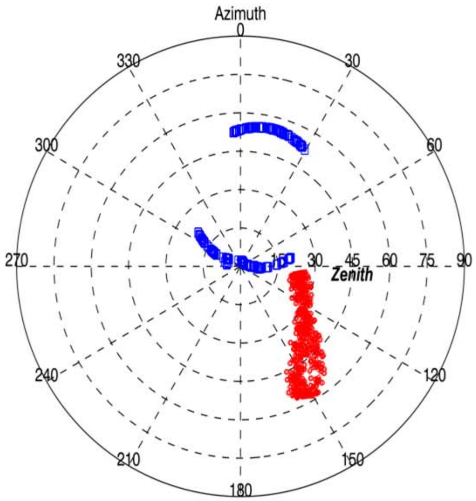

AATSR

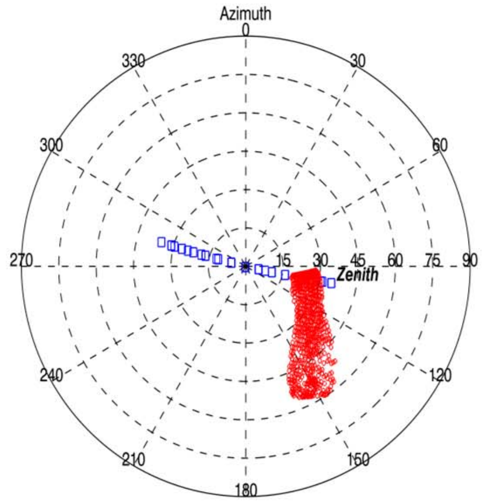

MERIS

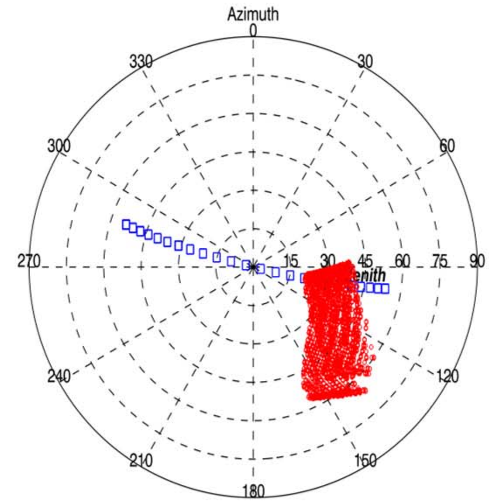

GOME-2

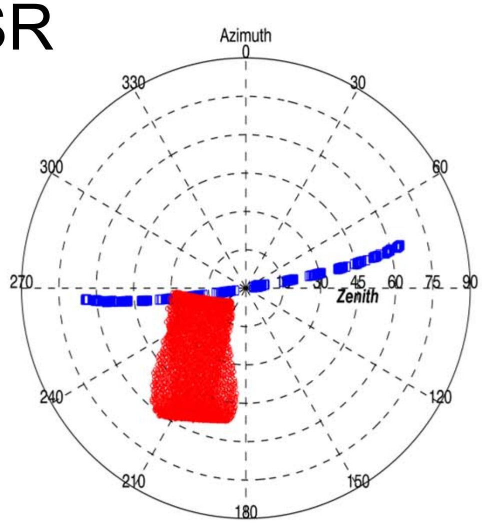

MODIS-A

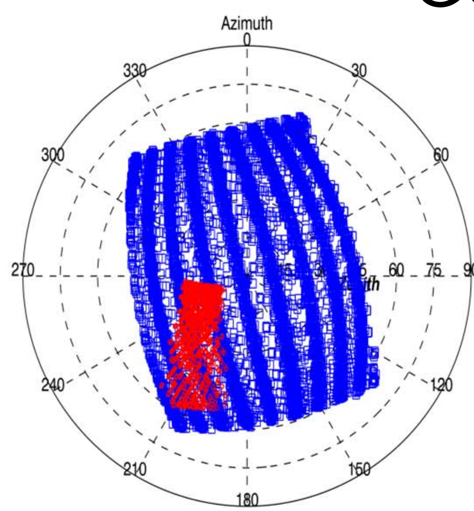

PARASOL

Libya-4 Site Spectra

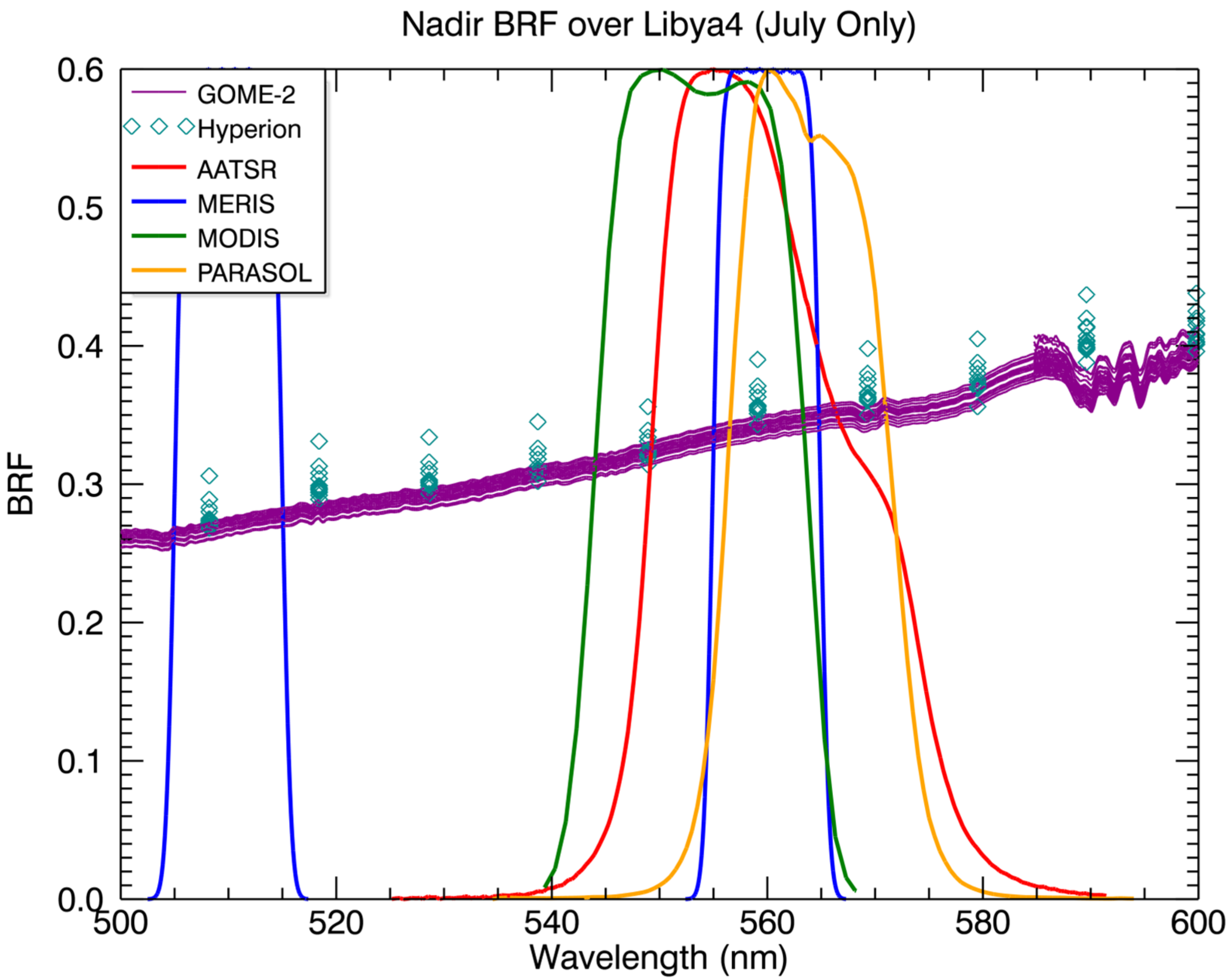

500-600nm

Atmos mainly scattering + O_3

Libya-4 Site Spectra

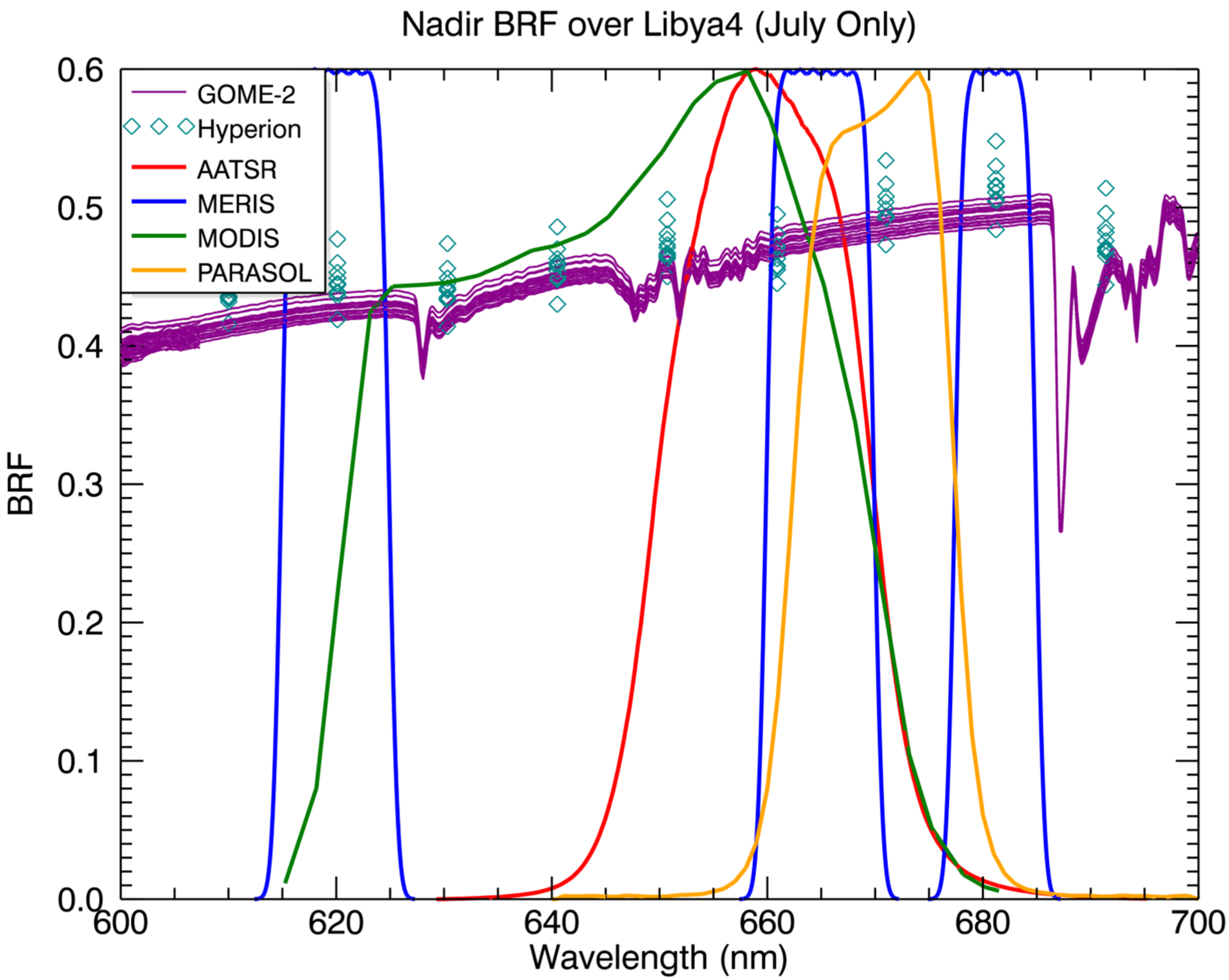

600-700nm

Atmos mainly scattering + O_3 +H_2O

Intercomparison – AATSR vs. MERIS Time Series

Gome-2 Spectra Integrated over sensor spectral bands

Reference is Meris 559nm, 666nm and 681nm

AATSR drift correction applied no bias correction

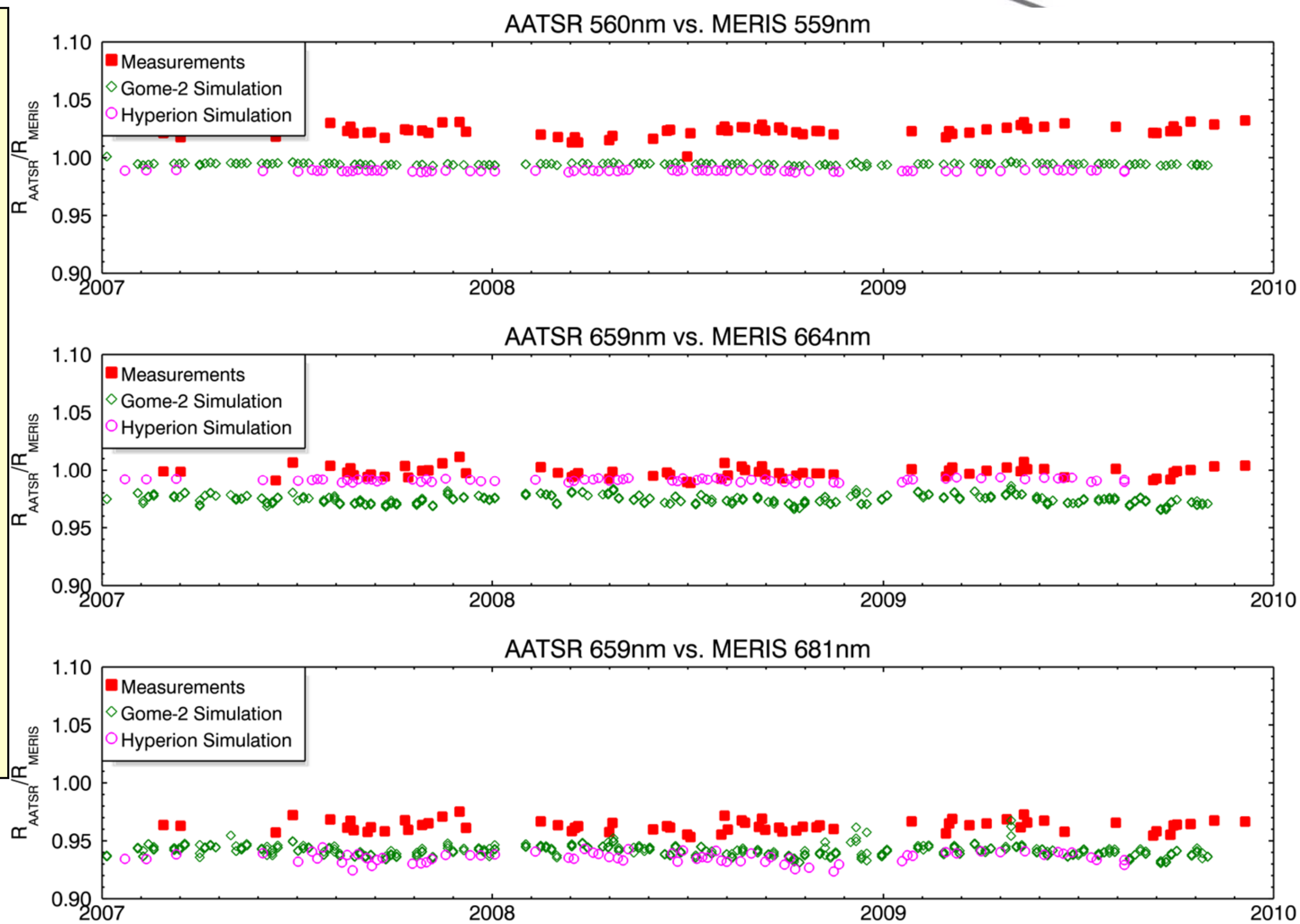

Intercomparison – AATSR vs. MERIS Time Series

Gome-2 Spectra Integrated over sensor spectral bands

Reference is Meris 559nm, 666nm and 681nm

AATSR drift correction + 3% bias adjustment applied

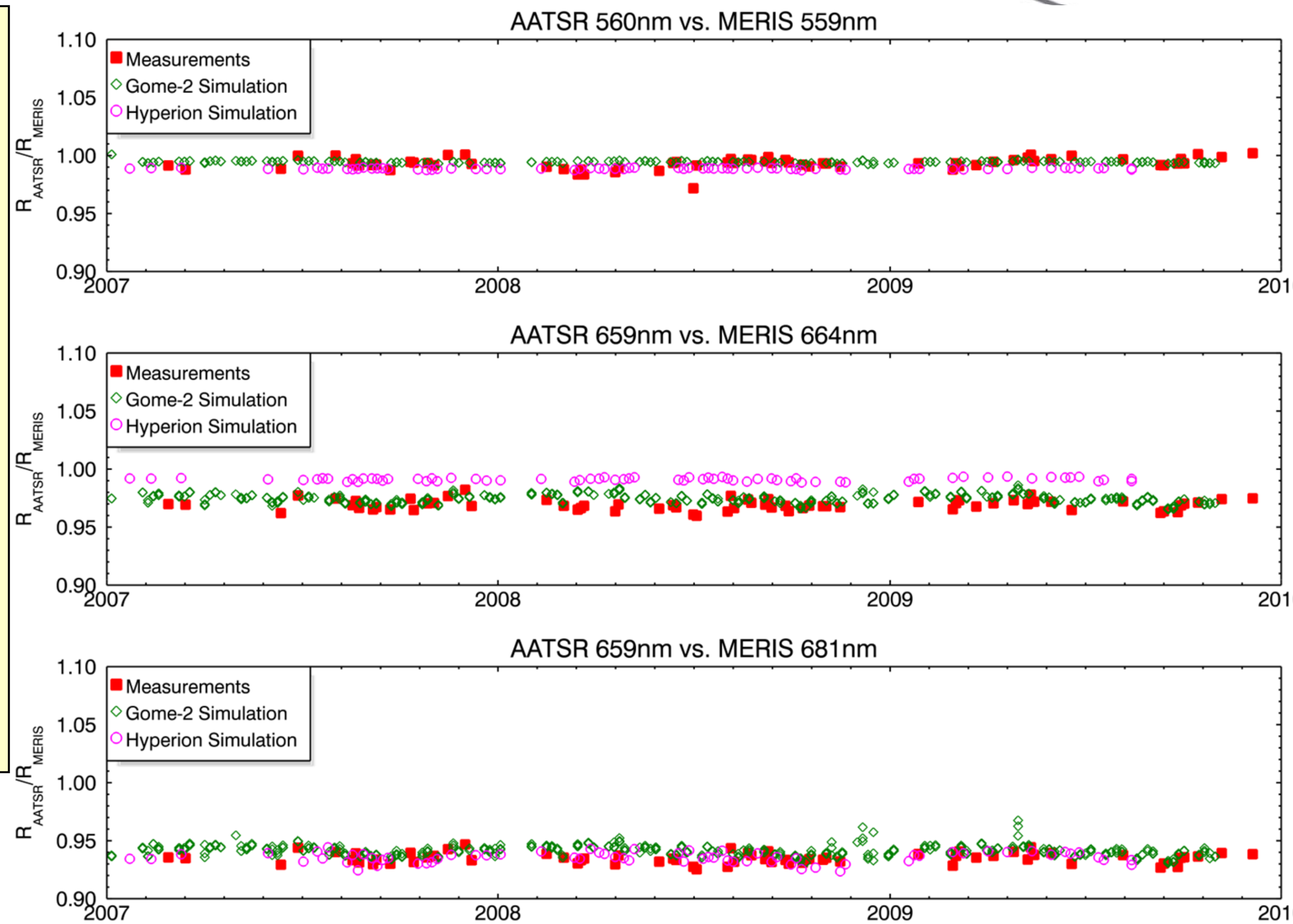

Intercomparison – AATSR vs. MERIS vs. View Angle

Gome-2 Spectra Integrated over sensor spectral bands

Reference is MERIS 559nm, 666nm and 681nm

$35^{O} < SZA < 45^{O}$

AATSR drift correction + 3% bias adjustment applied

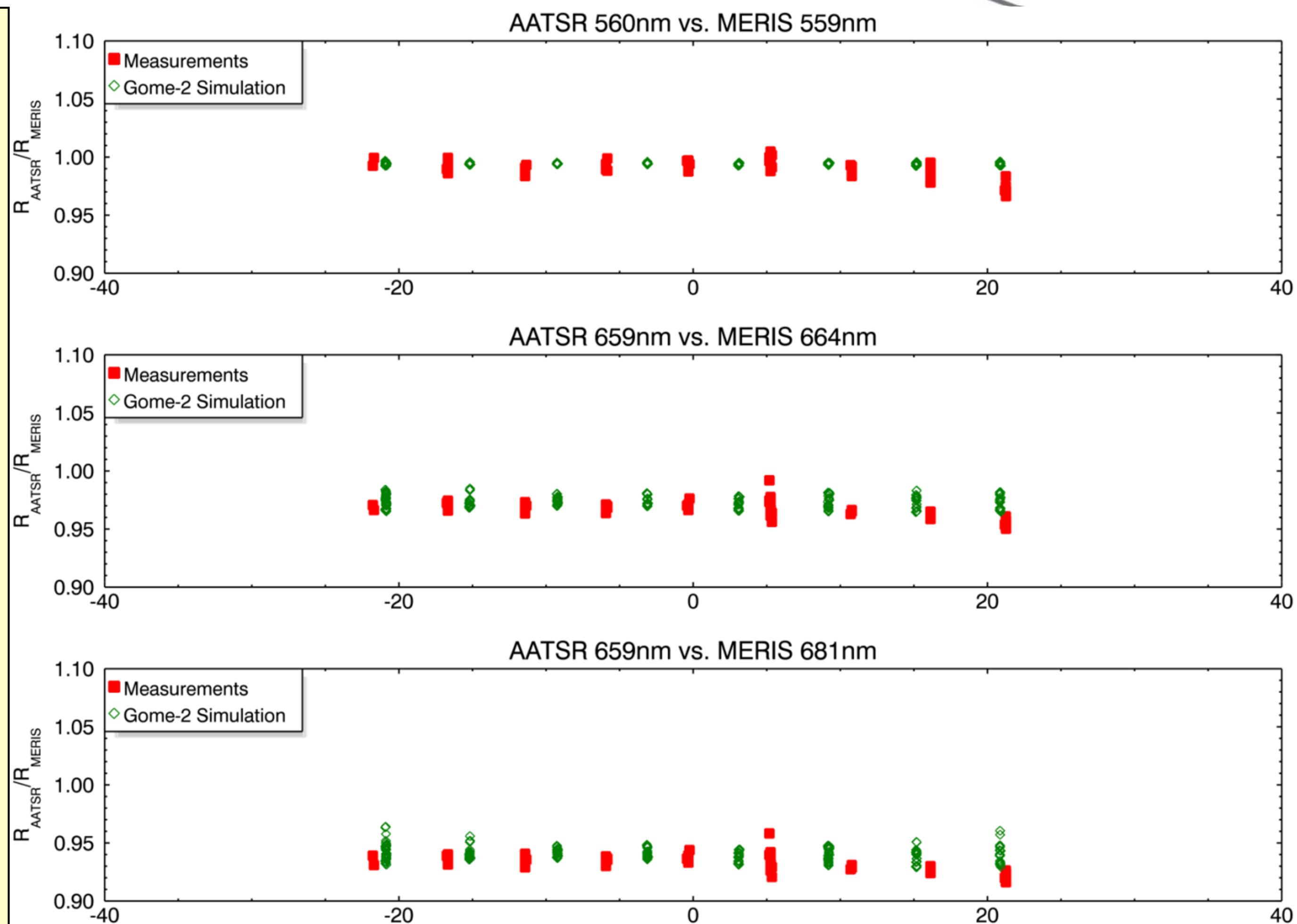

Intercomparison – MODIS vs. MERIS Time Series

Gome-2 + Hyperion Spectra Integrated over sensor spectral bands

Reference is MERIS 559nm, 666nm and 681nm

MODIS geometrically corrected to MERIS

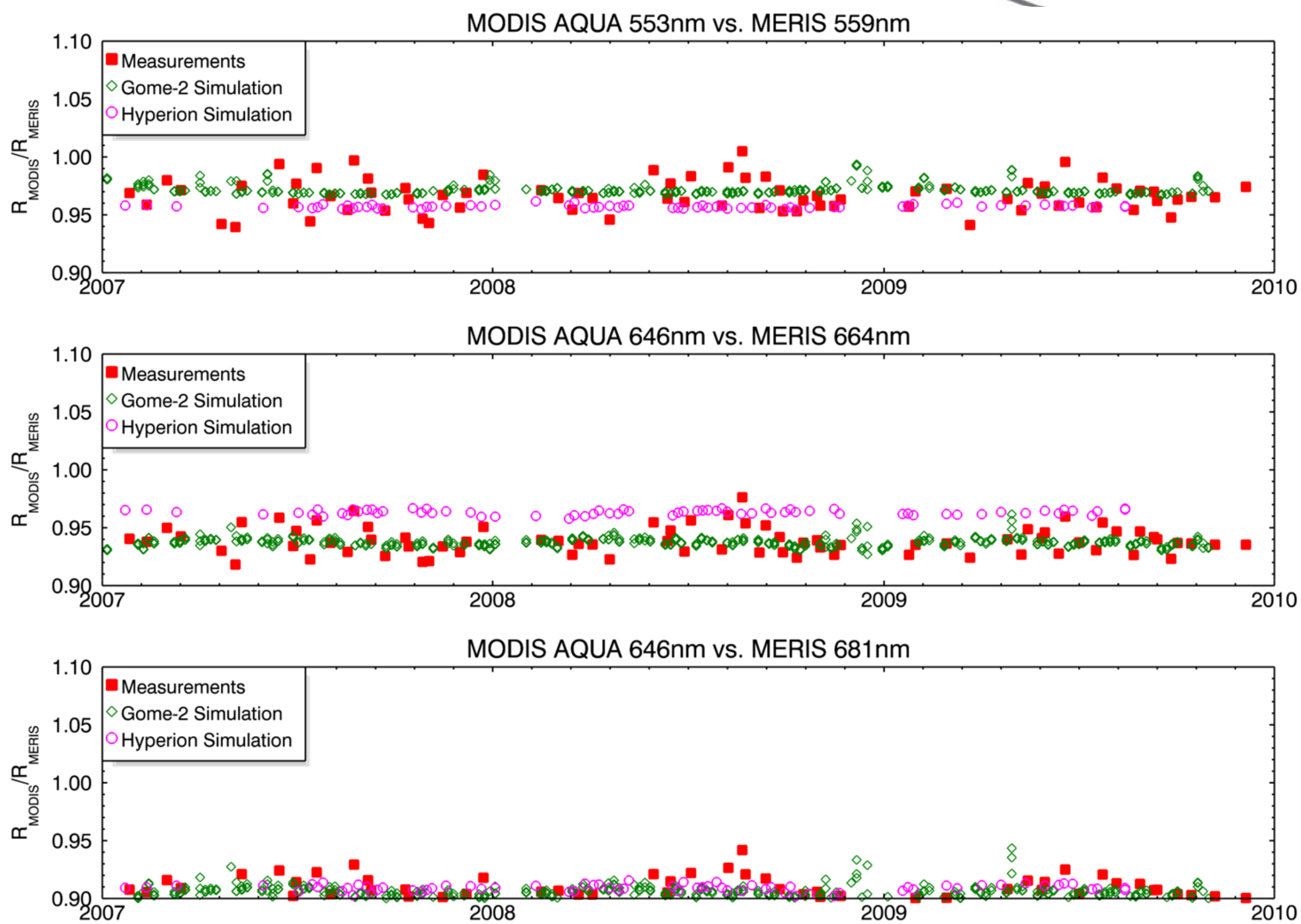

Intercomparison – MODIS vs. MERIS Vs. View Angle

Gome-2 Spectra Integrated over sensor spectral bands

Reference is MERIS 559nm, 666nm and 681nm

$35^{O} < SZA < 45^{O}$

MODIS geometrically corrected to MERIS

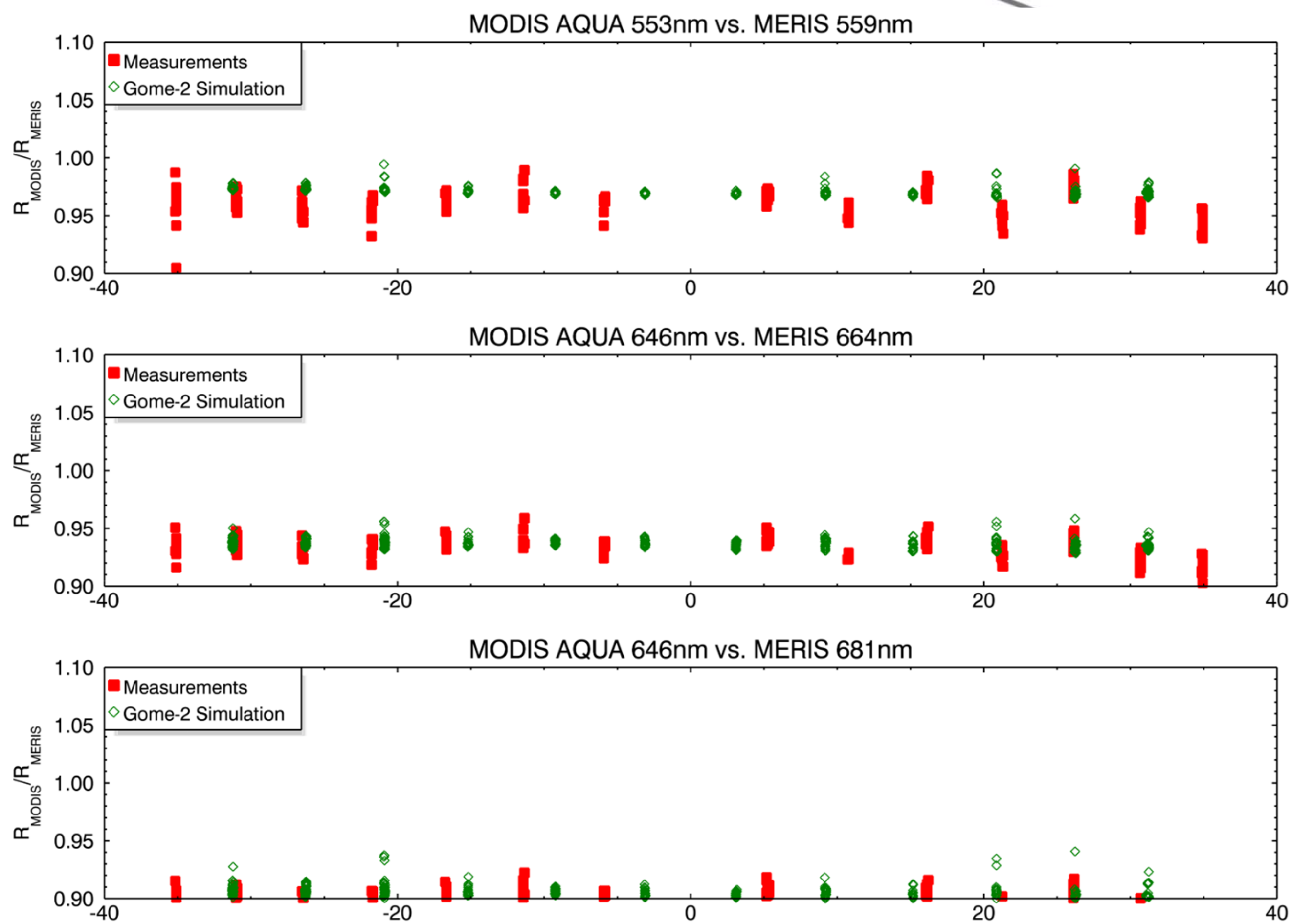

ATSR-2 Calibration

Current version as processed (V2.2 table)

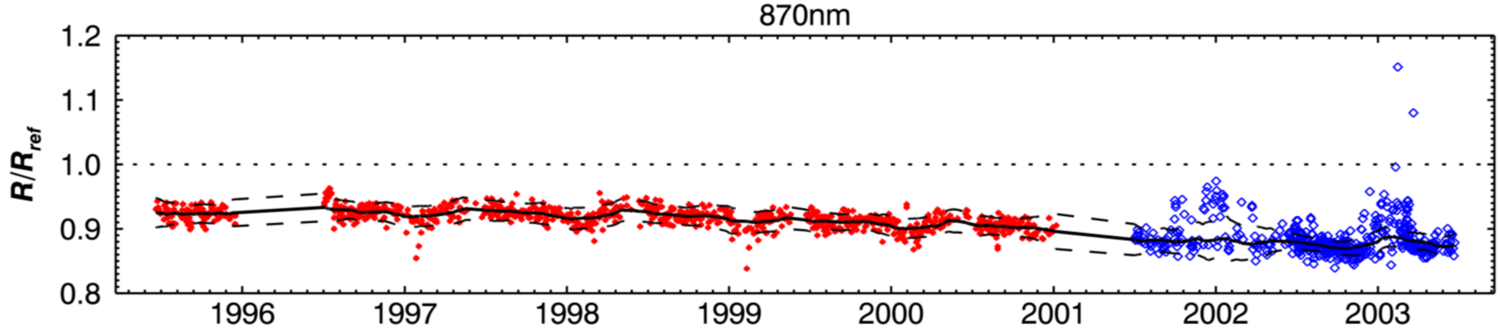

VISCAL Smoothing

- Loss of ERS-2 gyros affected the pointing of the VISCAL wrt. Sun leading to many poor acquisitions of calibration signal (blue points).

- Filtering by using a histogram test enables only ‘good’ measurements to be used for calibration (red points).
  - Not implemented for first version of .E1 product

- Next reprocessing will incorporate this filtered table

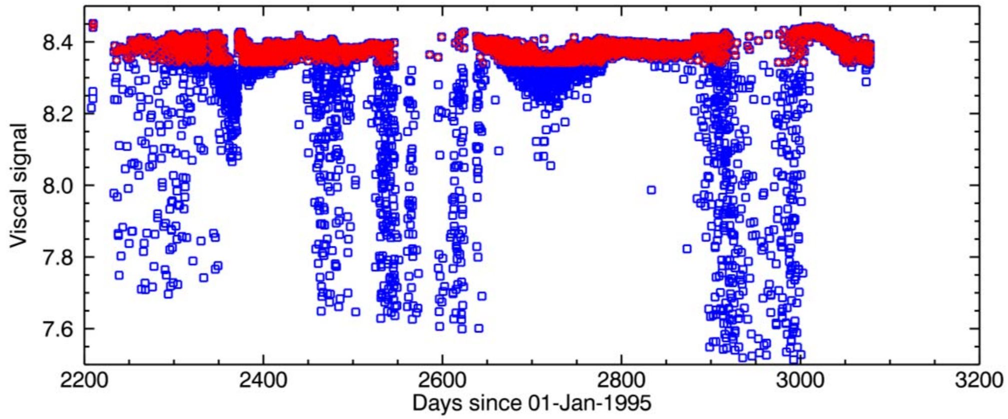

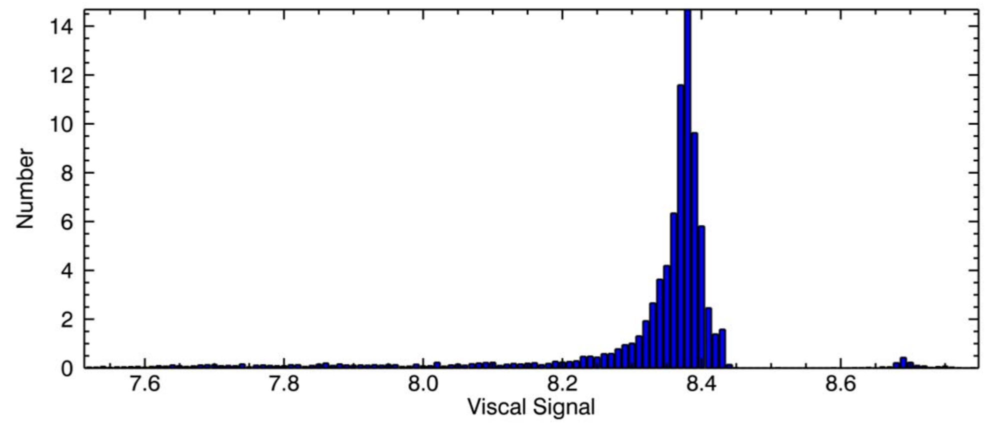

ATSR-2 Calibration

Current version as processed (V2.2 table)

Recalibrated using filtered table (V3.0)

Filtered, Drift corrected + Adjusted to AATSR (V4.0)

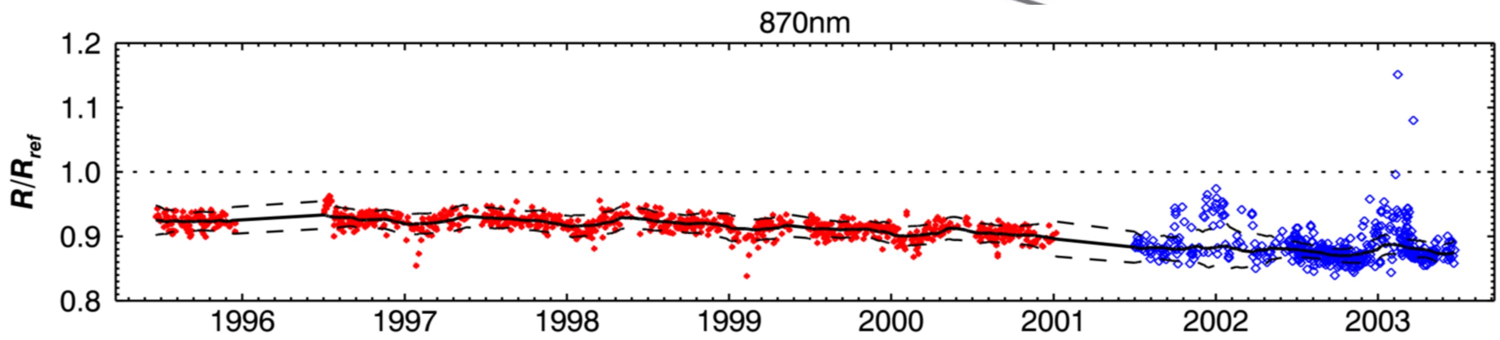

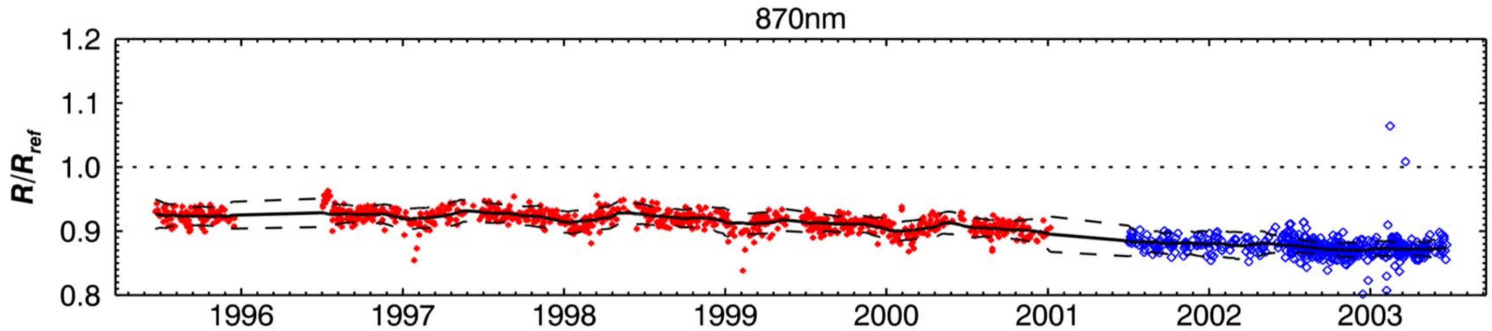

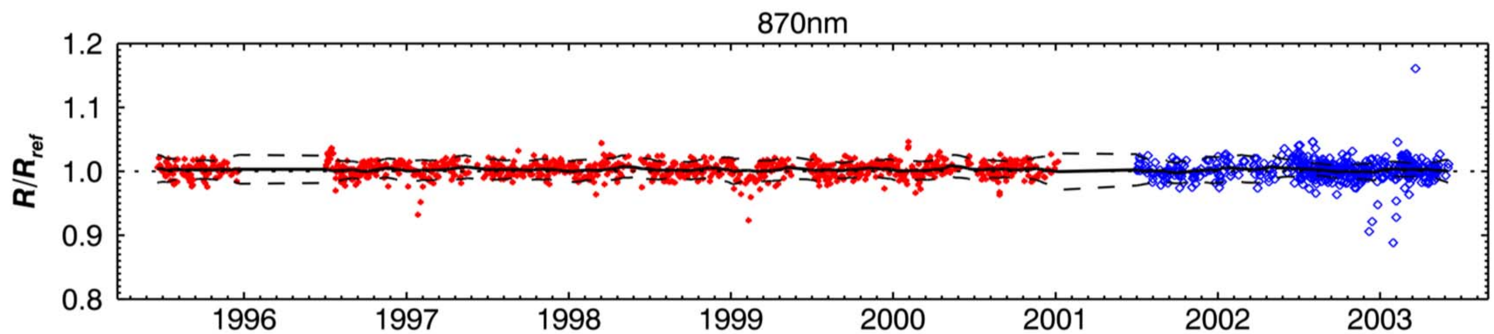

ATSR-1

- Drift table has been generated to account for new calibration coefficients and Sun-Earth distance

Original Calibration

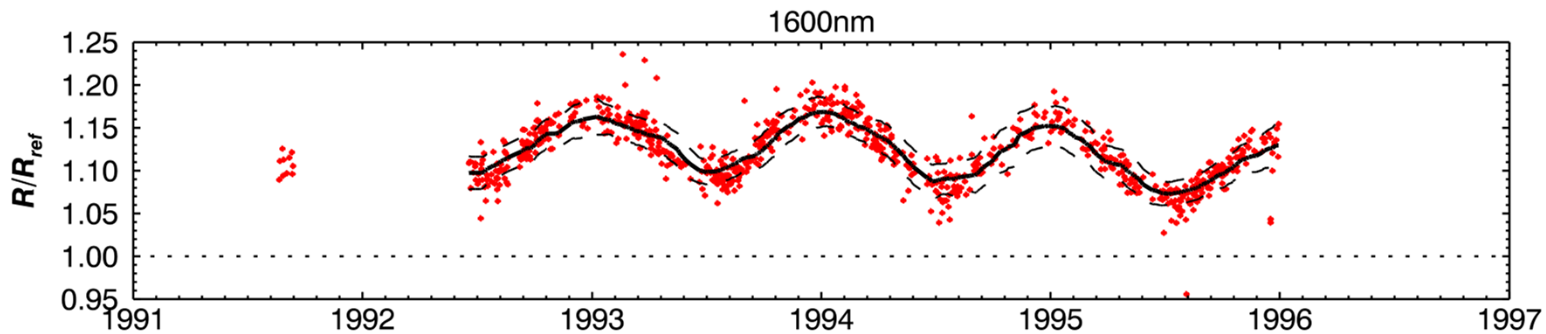

Revised Calibration

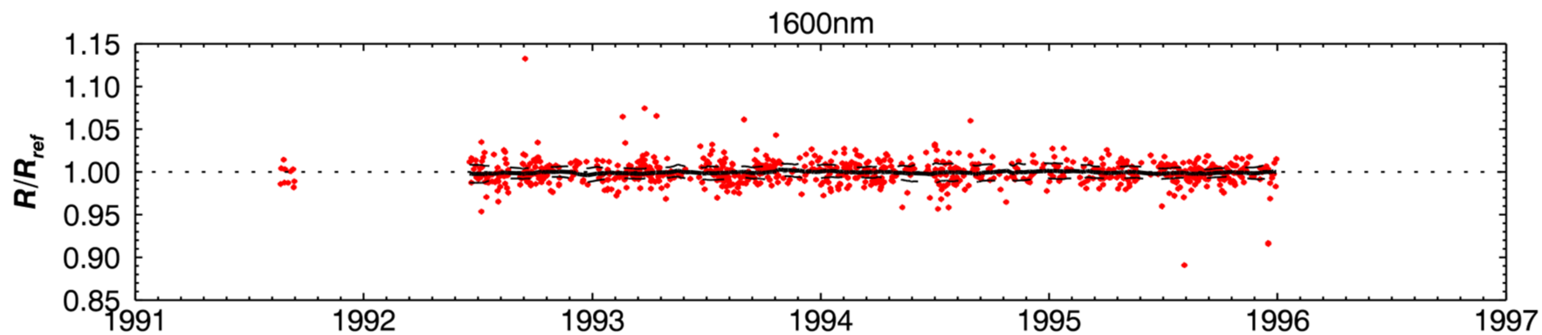

ATSR-1 relative to AATSR – corrected for directional effects

ATSR-1

- First release of the ATSR-1 L1b products in ENVISAT format (.E1 files) uses the following calibration

```
aav16_nad[scans][i]  = (int)((double)aav16_nad[scans][i] * cor1 + cor2)
```

```
cor1 = 1.95664, cor2  = -1.85314
```

- Calibration did not account for two factors
  - ATSR-1 calibration does not allow for variation in Sun-Earth distance.
  - ATSR-1 UBTs are scaled in range 0-10000 which is inconsistent with scale of cor2

- Calibration coefficients have been recomputed taking into account these factors so

```
cor1 = 1.778615, cor2  = 0.0
```

Libya-4 BRF - Uncorrected

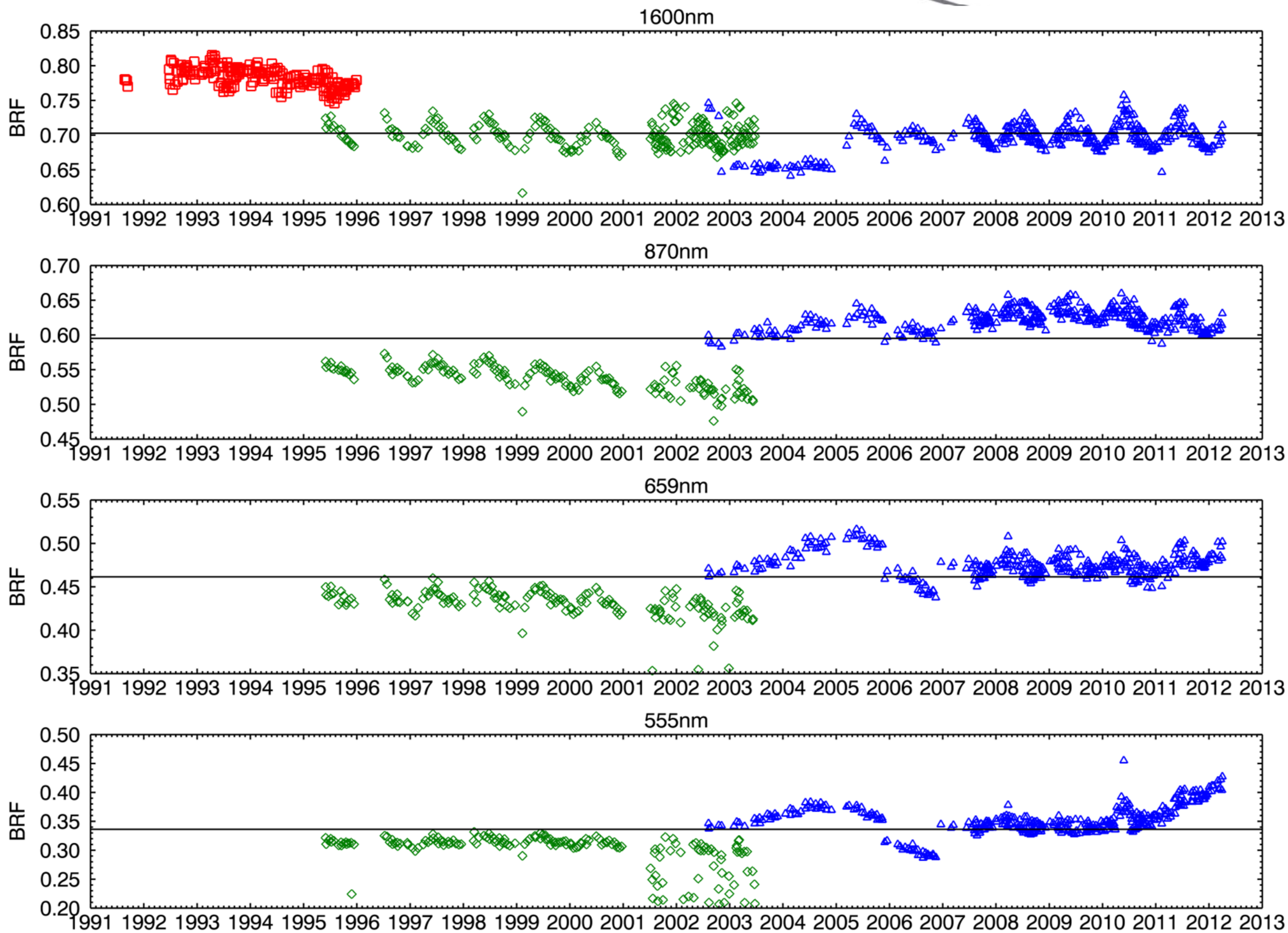

Libya-4 BRF – With Corrections (full swath)

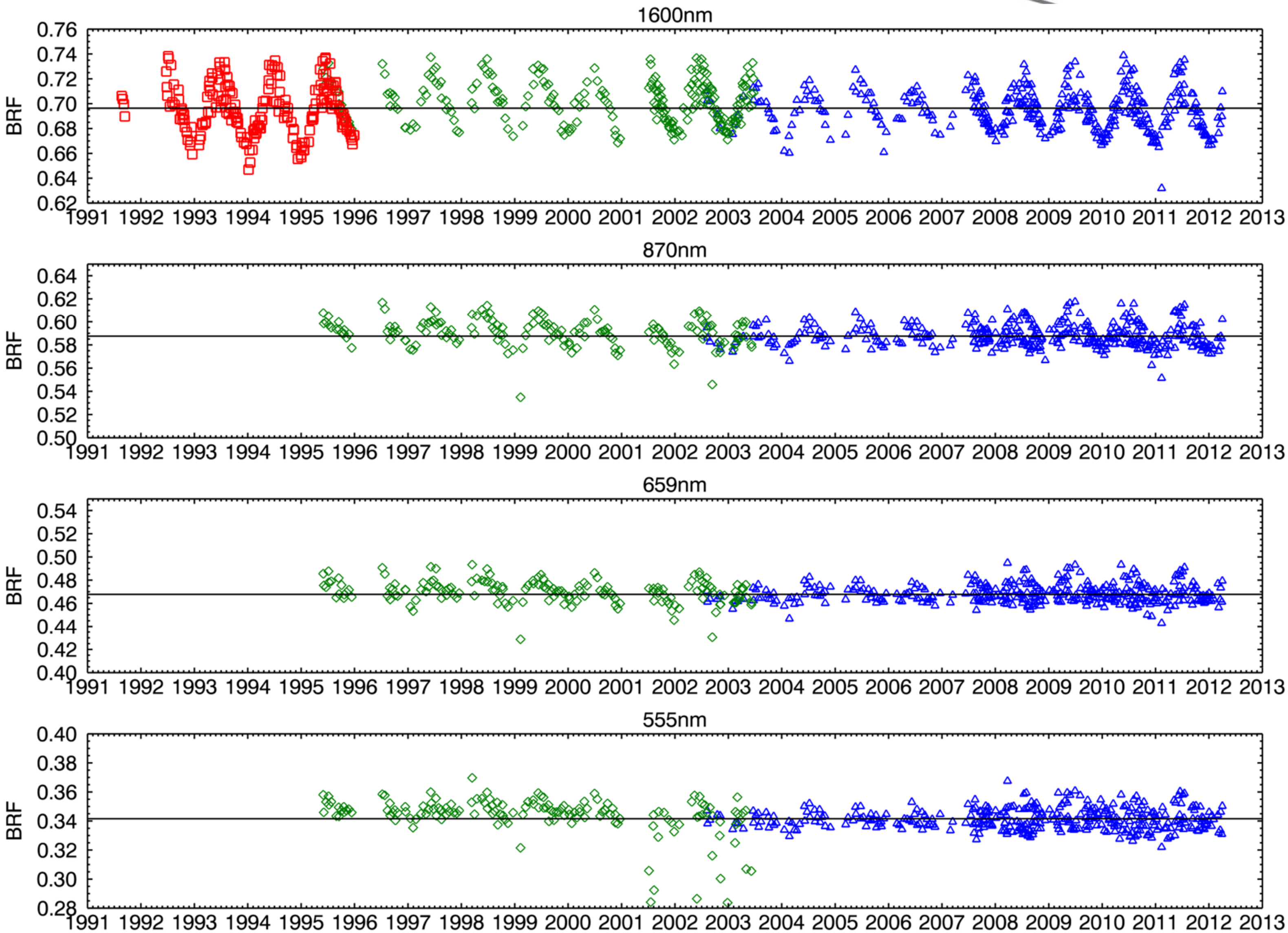

Libya-4 BRF – With Corrections (view < 7.5º)

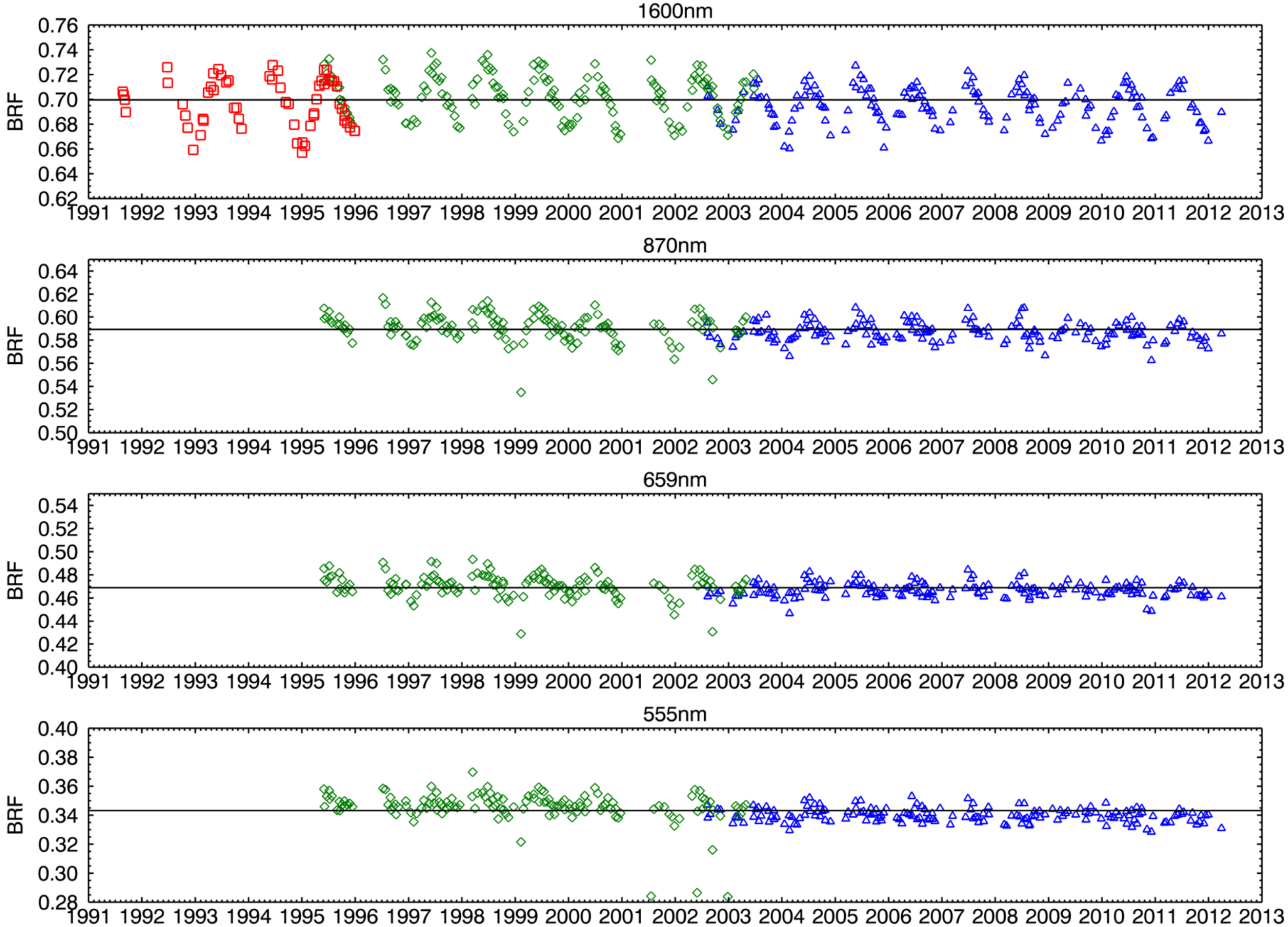

3rd Reprocessing calibration checks

- Site data extractions are performed for trial month V2.1 products as per v2.0 but this time straight from full orbit L1b products in archive.
  - I.e. No child product needed
- Top of atmosphere reflectances and BTs are obtained for all calibration sites used for previous long term calibration analysis and saved to netcdf files.
- Results from reprocessed data are compared against original v2.0 extractions
  - As per original v2.0 product
  - Corrected for drift and bias
- Comparisons show that reprocessed data are in line with expected results
- Analysis to be performed for full mission once data becomes available on archive.

AATSR – Trial Month

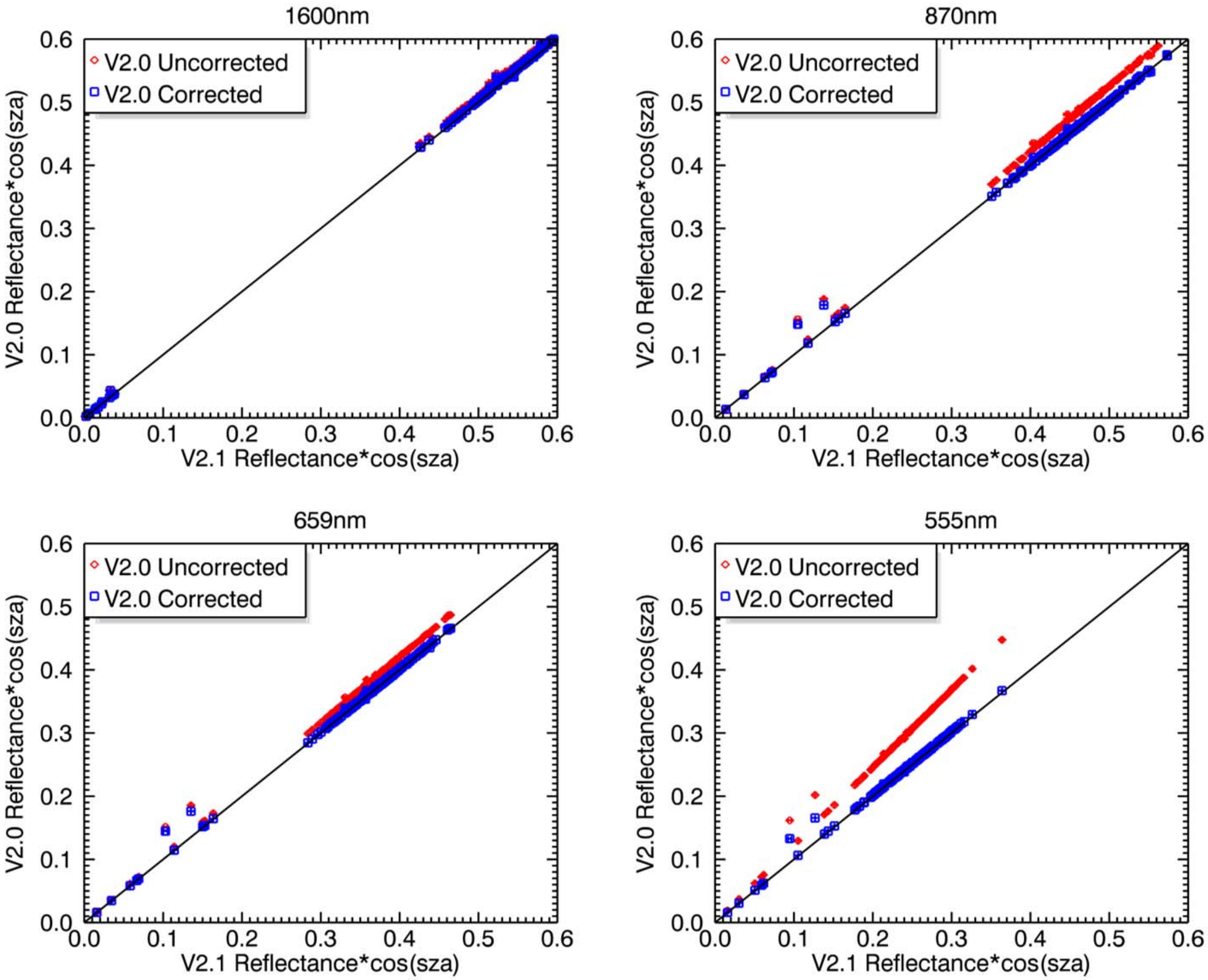

Slight negative bias compared to expected values - to be investigated once full mission processed

Band	Mean V2.1/V2.0	Stdev V2.1/V2.0	N samples
1600nm	0.99168753	0.019933087	160
870nm	0.99478095	0.029124789	162
659nm	0.99294823	0.028790752	162
555nm	0.98968705	0.028335044	162

ATSR-2 – Trial Month

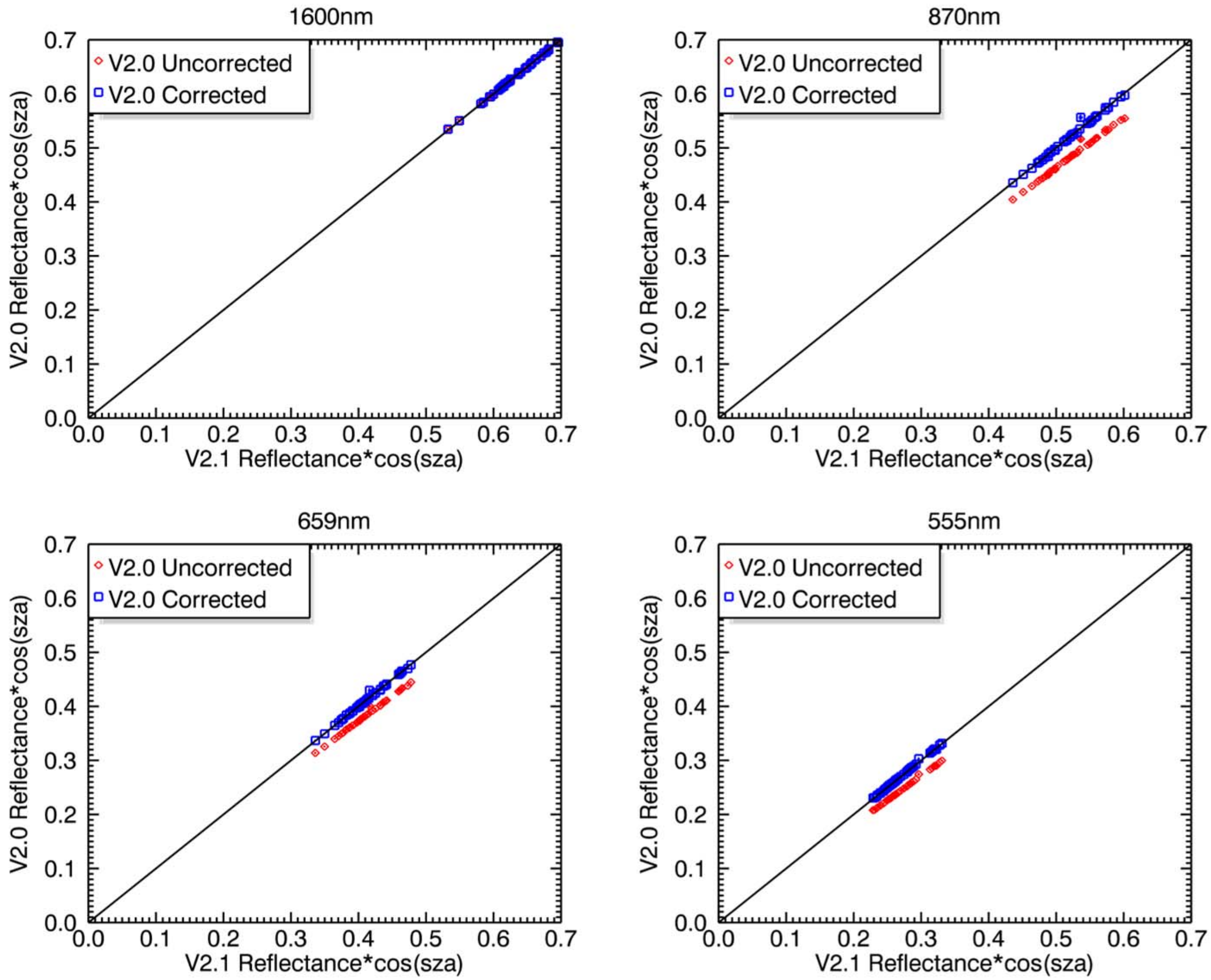

Band	Mean V2.1/V2.0	Stdev V2.1/V2.0	N samples
1600nm	0.99924240	0.0050003643	41
870nm	1.0014385	0.0064933719	41
659nm	0.99988379	0.0053706799	41
555nm	0.99833581	0.0039791559	41

ATSR-1 – Trial Month

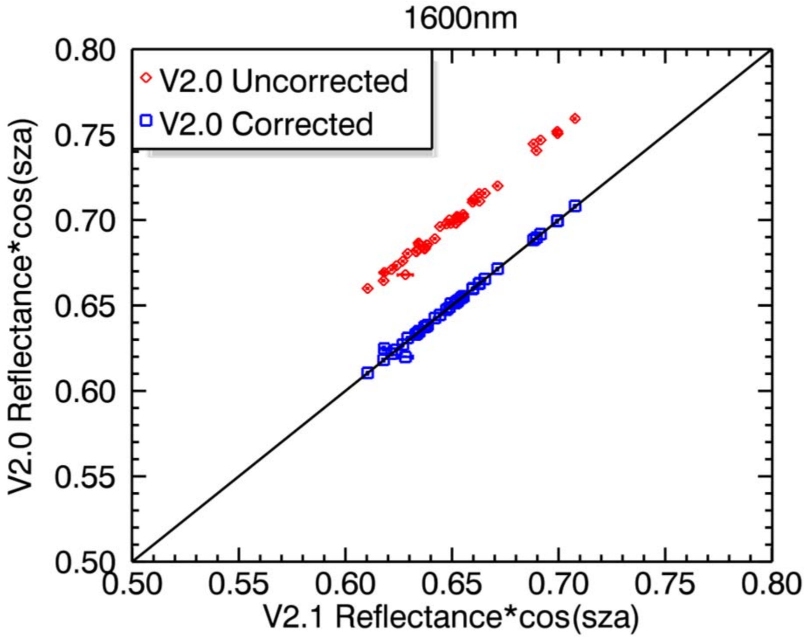

Band	Mean V2.1/V2.0	Stdev V2.1/V2.0	N samples
1600nm	0.99980490	0.0027636131	40

Further Activities

- Preparations for SLSTR
  - S3ETRAC – Sentinel-3 Extraction Tool for Radiometric Analysis and Calibration
    - ATBD describing extraction methodology has been issued and iterated with ESA/CNES
  - Current analysis tools can be adapted for SLSTR
  - Investigate methodologies to be used for new SLSTR SWIR channels
  - Investigate impact on geometric differences between AATSR
- Improvements to cloud detection over deserts
- Implement CNES BRDF model for Libya-4

Further Activities

- Use GOME-2 data (possibly SCIA?) for validating spectral correction factors over Desert and Ice targets to improve the spectral corrections.
  - Extend this for ATSR-2 using GOME-1

- Investigate possible use of ‘dark’ sites other than water

- Investigate impact on spectral differences between AATSR, ATSR-2 and ATSR-1

- Investigate ATSR-1 offset calibration using dark waters.

Geometric Calibration

(A)ATSR Geolocation Model

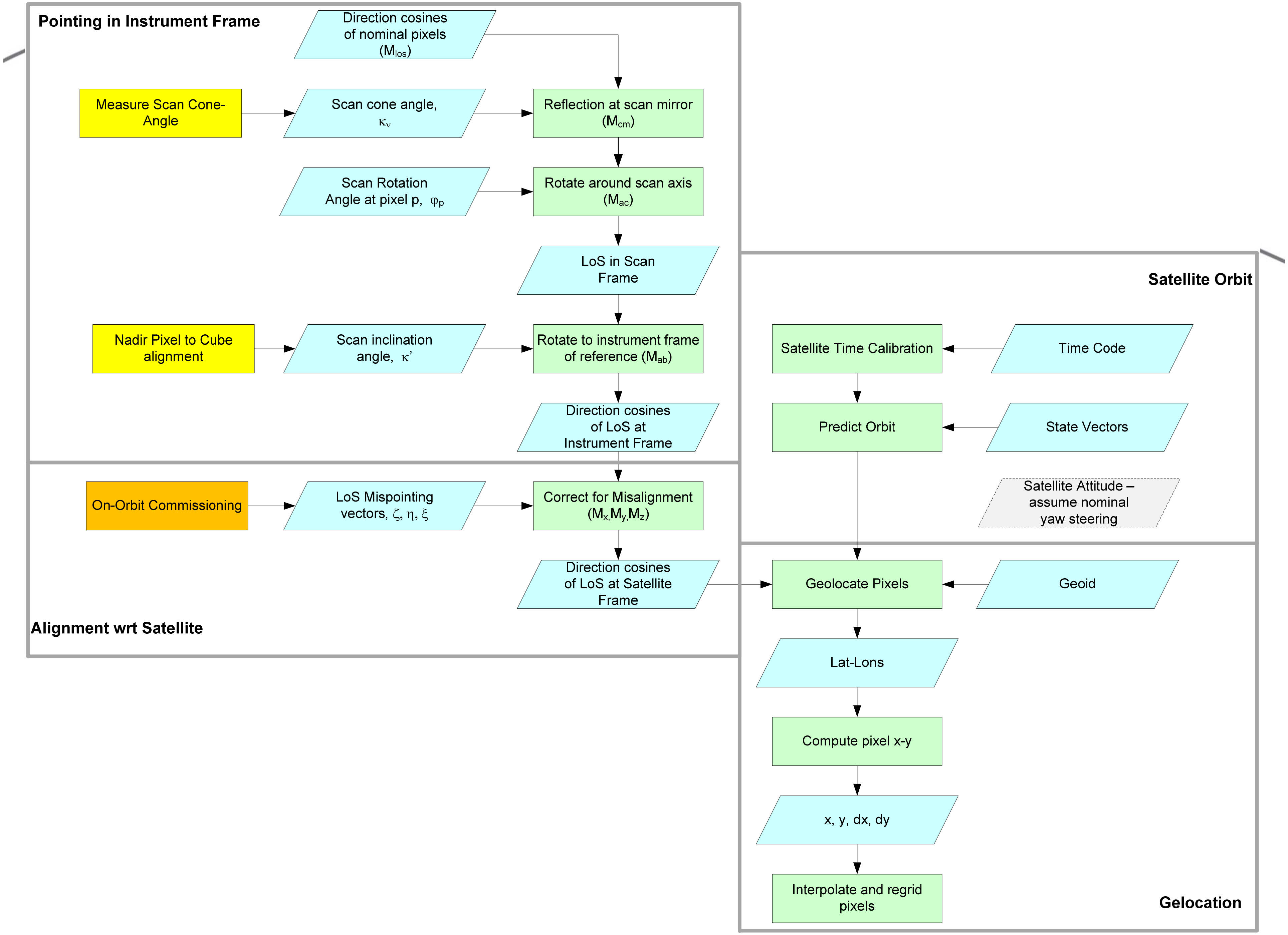

Error Sources

Term	Random	Systematic	Cause(s)	Solution
Regridding	±1km? (Not Gaussian) – depending on input parameters and scan mirror stability	Negligible	(A)ATSR uses nearest neighbour regridding to avoid loss of data!	For most accurate geo-referencing should use ungridded data NOT regridded data.
Geo-location	Dependent on DEM surface and interpolation method	Dependent on DEM	(A)ATSR geo-locates to geoid	Ortho-geolocate pixels to with use of 30m DEM
Satellite Orbit	Negligible	ATSR-1 and ATSR-2 dependent on state vectors Also ERS-2 in zero gyro mode will have high errors	State vectors	ATSR-1 and ATSR-2 should use restituted state vectors – modification to APP needed
Satellite Attitude	Dependent on attitude control stability I.e. ERS-2 after yaw steering failure will have high random errors.	AATSR and ATSR-1 assumed to be OK ERS-2 in zero gyro mode will have high errors	Attitude control stability	Will need external aux files to account for actual altitude and attitude. For ATSR-2 this is already done using Hey files

Error Sources

Term	Random	Systematic	Cause(s)	Solution
Alignment wrt. Spacecraft	Negligible	Assumed constant but could vary around orbit and with season	Measurement error Thermo-elastic distortion	Pre-launch test results. Quantify orbital/seasonal variations using observations over many reference targets.
Scan Cone Angle	Negligible	Assumed constant	Measurement error	Assessment of nadir/forward co-registration
Scan rotation angle for each pixel	NOT Gaussian!	Variable around scan – not consistent over the lifetime of the instrument.	Scan mirror jitter Alignment of encoder Bearing roughness Cogging Torque	Quantify scan dependent biases using observations over many reference targets - assuming all scans are same!

AATSR Pixel Field Of View

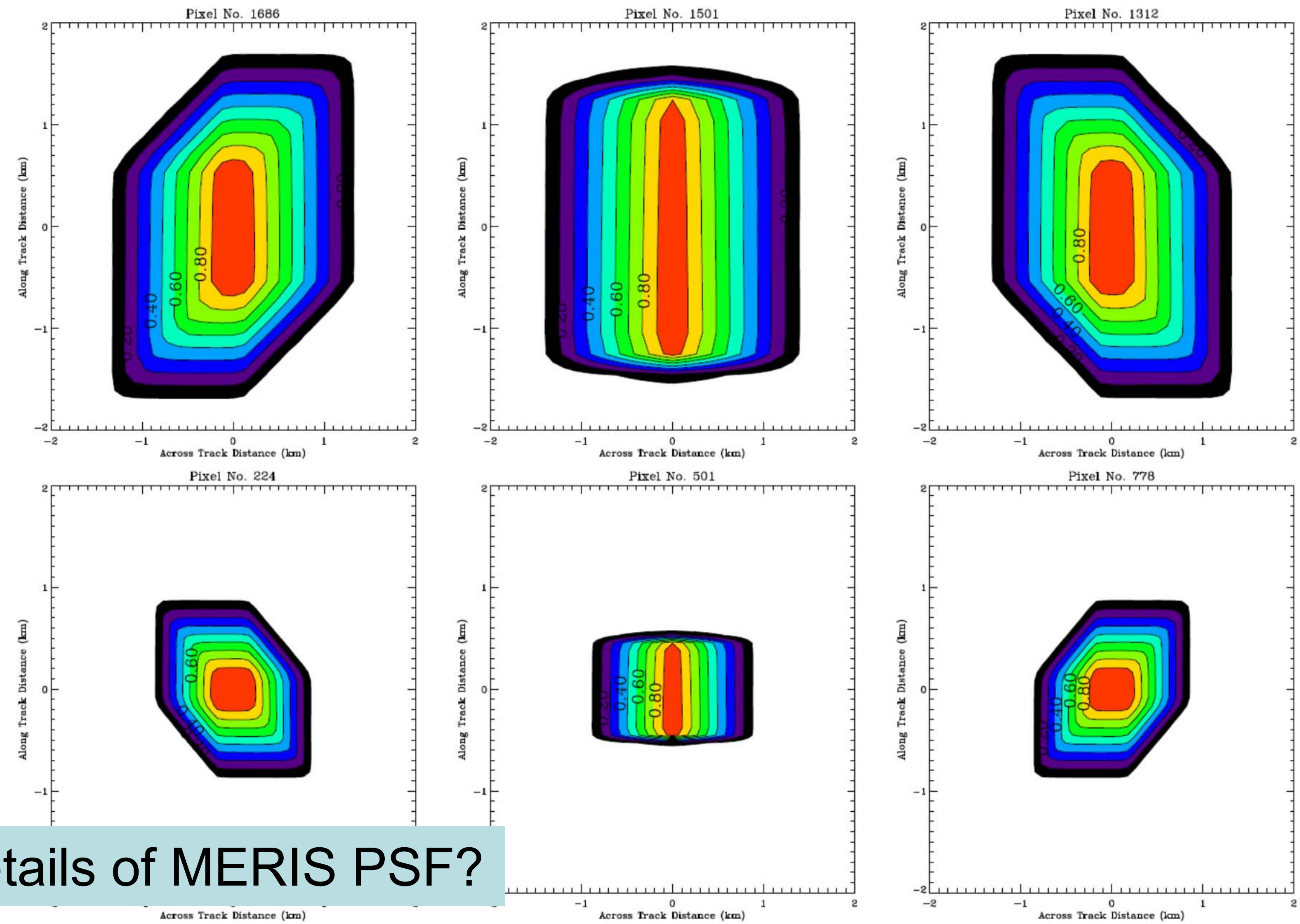

Details of MERIS PSF?

Geolocation / new CH1 (2)
Pixel identification

AATSR

MERIS

ATSR-2 Trial Month Reprocessing Checks

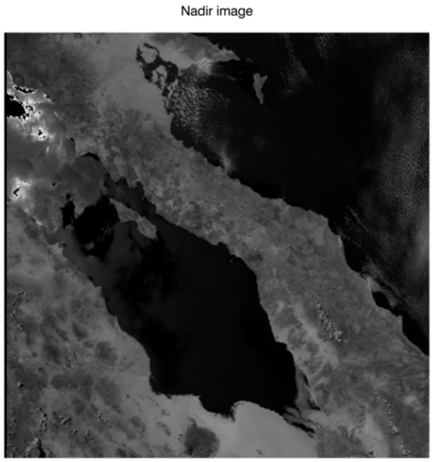

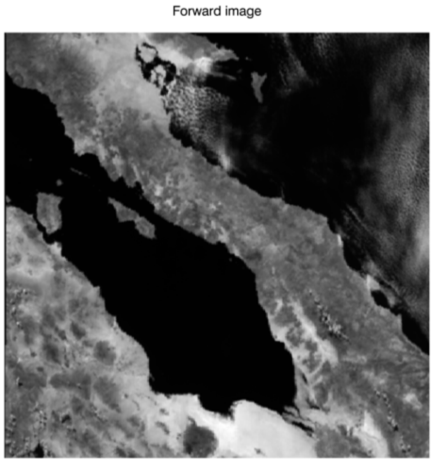

ATSR-2 V2.0 – Original

Along track shift of -1 pixel

Scan inclination angle adjustment needed

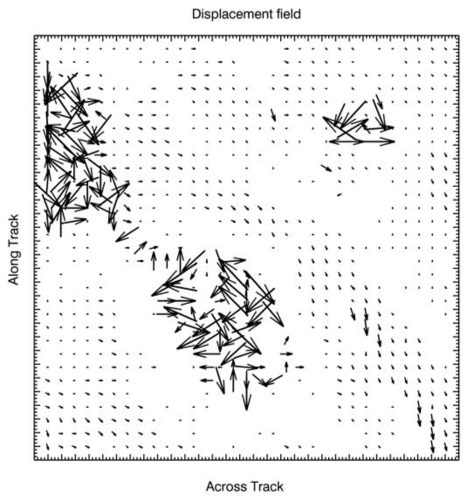

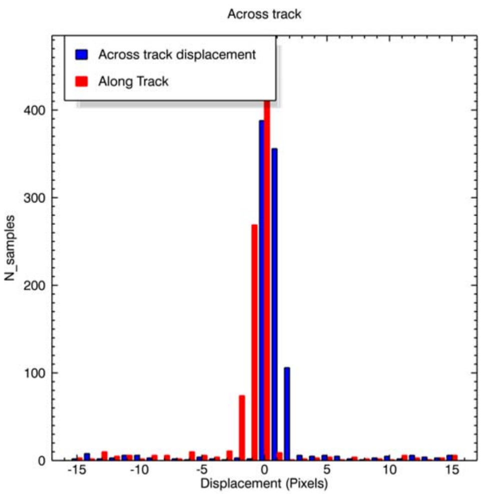

ATSR-2 Trial Month Reprocessing Checks

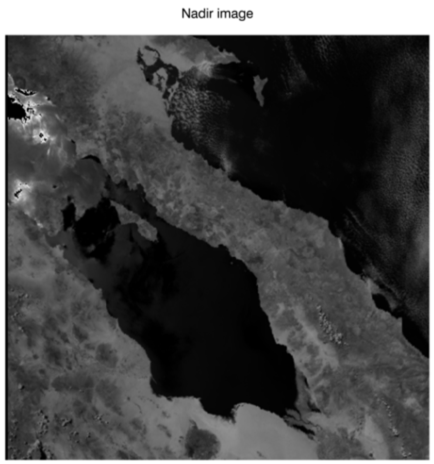

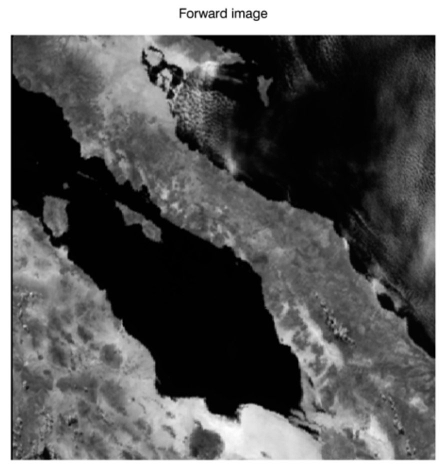

ATSR-2 V2.1 – Reprocessed

Nadir/Forward Co-registration improved

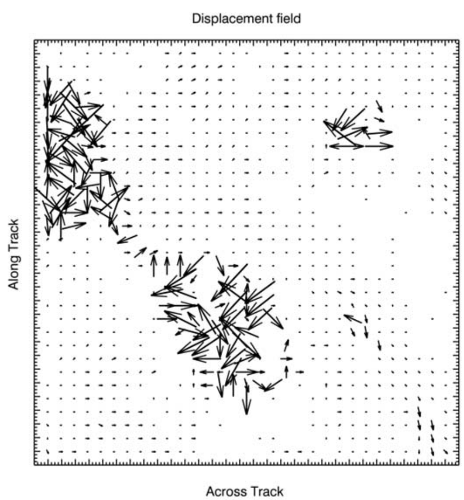

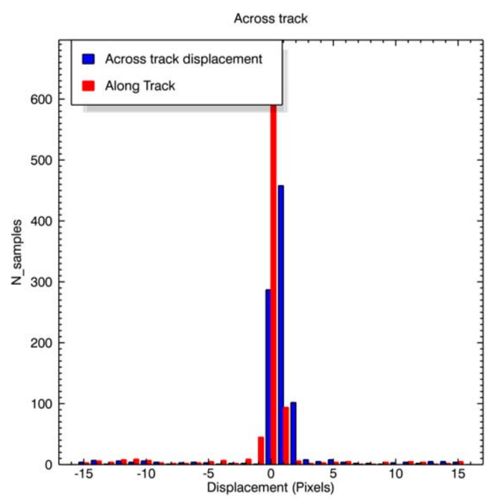

AATSR Trial Month Reprocessing Checks

AATSR V2.0 – Original

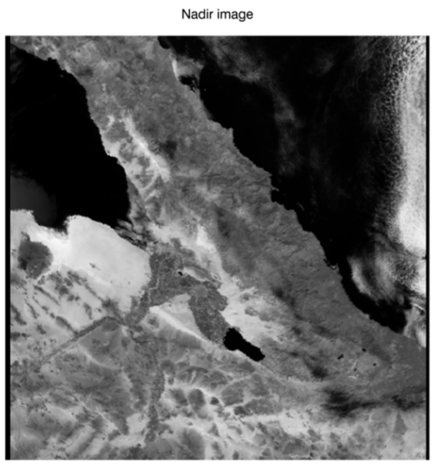

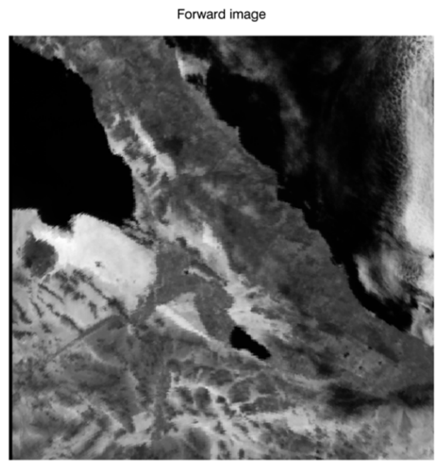

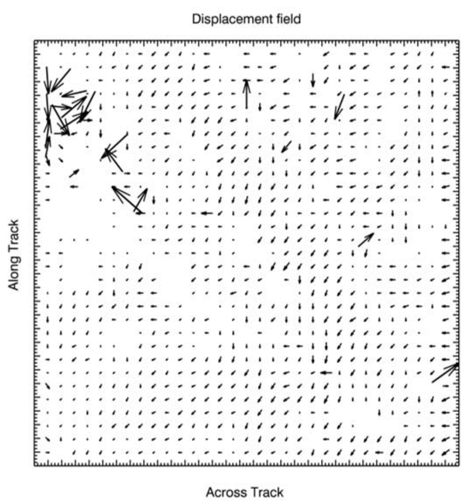

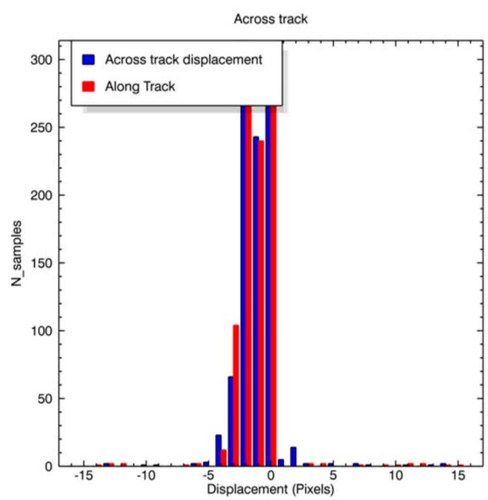

AATSR Trial Month Reprocessing Checks

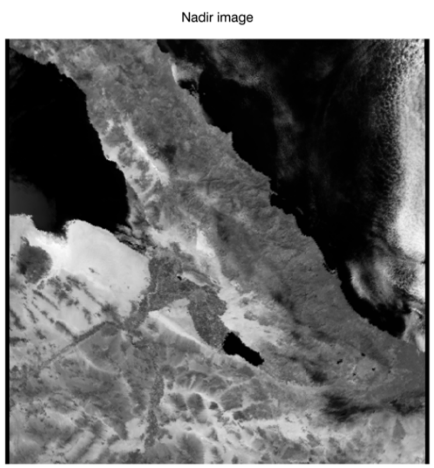

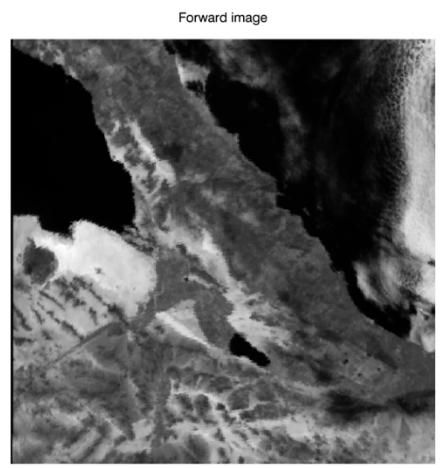

AATSR V2.1 – Reprocessed

Nadir/Forward Co-registration significantly improved

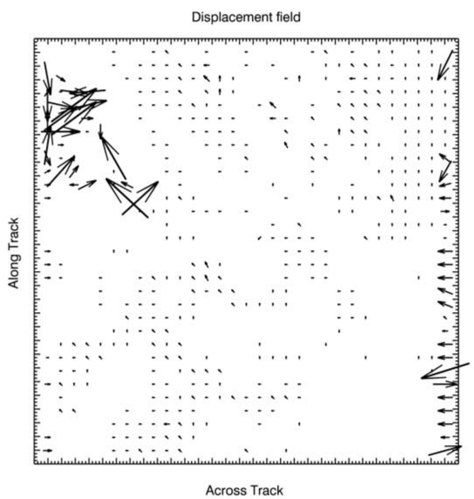

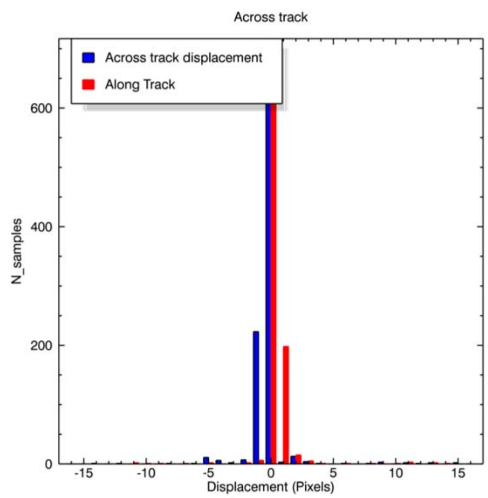

Conclusions

- Improvements to absolute geo-location can be made by using:
  - Ortho geolocation of pixels to DEM
  - Restituted state vectors for ATSR-1/2
  - Attitude and Altitude information

- Analysis of data over reference targets can be used to determine systematic offsets
  - Alignment errors
  - Scan dependent and thermal effects (possibly if scan mechanism is stable)
  - Prerequisite is to implement the improvements highlighted above.

- (A)ATSR geo-location will always be limited by the uncertainty in the scan rotation angle
  - Due to bearing noise
  - Even with improvements to constant pointing offsets, satellite attitude and ortho-geolocation…
  - ATSR-2 jitter levels are probably too severe to obtain meaningful corrections
  - SLSTR will have angular position for each pixel.

SLSTR

Sea and Land Surface Temperature Radiometer

Nadir swath	>74°	(1300 km min up to 1800 km)
Dual view swath	49°	(750 km)
Two telescopes	Φ110 mm / 600mm focal length	
Spectral bands	TIR : 3.74μm, 10.85μm, 12μm SWIR : 1.38μm, 1.61μm, 2.25 μm VIS: 555nm, 659nm, 859nm	
Spatial Resolution	1km at nadir for TIR, 0.5km for VIS/SWIR	
Radiometric quality	NEΔT 30 mK (LWIR) – 50mK (MWIR) SNR 20 for VIS - SWIR	
Radiometric accuracy	0.2K for IR channels 2% for Solar channels relative to sun	

AATSR Performance is Maintained!

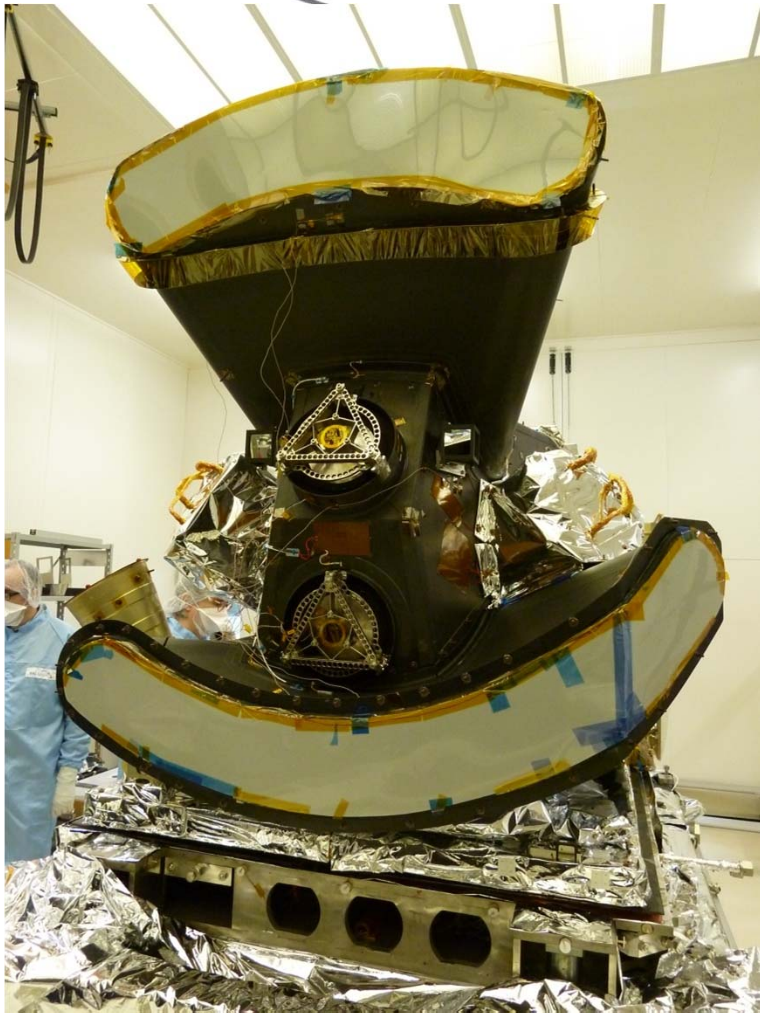

AATSR/SLSTR Comparison

	AATSR	SLSTR	
Swath width	512km – Nadir 512km – Forward View	1500km – Nadir 750km – Backward view	
Channels	0.555, 0.660, 0.870, 1.6, 3.7, 10.8, 12 micron	0.555, 0.660, 0.870, 1.375, 1.6, 2.25, 3.7, 10.8, 12 micron	
Number of detector elements per channel	1 – all co-registered behind common field stop	2 for IR 4 for VIS 8 for SWIR	Optically aligned!
Number of telescopes and scanners	1	2	
Black-Body Sources	Hot, cold – view every scan common to both views	Hot, cold– view alternate scans for each earth view	
VISCAL	Illuminated near north pole	Illuminated near south pole	
TIR Dynamic range	210K-320K	200K – 330K – normal 300K – 500K - Fire	

SLSTR Calibration Facility

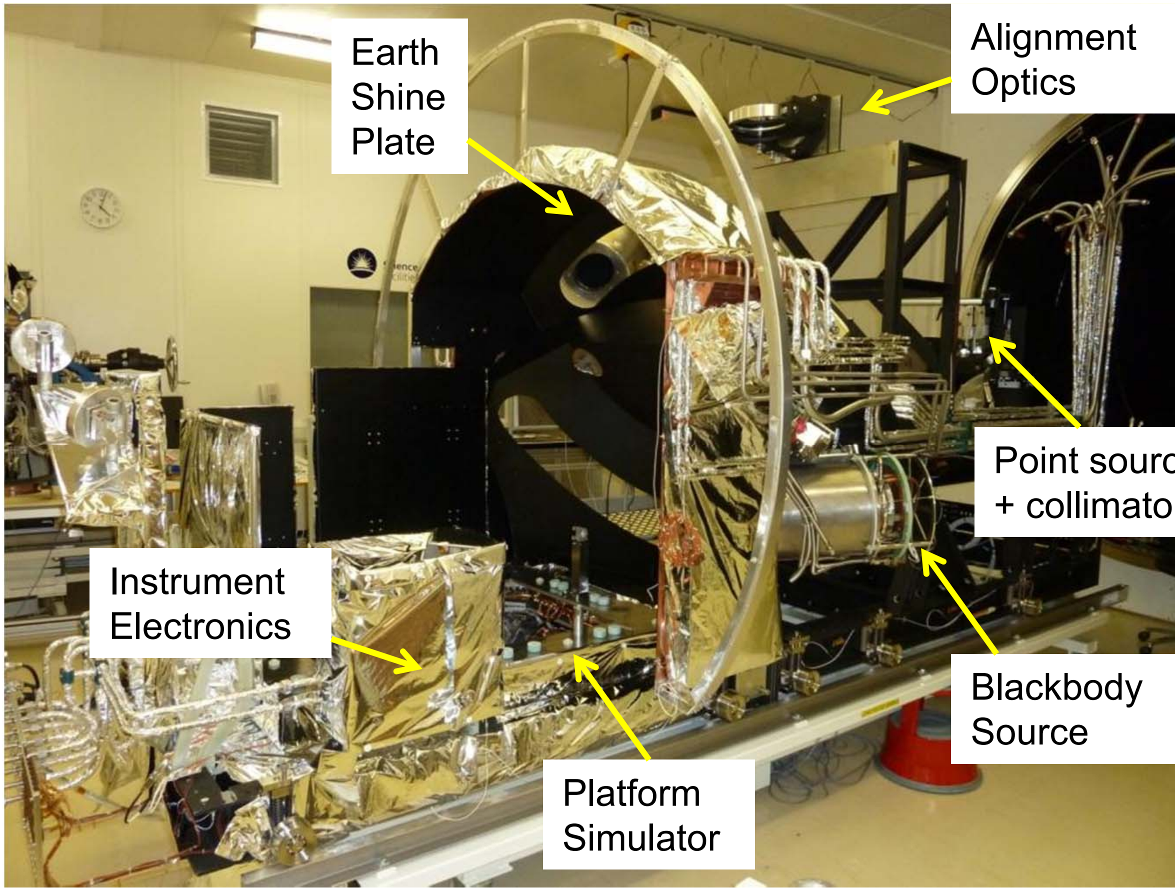

- Facility commissioning completed March 2012
- Tests with STM completed April-2012
- FM Testing scheduled for Q2 2014

ESA requirement: to perform calibration under flight representative conditions.

- *Thermal balance*
- *Steady State*
- *Instrument fully operational*

Issues for Sentinel-3 SLSTR

- Bands at 1375nm and 2250nm
  - Use MODIS-A for reference BRF
  - Spectral matching?

- SLSTR has significantly wider FOV – 1500km compared to 500km

- Nadir pixel is offset by -5º
  - Not exact coincidence with OLCI at Nadir
  - Matching geometry at swath edges

- Inclined view in opposite direction to (A)ATSR
  - Hence in backscatter direction in northern hemisphere
  - Good for match-ups with GEO sensors

- Multiple detectors per channel

- Detectors not aligned to common field stop – hence co-registration

SLSTR v AATSR Swath